# The Immune Response in Parkinson's Disease

**Arman Lira, B. Sc.**

Thesis submitted to the Faculty of Graduate and Postdoctoral Studies in partial fulfillment of the requirements for the Philosophy Doctor (Ph.D.) degree in Neuroscience.

Department of Cellular and Molecular Medicine,

Faculty of Medicine, University of Ottawa

# Abstract.

Microglia activity has been detected in Parkinson's disease (PD) post-mortem brains and experimental animal models; however the precise interplay between microglia and dopamine neurons of the SN*pc* is not well understood. In the blood plasma of PD patients, our laboratory found elevated levels of interferon-gamma (IFN-γ), a proinflammatory cytokine and potent activator of microglia. Given this, we sought to untangle the immune responses relevant to PD in mice, examining IFN-γ's involvement and signaling mechanism using an inflammatory co-culture model of microglia and midbrain neurons treated with rotenone. By means of RT-PCR, we discovered IFN-γ mRNA transcripts are produced by microglia, and this expression increases upon exposure to rotenone. We delineated IFN-γ's signaling mechanism in co-cultures using different IFN-γ receptor deficient cells, and showed it engages receptors in an autocrine (not paracrine) manner to further microgliosis and dopamine cell loss.

After exploring the innate immune response in a model of PD, we subsequently shifted focus to an *in vivo* system to better investigate any involvement of the delayed humoral arm of the adaptive immune system. Needing a time appropriate death paradigm, we developed a protracted low dose regimen of MPTP, which elicits dopaminergic cell death after 2 weeks of treatment. Subjected to this paradigm, Rag 2 mutant mice (deficient in both T and B cells) exhibit resistance to dopamine cell loss, microglia activation and motor impairments. Further evidence in support of immune involvement came with the resensitization of Rag2 mice to MPTP after reconstitution with WT splenocytes. Additionally, mice deficient in Fcγ receptors exhibited neuroprotection in our protracted degeneration model. Taken together, these data

indicate the innate and humoral arm can modulate the microglial response to dopaminergic degeneration and may participate in Parkinson's disease.

# Table of contents

## Acknowledgements

My sincerest appreciation and gratitude to my thesis supervisor: Dr. David S. Park. Under your leadership and mentorship, I grew to embrace the challenges of research and academic life. I will always be indebted and thankful for your unwavering support, altruism and friendship during my scientific pursuit.

Over the years, I amassed an enormous amount of respect and admiration for my advisory committee members, Dr. William Staines, Dr. Antonio Colavita, and Dr. Catherine Tsilfidis. I am truly grateful and very fortunate to have your scientific input and guidance through every challenge that comes with laboratory research.

To my mother, father, brother, grandparents and entire Lira and Reza family – I did not face a single day without your uplifting love and respect. This has been the cornerstone of my life, without which I would not stand as tall. And of course to those special friends who are like family, in and out of the laboratory, thank you for standing by me every step of the way and never doubting me.

## List of Manuscripts

**I.** **Lira A,** Kulczycki J, Slack R, Anisman H, Park DS (2011) Involvement of the Fc gamma receptor in a chronic N-methyl-4-phenyl-1,2,3,6-tetrahydropyridine mouse model of dopaminergic loss. **Journal of Biological Chemistry** 286(33):28783-93

**II.** Mount M, **Lira A**, Grimes D, Smith P, Faucher S, Slack R, Anisman H, Hayley, and Park DS (2007) Involvement of Interferon-gamma in Microglial-Mediated Loss of Dopaminergic Neurons. **Journal of Neuroscience** 21;27(12):3328-37

## Appended Articles

**III.** Qu D, Rashidian J, Mount M, Aleyasin H, Parsanejad M, **Lira A**, Haque E, Zhang Y, Callaghan S, Daigle M, Rousseaux M, Slack S, Albert P, Vincent I, Woulfe J and Park DS (2007) Role of Cdk5-mediated phosphorylation of Prx2 in MPTP toxicity and Parkinson's disease. **Neuron** 5;55(1):37-52.

**IV.** Juma WM, **Lira A**, Marzuk Z, Hakim AM, Thompson CS (2011) C-reactive protein expression in a rodent model of chronic cerebral hypoperfusion. **Brain Research** 1414:85-93

# List of Abbreviations

| | |
|---|---|
| Ab | Antibody |
| Ach | Acetylcholine |
| ANOVA | Analysis of variance |
| APC | Antigen presenting cell |
| BBB | Blood brain barrier |
| Cd11B | Cluster of differentiation 11B |
| DA | Dopamine |
| DAT | Dopamine transporter |
| COMT | Catechol-O-methyltransferase |
| GLA | Galactosidase A |
| HVA | Homovanillic acid. |
| IgG | Immunoglobulin G |
| IFN-γ | Interferon-gamma |
| IL- | Interleukin |
| FcγR | Fc-gamma receptor |
| MHC I & II | Major histocompatibility complex class I & II |
| MPTP | 1-methyl-4-phenyl-1,2,3,6 –tetrahydropyridine |
| MPP+ | N-methyl-4-phenylpyridinium ion |
| NMDA | N-methyl-D-aspartate |

| | |
|---|---|
| PD | Parkinson's disease |
| UPS | Ubiquitin proteasome system |
| Rag 2 | Recombinase activating gene 2 |
| ROS | Reactive oxygen species |
| SN*pc* | Substantia nigra *pars compacta* |
| TH | Tyrosine hydroxylase |
| ThC | T- helper cell |

# Chapter 1

# General Introduction.

## Parkinson's disease:

Parkinson's disease (PD) is the most prevalent motor movement disorder, and the second most common neurodegenerative disorder, after Alzheimer's disease (Lees *et al.*, 2009). It affects approximately 1% of the population over the age of 65, and 4% of the population over the age of 80 (Nussbaum and Ellis, 2003; de Lau and Breteler, 2006). Roughly four million people worldwide and one million North Americans have PD (Olanow and Tatton, 1999). Each year in the United States alone there are 60, 000 new cases reported, and with the increase in life expectancy, the prevalence is climbing. PD normally develops in people over the age of 50, and is known as late-onset PD (Van Den Eeden *et al.*, 2003). Prior to this age, incurring the disease would be referred to as early-onset PD (Cookson and Bandmann, 2010; Crosiers *et al.*, 2012). Far less common, juvenile-onset is the term used to represent those afflicted before the age of 20 (Denison *et al.*, 2003a).

PD involves the progressive, neurodegeneration of the extrapyramidal dopaminergic system. Pathological features include loss of dopamine (DA) neurons in the substantia nigra *pars compacta* (SN*pc*), Lewy body formation, and reactive gliosis (Benner *et al.,* 2008). Lewy bodies are cytoplasmic inclusions made up primarily of an alpha-synuclein core and enclosed by a halo of fibrils. Lewy bodies are thought to be formed by an aggresome response in neurons (Tanaka *et al.*, 2004). Other aggregates such as ubiquitin, Tau proteins, alpha B crystalline, and neurofilament proteins may be present inside Lewy bodies (Engelender, 2008; Ishizawa *et al*., 2003). Parkinsonism is often the term given when PD-like symptoms are present and Lewy bodies are not.

The SN*pc* regulates part of the direct and indirect motor circuitry that controls all voluntary movements, and is a functionally associated nucleus of the basal ganglia. PD patients have trouble initiating, terminating, and coordinating smooth physical movements. DA cell death manifests itself in the loss of dopaminergic neurotransmission to the striatum, thereby weakening the communication between the basal ganglia motor circuit and deteriorating the coordination of muscular movement. This communication worsens as more DA cells degenerate, eventually rendering the basal ganglia unable to regulate motor movement (Fix, 2008; Stocco *et al.*, 2010)

Accordingly, PD patients exhibit basal ganglia dysfunction clinically characterized by the key clinical symptoms of bradykinesia, resting tremor (4-6Hz), gait disturbances, cogwheel rigidity, and postural instability (Wichmann *et al.,* 2003; Dauer *et al.,* 2003). Tremors usually begin on the hands and eventually spread to the head, tongue, lips and feet as the degeneration ensues. The tremor may be 'pill-rolling', between finger and thumb, which worsens when tired or stressed, and goes away during sleep.

Concurrently, behavioural problems, mood and cognitive decline may occur (Alder CH, 2005). Dementia is another devastating feature associated with advanced PD, and it affects judgement and memory. Other clinical signs include masked facies, depression, hypophonia, hypokinetic dysarthria, micrographia, stooped posture, shuffled gait, trouble swallowing, conjugate gaze disorders, fatigue, constipation, hallucinations, slowness in blinking, drooling, muscle aches and pains, difficulty eating, sweating, lack of body temperature and low blood pressure (Weerkamp *et al.*, 2013). PD patients can have difficulty swallowing, and are at a higher risk for aspiration pneumonia. Typically,

progressive decline of the motor system continues until akinesia, autonomic dysfunction, gait instability, and failure to respond to medication ensue.

PD is a multifactorial disease that is very difficult to treat. Symptoms occur after the majority of DA cells are degenerated in the SN*pc* (Fearnley J. M. and Lees, 1991; Marsden, 1994). Given the low percentage of remaining, healthy dopamine neurons, therapeutic avenues are inherently limited. As such, early detection is a key strategy to deal with PD. Since it is not known what causes degeneration of DA cells in most cases, PD medications can only temporarily dampen symptoms. And it accomplishes this primarily by increasing the level of DA.

Levodopa is commonly used to treat PD (Fahn *et al.*, 2004). It crosses the blood brain barrier effectively and is converted into DA. Carbidopa can be given concurrently with Levodopa. It inhibits DOPA decarboxylase, an enzyme required for the biosynthesis of DA from L-DOPA. Given that Carbidopa cannot cross the BBB, it acts to prevent the breakdown of L-DOPA in the periphery, thereby increasing its bioavailability in the DA-deficient brain. To help block DA degradation, a Catechol-O-methyl transferase (COMT) inhibitor can also be administered. COMT degrades catecholamines, such as DA (Bonifati *et al.*, 1999). Likewise, inhibitors of monoamine oxidase-B (an enzyme that breaks down DA) are used to increase the amount of DA in the basal ganglia (Schapira, 2003). Furthermore, physicians normally prescribe DA receptor agonist to buy time and quality of life for PD sufferers (Lida *et al.*, 1999; Schapira *et al.*, 2003). This only provides temporary relief. Unfortunately, PD medication merely masks the problem by increasing levels of DA, and does not interrupt

the degenerative or neuroinflammatory process. Treatments are usually beneficial for 4-8 years, after which they lose effectiveness; all the while degeneration of DA neurons continues (Wu *et al.,* 2003; Olanow and Tatton, 1999). Eventually PD sufferers develop uncontrollable, jerky movements called dyskinesias. In late stage PD, when medication is no longer effective, PD sufferers may turn to surgery for relief of their dyskinesias. The FDA has approved deep brain stimulation for treatment of PD. It is an electrical device similar to pacemakers for correcting heart arrhythmias, with the intent on short-circuiting the basal ganglia. It is similar to pallidotomy, without permanently lesioning the globus pallidus (Bronstein *et al.*, 2010).

PD medications have a short therapeutic window, and do not target any of the underlying cellular dysfunction. After a few years, patients usually develop dose-limiting effects to their medications, such as dyskinesia, and physical symptoms worsen. It is clear that for new medications to effectively stabilize motor symptoms, they need to interrupt the degenerative mechanism driving DA cell death in the SN*pc*.

Accumulating evidence suggests genetic and environmental components strike a common chord with key signaling pathways (Chuang *et al*., 2013; MacLeod *et al*., 2013). Merely 15 % PD sufferers have a 'first degree' relative with the disease (Samii *et al*., 2004). Familial PARK gene members include PARK1 (alpha-Synuclein), PARK2 (Parkin), PARK5 (UCH-L1), PARK6 (PINK1), PARK7 (DJ-1), PARK8 (LRRK2), PARK9 (ATP13A2) and VSP 35 (Cookson, 2005; Moore *et al*., 2005; Schiesling *et al*., 2008 ; Vilarino-Guell *et al*., 2011). These genetic mutations can play a role in idiopathic (sporadic) cases of PD. In most cases, PD develops sporadically with no

familial pattern of inheritance. Although the cause of degeneration in sporadic cases remains elusive, scientists have gathered clues from some of the genetic components of PD to piece together underlying mechanisms of DA cell death, enabling for improved medications and symptom management.

## PD Genes:

The PARK1 gene is also known as PARK4 and encodes alpha-synuclein, the non Abeta component of amyloid fibrils in Alzheimer's disease? (Xia *et al.*, 2001; Xia *et al.*, 2002). Alpha-synuclein mutants are inherited in an autosomal dominant pattern (Corti *et al.*, 2011). Alpha-synuclein protein is predominantly expressed in the brain, within presynaptic terminals and is the most prominent component of Lewy bodies. Although its function is not well understood, alpha-synuclein is thought to regulate the release of synaptic vesicles (George *et al.*, 1995).

At least 18 mutations in SNCA have been shown to cause PD, and they are associated with the early-onset of the disease. Two kinds of mutations result in protein misfolding, namely Ala53Thr and Ala30Pro (Li *et al*., 2001). Conversely, SNCA gene copies can duplicate or triplicate, leading to an overexpression of the protein (Singleton *et al.*, 2003). Both the misfolding or overexpression mutations facilitate protein aggregation, which may become neurotoxic and be involved in Parkinson's disease, multiple system atrophy (Arima *et al.*, 1998a) and Alzheimer's disease (Yokota *et al.*, 2002). Reports also show aggregation of alpha-synuclein can interfere with the

ubiquitin-proteasome system (Snyder H and Wolozin B, 2004), thereby causing a build-up of abnormal proteins that impede neuronal function (Cookson, 2009).

Dementia with Lewy bodies is also caused by alpha-synuclein mutations (Arima *et al.*, 1998b). This disorder can be accompanied with visual hallucinations, attention deficits, and PD-like symptoms. Compared to PD, dementia with Lewy bodies have more widespread deposits of Lewy bodies throughout the brain. Additionally, alpha-synuclein gene alterations have been linked to multiple system atrophy, another progressive neurodegenerative disease impinging on motor movement and balance (Arima *et al.*, 1998a).

The PARK2 gene encodes Parkin, an E3 ubiqitin protein ligase. It is one of the largest genes in the human genome, located on chromosome 6 in an area known as FRA6E, which is prone to rearrangements (Denison *et al.*, 2003b). The PARK2 gene has an autosomal recessive pattern of inheritance. Parkin and other E3 ubiquitin ligases covalently attach ubiquitin to proteins for degradation by the proteasome or autophagosome. The ubiquitin-proteasome system regulates concentration of proteins, including those tightly controlled with timing of cell division, by degrading misfolded and aberrant proteins (Dawson and Dawson, 2010). Parkin carries out some of its function in mitochondria; reportedly it aids in the degradation of abnormal mitochondria by autophagy (Chang *et al.*, 2013). It also has a role in the release of synaptic vesicles.

Parkin may be a tumor suppressor protein, as some of its mutations have been shown to cause cancers. There are over 200 Parkin mutations found to cause juvenile and late-onset PD (Denison *et al.*, 2003a). These mutants cause dysfunctional Parkin proteins, or truncated forms that are degraded. Mitochondria function is also altered by

some Parkin gene modifications. Lastly, Parkin gene mutations may increase risk of developing leprosy (Kay *et al.*, 2010; Mira *et al.*, 2004). Altering the ubiquitin-mediated autophagy facilitates contracting this infection (Manzanillo *et al*., 2013)..

PARK5 is named UCH-L1 (ubiquitin carboxyl-terminal esterase L1) (Yasuda *et al.*, 2009). It is involved in degrading unwanted proteins, although it is not clear exactly how it accomplishes this. UCH-L1 inherently possesses two kinds of enzymatic activity: hydrolase and ligase activity. Hydrolase remove and recycles ubiquitin once unwanted proteins are broken down, while the ligase activity brings together ubiquitin molecules for tagging purposes.

A polymorphism (Ser18Tyr) in the UCH-L1 gene appears to reduce the likelihood of getting PD. This polymorphism minimizes the ligase activity (Xilouri *et al.*, 2012). Conversely, replacing isoleucine with methionine at position 93 may increase the chance of developing PD (Kabuta T and Wada K, 2008). The hydrolase activity is impeded in this mutant form, leading to the over accumulation of unwanted proteins that may become neurotoxic.

The PARK6 gene is an autosomal recessive PD gene, encoding PTEN induced putative kinase 1 (PINK1), which is expressed on the surface of mitochondria throughout the body (Narendra *et al*., 2010). Though its function is unclear, PINK1 seems to protect the mitochondria during times of high demands for energy. Without an adequate energy supply, as is the case during mitochondrial dysfunction, the cell can die. During mitophagy, PINK1 recruits Parkin to the outer mitochondrial membrane to remove damage mitochondria (Youle *et al*., 2011). PINK1's mitochondrial-targeting motif and the kinase activity are functionally important. More than 70 mutations have been found

to cause early onset PD; these normally disrupt its kinase activity, though mitochondrial-targeting motif mutations have also been linked to PD (Narendra *et al*., 2010).

DJ-1 is the protein encoded by the PARK7 gene, and it is expressed throughout body and brain, helping protect against oxidative stress by helping regulated mitophagy (Canet-Avilés *et al*., 2004; Junn *et al*., 2009). The dopamine neurons of the SN*pc* are particularly vulnerable to free radicals. DJ-1's chaperone activity is used to deliver proteins to the proteasome system (Lev *et al*., 2008). Over 25 DJ-1 mutations have been identified, which alter its protein structure or reduce its expression, to cause PD (Blackinton *et al*., 2005).

The PARK8 gene encodes leucine-rich repeat kinase 2 (LRRK2), which is also known as dardarin. LRRK2 is as autosomal dominant PD gene. Notably, it has a leucine-rich region, used in protein-protein interaction, and a kinase motif, which phosphorylates by transferring a phosphate group from ATP to an amino acid of a protein. LRRK2 additionally has GTPase activity in its ROC domain. The ROC domain is responsible for regulating homodimerization with LRRK2 (Lee *et al.*, 2012). Over 100 LRRK2 mutants have been found to cause late-onset PD . In 3-7 percent of familial PD cases, there is the LRRK2 mutation Gly2019Ser. It is also found in 1.6 percent of sporadic PD cases (Davie *et al*., 2008). The LRRK2 mutation is the most common cause of familial and sporadic PD (Davie *et al*., 2008; Lesage *et al*., 2009). A mutation in Arg1441Gly is common in the Basque region. A Gly2385Arg mutation was found to increase the risk of PD in a Chinese and Japanese population.

PARK9 encodes the ATPase type 13A2, which is intimately involved in autophagy. Accumulating evidence suggests autophagy is involved in pathogenesis of

PD. Autophagy is the process by which proteins or organelles are degraded and recycled by fusion of autophagosome and lysosomes (Lin *et al*., 2012). Targeted proteins or organelles are engulfed by autophagosome before mixing with digestive enzymes within lysosomes (Patel *et al*., 2012). There are three types of autophagy: macroautophagy, microautophagy and chaperone mediated autophagy (Peracchio *et al*., 2012). Autophagy can also be an adaptive survival mechanism, or it can promote cell death, and is referred to as autophagic programmed cell death (Nixon *et al*., 2013; Patel *et al*., 2012; Tsujimoto *et al*., 2005).

ATPase type13A2 is a P5 subfamily of lysosomal ATPase serving to transport substrates, including inorganic cations (Schultheis *et al*., 2004). It is involved in homeostasis of neuronal integrity and intracellular cations (Ramonet *et al*., 2012). Persons with PD and dementia with lewy bodies have higher levels of ATPase type 13A2 (Ramonet *et al*., 2012; Ramirez *et al*., 2006).

GBA stands for glucosidase, beta, acid – a gene which makes glucocerebrosidase, which is a lysosomal hydrolase enzyme and aids the breakdown of the large molecule glucocerebroside into glucose and ceramide, a lipid. It has been implicated in PD. GBA mutations increase the risk of developing sporadic PD (Lesage *et al*; 2009). It is still not well understood how GBA mutants can cause PD, although it is thought that the lysosomal dysfunction can lead to toxic deposition of defect proteins.

GBA mutations can cause Gaucher disease, where glucocerebroside accumulates in macrophages, and becomes detrimental to different organs macrophages invade (Lesage *et al*., 2009). Gaucher sufferers have a higher chance of

developing PD. Likewise, carriers of mutations in GBA have a higher likelihood of developing dementia with lewy bodies. Another lysosomal hydrolase, alpha-galactosidase A (GLA) has been implicated in PD pathogenesis (Wu *et al*., 2011).

A screening of idiopathic PD patients for lysosomal hydrolase activities highlighted a reduction in alpha-galactosidase A (Wu *et al*., 2011). Furthermore, their data indicated that a sequence variant in the GLA gene's transcription binding site could modulate its expression and be involved in PD pathogenesis.

The most recent genetic mutation linked to PD is vacuolar protein sorting-associated protein 35 (VSP35), and was discovered by Matt Farrer's research group using exome sequencing (Vilarino-Guell *et al*., 2011). This new technique reveals all mutated genes in a person. VPS35 is an important part of the retromer, protein recycling system (Zhao *et al*., 2007). The retromer is needed to recover and recycle lysosomal enzyme receptors (IGF2R and M6PR) from endosomes to the trans-Golgi network. Additionally it is needed to manage transcytosis of the immunoglobulin receptor IgR-IgA. Vsp35 is particularly critical for membrane protein sorting, rescuing, and recycling. It is the largest subunit in the retromer complex, and functions as the central platform upon which Vsp26 and Vsp29 are assembled (Hierro *et al*., 2007). The cargo binding function of this complex is attributed to its interactions with different cargo molecules. An aspartic acid to asparagine mutation was found to be a genetic determinant of late-onset PD (Zimprich *et al*., 2011). Similarly, defects with the retromer system have been associated with Alzheimer's disease (Muhammad *et al.*, 2008) and Charcot-Marie-Tooth (Verhoeven *et al.*, 2003). The retrograde pathway plays an important role by maintaining the distribution of cell surface factors and signaling molecules. Additionally, it is involved in

the removal of toxic metabolites that may cause aggregation and neuronal dysfunction (Burd, 2011).

Factors involved with pathogenesis of PD can be grouped as either primary conserved players directly affecting critical pathways of DA neuron function, or indirect associative factors modulating activity of such conserved factors (Simunovic *et al*., 2009). Deregulating either primary or secondary factor can result in PD. Moreover, there is significant functional overlap between PARK family gene members. Evidence from genetic analysis and animal model studies show different PARK genes, for example LRRK2, PARK16, and VSP35 converge onto a common cellular pathway which ultimately results in DA cell death.

Mitochondrial dysfunction, ubiquitin-proteasome system defects, and reactive oxygen species generation are general concepts underling genetic dysfunction in PD. In mitochondrial dysfunction, energy manufacturing is disrupted and free radicals are generated. Likewise, normal antioxidant activity of dopamine neurons is diminished, leading to a rise in free radical damage.

The ubiquitin-proteasome system is responsible for targeted degradation of damaged, abnormal, or misfolded proteins. It accomplishes this by way of proteolysis, or breaking peptides bonds with proteases (Lodish *et al*., 2004). Proteins are marked with ubiquitin, and consequently processed for degration through the proteasome. Proteolytic dysfunction causes a buildup and clustering (aggregation) of these proteins - the primary discernible being alpha-synuclein in Lewy bodies (Olanow and McNaught, 2006). There is a marked downregulation of genes associated with proper function of mitochondria, ubiquination, chaperone proteins, proteosomal subunits and lysosomes (Simunovic *et al*.,

2009). The UPS is used to regulate essential cellular activities such as the cell cycle, oxidative stress responses, and gene expression regulation (Lodish *et al*., 2004).

Dysfunction of the ubiquitin-proteasome system and mitochondrial have long been linked to PD and programmed cell death (Bredesen *et al*., 2006; Gomez *et al*., 2007). Defects with mitochondria typically entail complex I inhibition of the electron transport chain, reactive oxygen species generations, ATP depletion, and cytochrome-c release, and caspase-3 induction. Antioxidant enzyme genes, such as superoxide dismutase, have been found to be downregulated in DA neurons of PD patients (Simunovic *et al.*, 2009).

Not only are the PARK gene family members deregulated, but also are the secondary associative factors of PD pathogenesis affecting programmed cell death and survival. PD patients display genetic abnormalities causing dysfunctional neurotransmission and ion channels, reinforcing the idea that dopamine neurodegeneration can arise from changes to electrical activity, according to Simunovic *et al* (2009).

They conducted a microarray profile of gene expression using laser micro-dissected single DA neurons from the SN*pc* of PD patients, as opposed to traditional dissections of entire midbrain, and they compared with age-matched sporadic PD subjects. They demonstrate that cell electrical activity is important in DA neuronal survival (Simunovic *et al.*, 2009). Neuronal electrical properties are contingent on sodium, potassium, and calcium channels. They report a downregulation of ATP1B1, a $Na^+/K^+$-ATPase carrier protein, which supports the electrochemical gradient. Mutations

of its gene have been found to cause rapid-onset dystonia Parkinsonism (de Carvalho Aguiar *et al*., 2004).

Likewise, Michel *et al* (2007) extrapolated a model whereby mitochondrial dysfunction causes $K_{atp}$ (adenosine triphosphate-sensitive) channel-mediated hyperpolarization, making dopamine neurons vulnerable to degeneration. In a similar context, superoxide dismutase overexpression blocked K+ -mediated hyperpolarization (Simunovic *et al*., 2009). Downregulation of calcium channel subunits have also been detected in these genetic studies.

L-type calcium channels sequestered by the endoplasmic reticulum and mitochondria use ATP-dependent transporters (Surmeier *et al*., 2007). These high metabolic rates and energy consumption require oxidative phosphorylation, which in addition to ROS production and mitochondrial defects, enhance ageing and may contribute to protein abnormalities (Surmeier *et al*., 2007).

Other ions channels have been linked to neuron death. NMDA receptors can contribute to neurons death via excitotoxicity. Conversely, nicotinic ACh receptors have been shown to be neuroprotective in MPTP and 6-OHDA models of PD. This protection is mediated by diminishing the glutamate-driven excitotoxicity, as well as by increasing intracellular calcium. As such, controlling DA neuron's electrical activity can promote survival (Matsubayashi *et al*., 2004; Quik *et al*., 2007).

Evidently, many genes are deregulated that do not belong to the PARK family of genes, and are rather associated with increased likelihood of developing the Parkinson's disease. They are functionally grouped by their involvement in different cellular processes, such as certain heat shock proteins and ubiquitin peptidases associated with

protein degradation pathways; caspase-9, cytochome-c oxidase subnits, TNF-alpha receptor and Fas associated with programmed cell death and mitochondrial function; calcium-dependent secretion activator, transport vesicles and docking proteins associated with synaptic function; connective tissue growth factor and NF-KB binding protein associated with growth factors, dopamine receptor D1, sodium and potassium channels associated with receptors and ion-channel; and finally immune genes encoding for interferon-gamma, interleukin 6 receptor, CD40, and different chemokines (Bredesen *et al*., 2006; Gomez *et al*., 2007; Duke *et al.,* 2006; Olanow *et al*., 2006; Moran and Graeber *et al*., 2008; Simunovic *et al.*, 2009).

Moran and Graeber *et al* conducted a microarray analysis of close to 900 genes from SN cells of PD patients, and discovered a strong associate with inflammatory genes. An independent study found 51 immune related genes were deregulated in DA neurons from PD patients (Simunovic *et al.*, 2009). These genetic analyses are consistent with experimental evidence of immune system involvement in DA neuron death (Whitton *et al*., 2007).

Defective groups of genes may reflect part of the neurodegenerative trigger. By understanding all the different mechanisms of dopamine cell death, better preventative treatments can be formulated to prevent further debilitation in PD patients.

## Environmental Risk Factors for PD:

Alongside the diverse genetic risk factors, there exist a multitude of environmental susceptibilities contributing to the development of PD (Chuang *et al*., 2013). Exposure to infectious diseases early in life may predispose individuals to neuron death later on in adulthood. For example, early childhood encephalitis could sensitize neurons and become increasingly vulnerable to future infections (Liu *et al*., 2003).

Microglia become activated in response to various stimuli, including foreign matter, viruses, and bacteria. Lipopolysaccharides (LPS) are a component of outer cell wall membrane of Gram-negative bacteria's. When exposed to the immune system, they generate a strong reaction. LPS induces secretion of pro-inflammatory cytokines, chemokines and prostaglandins particularly from B cells and macrophages, after engaging the CD14/TLR4/MD2 receptor complex (Rock *et al*., 2004). They also release the chemokine IL-8 for B cell differentiation. Scientists have demonstrated LPS activates iNOS and TNF-alpha secretion (Lee *et al.*, 1999; Lee *et al.*, 2003). As the classic inflammatory molecule, LPS was traditionally used in various models of PD to study mechanistically how the innate immune system mediates dopaminergic cell injury.

LPS-induced DA neuron loss and proinflammatory gene expression has been examined in co-cultures of microglia and midbrain neurons (McCoy *et al.*, 2006; Qin *et al.*, 2004) and macrophages (Lin *et al.*, 2007). Microglia activation with LPS treatment was sparked by NADPH oxidase, the main superoxide producing enzyme in microglia. LPS caused this enzyme to incite DA neuron loss by generating ROS and stimulating proinflammatory TNF-alpha gene expression.

LPS was widely used to study the innate immune system in PD, given DA neurons of the SN*pc* are inherently susceptible to inflammation and oxidative stress. Nowadays however, the use of LPS in PD models is diminished because its generalized toxic effects and pyrogenicity have been superseded by more practical and selective agents of dopaminergic injury.

Furthermore, LPS fails to reproduce the complex I inhibition commonly exhibited in PD. Complex I of the electron transport chain is formed by two enzymes: Coenzyme Q10 and NADH dehydrogenase. There is a staggering 30-40% reduction in complex I activity in PD brains, which is why coenzyme Q10 therapy has proven to be neuroprotective against the dopaminergic neurotoxin MPTP. Compared to LPS, more clinically relevant promoters of DA cell death are pesticides, which inhibit mitochondrial complex I and elicit many common features of PD (Gao *et al*., 2013; Yang *et al*., 2007; Ding *et al*., 2001).

## Pesticides:

Pesticides and herbicides are risk factors for developing PD (de Lau *et al*., 2006; Hayley *et al.*, 2004; Brown *et al.*, 2006). Pesticides and agrochemicals have long been suspected culprits causing dopaminergic cell death ever since farming communities exhibited a higher incidence of PD. Those exposed to 'agent orange', a herbicide used during the Vietnam War, had an increased likelihood of developing PD (de Lau *et al*., 2006). Pesticides were initially used in PD research because paraquat, a herbicide, structurally resembles MPP+. Rotenone was first extracted from the roots and stems of

several tropical and subtropical plant species. Tribesmen initially used rotenone in water to stun and kill fish. Nowadays, rotenone is a pesticide used in many models of PD because it kills dopamine neurons selectively at low concentrations by inhibiting complex I of the mitochondrial electron transport chain causes DA cell death (Greenamyre *et al.*, 1999; Jenner, 2001). It also elicits microglia activation, Lewy body formation, and motor movement impairments (Gao *et al.*, 2002a). Accordingly, rotenone's neurotoxic effects as a complex I inhibitor and activator of microglia make it an ideal candidate for use in neuroinflammatoy research, specially compared to the classic inflammagen LPS, which elicits a more broad generalized toxicity (Sherer *et al.*, 2003b).

Evidence suggests sporadic PD arises from the culmination of genetic and environmental factors impinging on central signaling pathways within DA cells (Wu *et al*., 2011; Chuang *et al*., 2013). Given the devastating course of PD and the lack of suitable treatment, the impetus is on understanding the way by which DA neurons degenerate, in hopes of designing effective preventative therapies. A multifactorial treatment strategy is needed to not simply replace DA, but to prevent further cell death and halt the immune reaction. Interfering with the complex immunological network may protect DA neurons, and give current PD medications a better opportunity to ameliorate motor system impairments.

The immune system can exacerbate particular PARK gene deficits, and vice versa members of the PARK gene family encode proteins that can activate the innate or adaptive immune response. For instance, microglia activation generates a battery of reactive oxygen species, which can combine with the free radicals from the genetic mutations that cause mitochondrial dysfunction or DJ-1 defects (Yang *et al.*, 2007;

Rhodes *et al.*, 2013). Modulating reactive oxygen species is an important control for any cell, specially those of the SN*pc*, which appear highly susceptible to oxidative stress. DJ-1 possesses antioxidant properties, and our laboratory has shown DJ-1 post-translational modification has huge impact on its function to protect DA cells (Aleyasin *et al*., 2010). Parkin encodes a E3 ubiquitin protein ligase. Mutations in the ubiquitin-proteasome system lead to an accumulation of excess or aberrant proteins, such as alpha-synuclein, that can elicit aggregation, inflammation, and antibody production (Benner *et al*., 2008). Aside from the interplay between immunological processes and PD genes, there are also genetic mutations of the immune system itself that can increase the likelihood of developing PD. Furthermore, environmental risk factors such as exposure to pesticides or CNS infections, can invoke neuroinflammatory responses to yield neurodegeneration. Even though, the majority of PD cases are idiopathic, the replete list of evidence for innate immune involvement made it a pathological feature of PD (Benner *et al*., 2008).

## Innate Immunity in PD:

The innate immune system responds immediately to defend the body against foreign pathogens, bacteria, viruses, or cellular debris, by acting as a physical or chemical barrier and recruiting immune cells to the site of injury or infection. It accomplishes this by secreting cytokines, chemokines, ROS, activating phagocytosis, or promoting the complement cascade and infiltration of specialized white cells to remove infected or dying cells. The innate immune system is also known as the non-specific immune system, and can activate the adaptive 'specific' immune system by presenting antigens.

Microglia are the resident immune cell in the central nervous system and the primary active defense (Dissing-Olesen *et al*., 2007). They make up 20% of all glia in the brain, and are the first responders, capable of very sensitive detection of low levels of pathogens (Aguzzi *et al*., 2013; Lawson *et al*., 1992; Kreutzberg *et al*, 1995). This high acuity in sensing their environment is partially accomplished by using a unique potassium channel, capable of detecting subtle changes in extracellular potassium levels (Gehrmann *et al*., 1995; Kreutzberg *et al.,* 1995). Microglia display high level of plasticity in order to combat different immunological challenges, and therefore do not need to be constantly replaced (Aguzzi *et al*., 2013; Kreutzberg *et al.,* 1995).

As macrophages, microglia constantly survey their environment, and target pathogens, foreign bodies, plaques, injured and dying cells (Kreutzberg *et al.,* 1995). Microglia can destroy foreign bodies or infected cells via phagocytic and cytotoxic activity. Microglia can phagocytose material and display digested peptides on major histocompatibility complex (for T cells). They are very efficient antigen presenting cell of the central nervous system (Aloisi, 2001; Gehrmann *et al*., 1995).

Amoeboid microglia scavenge and phagocytose debris but are not ideal for antigen presentation or inflammation. They are prominent in development and rewiring of the brain, when debris and apoptotic cells need to be removed (Kreutzberg *et al.,* 1995; Ferrer *et al*., 1990; Christensen *et al*., 2006). Additionally they do not have major histocompatibility complex class I and class II, no intereferon-gamma, CD45 antigens, and other factors involved in antigen presentation and cytotoxicity.

Quiescent microglia are not typically replaced by myeloid progenitor cells, due to the tight knit blood brain barrier. However, upon serious infection, bone chimera studies demonstrate the blood brain barrier weakens to allow for peripheral macrophages and myeloid progenitor cells (Gehrmann *et al*., 1996). The resting form of microglia is ramified, and made up of branching processes constantly in motion in order to survey their environment. Their main purpose is detecting infection and cell injury. They are unable to phagocytose (unlike the other two types), have no major histocompatibility complex class I and class II, and are poor antigen presenter (Aloisi, 2001; Christensen *et al.*, 2006).

On the other hand, activated microglia can be non-phagocytic or phagocytic (Blaylock *et al.*, 2013). Non-phagocytotic microglia are activated by glutamate receptor agonist, lipopolyssacharides, cytokines, extracellular potassium changes, which occurs upon cells rupturing, and cell necrosis factors. Upon activation, microglial branches shorten, they expresses immunomolecules, including major histocompatibility complex I and II, and can secrete chemokines and cytotoxic factors. Subsequently, these microglia rapidly proliferate (Blaylock *et al.*, 2013).

Activated phagocytic microglia are the most immunoresponsive. They are highly mobile scavengers that phagocytose material, release cytotoxic and inflammatory factors upon encountering pathogens, foreign bodies, viruses, bacteria, damaged cells, dead cells, DNA fragments, neural tangles, plaques, and lipids. They possess the ability to present antigens, interact with astrocytes and neurons to maintaining homeostasis (Kreutzberg *et*

*al*., 1995; Aloisi, 2001). After phagocytosing as much material as they possibly can, microglia become gitter cells, which are generally non-reactive (Rissi *et al*., 2006).

Microglia activation, the primary hallmark of neuroinflammation, has been consistently observed in the SN and striatum of PD post-mortem brain and experimental animal models of the disease (McGeer *et al.,* 2003). However, neuroscientists were unsure whether microgliosis contributed to DA cell death, or presented itself as a consequence of the degenerative process (McGeer *et al.*,2003.

Phagocytosis is microglia's main function, although through cytotoxicity they can also destroy infectious organisms or infected cells. Microglia can release a wide variety of neurotoxic and neuroinflammatory factors including chemokines, glutamate, aspartate, and proteases, such as cathepsins B,L, and S, the matrix metalloproteinases (MMP -) 1,2,3 and 9 (Kim and Joh, 2006). Microglia also have been shown to secrete cytokines such as IL-1 alpha, IL-1 beta, and TNF-alpha, and Fas. If the release of cytokines is sustained, it becomes neurotoxic (Kim and Joh, 2006; Liu and Bing, 2011)).

Microglia secrete chemokine IL-8 for B cell differentiation and neutrophil recruitment (Ramesh *et al*., 2013; Tarassishin *et al*., 2011). IL -1 release inhibits IL-10 and TGF-beta, thereby downregulating inflammation and antigen presentation. Secretion of chemokines, such as the chemoattractant protein-1 (MCP-1), MDC, IL-8, and MIP-3beta recruit T cells and dendritic cells to the injury site. Prostaglandins prevent inflammatory cascade and downredulate Th1 (Aloisi, 2001). Microglia are also beneficial in that after inflammation , they can speed up considerably regrowth and remapping of neural tissue, by synaptic stripping (removal of branches from nerves near

site of injury), secreting anti-inflammatory cytokine and growth factors (Ritter *et al*., 2006; Gehrmann *et al*., 1995).

## Microglial Derived Reactive Oxygen Species:

Free radicals oxidize neighboring molecules as they extract electrons to complete their orbital. In microglia there exist three enzymatic sources of reactive oxygen species, namely NADPH Oxidase (PHOX), Inducible nitric oxide synthase (iNOS) and cyclooxygenase-2 (COX 2). Microglia's biggest superoxide producing enzyme, NADPH Oxidase, is upregulated in post-mortem brain from PD patients (Qin *et al*., 2004). Inhibiting its activation protects DA neurons in different models of PD (Gao *et al*., 2003c). Inducible nitric oxide synthase is calcium independent, and its activation is sustained longer than endothelial NOS, which is calcium dependent. Researchers report direct inhibition of iNOS reduces dopaminergic neurotoxicity of LPS and IFN-γ-activated microglia in vitro by 75% (Hemmer *et al*., 2001). COX-2 produces super oxide as a byproduct of prostaglandin synthesis. Overexpressing COX-2 can activate cell cycle genes and trigger apoptosis.

Upon activation, microglia generate cytotoxic levels of superoxide and nitric oxide. These two compounds can rapidly interact to form the peroxynitrite, a highly reactive oxidative species capable of traversing cell membranes, and causing lipid peroxidation, DNA damage, mitochondrial inhibition and nitrotyrosine formation (Dringen *et al*., 2005; Ischiropoulos *et al*., 2003). 3-nitrotyrosine is a marker for peroxynitrite, and has been detected in PD (Ischiropoulos *et al*., 2003). Peroxynitrite is

formed three times faster than superoxide dismutase converts super oxide in hydrogen peroxide (Beckman, 1994).

## Microglia Neurotoxicity and Reactive Microgliosis:

Microglia can become activated upon exposure to cytokines, chemokines, invading pathogens, antibodies, alpha-synuclein, amyloid-beta, lipopolysaccharides, misfolded proteins, extracellular debris, thrombin, pesticides (rotenone), and MPTP (Cardona *et al*., 2006). Microglia neurotoxicity has been implicated in PD, principally by secreting neurotoxic and inflammatory factors, including TNF-alpha, interleukin-1beta, nitric oxide, superoxide, and prostaglandin $E_2$ (Block *et al*., 2007b).

Injured or dying cells can also activate microglia. This occurs by soluble factors, including neuronal death signals, alpha-synuclein, μ-calpain, or changes in extracellular potassium. Similarly, dying neurons signal microglia to become active by the loss of cell to cell contact. This effect is mediated by the inhibitory CD200 receptor glycoprotein, which normally engages healthy neurons. Upon neuron withdrawal due to injury or death, the inhibition signal is lost and microglia become activated and neurotoxic (Lyons *et al*., 2007; Dentesano *et al*., 2012).

Microglia activation can sustain neurodegeneration via two distinct mechanisms. A proinflammatory insult, such as with the classic inflammagen lipopolysaccharide, can drive microgliosis to secrete neurotoxic and neuroinflammatory factors causing neurons to degenerate. This is called microglial neurotoxicity. Conversely, in a process known as reactive microgliosis, a neuron damage signal triggers microglia to become activated and

neurotoxic (Hong *et al*., 2007a). Reactive microgliosis is a self-propelling, vicious cycle of neuron injury causing more microglial activation, which triggers further neuron damage, and so forth (Streit *et al.*, 1999; Gao *et al*., 2003b; Huh *et al*., 2003; McGeer *et al*., 2003; Levesque *et al*., 2010).

Originally thought to be short-lived, reactive microgliosis is a self-repeating cycle lasting years after initial trigger is eliminated. Studies of accidental administration of MPTP by humans or its experimental use in primates, report reactive microgliosis endured years after the initial insult (Langston *et al*., 1999; McGeer *et al*., 2003). In 2010, Block *et al* discovered μ-calpain release from injured dopamine neurons precipitated reactive microgliosis. This consequential activation of microglia was marked by the generation of superoxide, which was toxic selectively to dopaminergic cells.

Additional lines of evidence implicating microgliosis in PD come from cytokine studies. Levels of pro-inflammatory cytokines such as interleukin-1beta (IL-1B) and tumour necrosis factor-alpha (TNF-alpha) are elevated in the substantia nigra in PD (Mogi *et al*., 1996). Treating midbrain cultures with neutralizing antibodies to either TNF-α or IL-1β reduced dopaminergic LPS-induced toxicity by approximately 50% (Gayle *et al*., 2002). Furthermore, the pro-apoptotic caspase-11, which is essential for production of IL-1β, has been found to play an important role in dopaminergic neurotoxicity (Arai *et al*., 2004). Additionally, mice deficient in IL-1B converting enzyme are markedly resistant to MPTP neurotoxicity.

The anti-inflammatory minocycline prevents MPTP-induced activation of microglia (Wu *et al.,* 2003). Moreover, it has been shown to prevent DA cell loss by

decreasing IL-1B formation, lowering the activity of NADPH Oxidase, iNOS, and decreasing 3-nitrotyrosine formation.

Lipopolysaccharide induces iNOS, and causes the release of TNF-alpha. It is noteworthy that chronic LPS infusion into the SN causes immediate microgliosis, followed by delayed and gradual loss of SN neurons after a month. As such, early-onset inflammation triggers progressive and selective neurodegeneration of dopamine neurons, which is in line with the nature of cell loss in PD (Ling *et al*., 2006).

Brain trauma and exposure to infectious disease early in life can predispose the SN*pc* to dopamine neuron death (Liu, *et al.* 2003; Bower *et al*, 2003). This is perhaps why the famous boxer Muhammad Ali developed early-onset PD (Brey *et al*., 2006; Matthews *et al*., 2006). It may also be the reason behind NFL football players having a higher likelihood of getting neurodegenerative diseases (Gavett *et al*, 2011).

Robust microglial activation with enhanced neurodegeneration has been observed in animal as well as many in vitro models of PD, including MPTP (Kurkowska-Jastrzebska *et al*., 1999; Wu *et al*., 2002), 6-OHDA (Cicchetti *et al*., 2002), rotenone (Gao *et al*., 2002a), and LPS (Levi *et al*., 1998).

## Interferon-gamma (IFN-γ):

Whereas microglial derived ROS is a well-established cause of DA cell loss, the role of cytokines is not as clear in models of PD. Given their proinflammatory potency and high level of coordination as immune messengers, we set out to study cytokine's regulation of microglial neurotoxicity. In collaboration with Dr. David Grimes, a

neurologist at the Ottawa Hospital, our laboratory measured the levels of several cytokines from the blood of PD patients versus age-matched control subjects. IFN-γ was the highest expressed cytokine in PD patient's blood, significantly more than all other cytokines examined, piquing our research interest (Mount *et al*, 2007). Little was known about its involvement in the CNS, and far less about its role in DA cell loss. In fact, no previous reports showed IFN-γ production in the central nervous system. Given the blood brain barrier's tight regulation, it was not clear how elevated levels of IFN-γ in the blood correlate with its activity in the brain. Moreover, IFN-γ's receptor is ubiquitously expressed, rendering it difficult to delineate how its signaling pathways may be involved in DA neuron death.

The interferon-gamma cytokine is the only member of the type II class of interferons (Ray *et al*, 1982). It is 143 amino acids long and has a monomer core is made up of six alpha-helices, and the C-terminal region has an extended unfolded sequence (Vanhaverbeke *et al*, 2004; Thiel *et al*, 2000; Ealick *et al*, 2001). The biologically active form is dimerized, and functions are mediated through the heterodimeric engagement of interferon-gamma receptor 1 and interferon-gamma receptor 2 (Ray *et al*, 1982). Consequentially, the JAK-STAT pathway is activated, modulating transcription of 30 genes. Interferon-gamma alternatively can bind glycosaminoglycan heparin sulfate to inhibit its biological activity (Sadir *et al*, 1998).

Interferon-gamma is critical for the innate and adaptive immune system. It is produced primarily by natural killer cells, natural killer T cells, CD4 Th1, CD8 cytotoxicity T lymphocytes, myeloid cells, dendritic cells, and macrophages (Schoenborn *et al*, 2007; Thiel *et al*, 2000). IFN-γ's immunoregulatory properties include increasing

the antimicrobial, antiviral, and tumoricidal activity of monocytes, macrophages, neutrophils, and natural killer cells (Schroder *et al*, 2004). IFN-γ toxicity is increased in iron loaded cells (Zhang *et al*., 2005), such as DA neurons (Chinta *et al*., 2005). Abnormal interferon-gamma levels are linked to autoinflammatory and autoimmune diseases. Additionally, genetic mutations of IFN-gamma can increase the likelihood of developing PD (Simunovic *et al*., 2009).

Even though IFN-γ was never shown to be produced in the central nervous system, we hypothesized under inflammatory conditions it can be produced by microglia, which is technically a macrophage. Moreover, being such a powerful microglial activator, we predicted IFN-γ will act in an autocrine manner to regulate microglia neurotoxicity. Our research objective was to highlight IFN-γ's mechanistic involvement in a rotenone-induced model of DA neuron death.

## Coculture Model of Neuroinflammation:

We chose a rotenone based model of neuroinflammation, to drive microglial production of the proinflammatory cytokine. Our intentions for choosing an *in vitro* coculture system, whereby purified microglia are added to neuron-enriched midbrain cells is to examine the mechanism of microglia mediated dopaminergic neurotoxicity, with the capability of isolating and focussing on the IFN-γ receptor from either microglia or dopamine neurons separately. Highlighting the importance of neuronal versus microglial IFN- γ receptors shed light on its mechanistic involvement in DA cell death.

Secondly, rotenone's well documented effects as a DA neurotoxin and inflammatory pesticide make it the more suitable toxin to employ compared to LPS which elicits broad generalized toxic effects. We also argue rotenone is better at eliciting a neuroinflammatory model than MPTP, which does not directly activate microglia. Note the DA transporter is responsible for bringing MPP+ into cells, and it is not possessed by microglia. In our coculture model we determined a concentration of rotenone that exerts selective dopaminergic toxicity via microglia activation, which was favourable to assess an inflammatory reaction (Mount *et al*, 2007). Moreover, we assess dopamine neuron survival in different experiments that interfere with IFN-γ signaling.

Microglial derived ROS and TNF-alpha have previously been reported in inflammatory models of DA cell death (Qin *et al*., 2004), rendering our *in vitro* system a unique, powerful tool in analysis of the neuroinflammatory attack on DA neurons, and sheds light on an important proinflammatory cytokine that was not well understood in the context of PD.

## The Adaptive Immune Response:

After exploring IFN-γ in an isolated *in vitro* co-culture system, we chose to broaden our scope of the immune system by studying the full response of the adaptive immune system to MPTP-induced injury, using a specialized *in vivo* mouse model. Whereas the innate neuroinflammatory reactions have been characterized, the adaptive immune response remains unclear (Chen *et al.,* 2005; Wahner *et al.,* 2007; Nagatsu *et al.,* 2000; Czlonkowska *et al.,* 2002; Whitton *et al.,* 2007). Evidence obtained from post-

mortem PD brains and experimental animal models suggests adaptive immunity is involved in the pathogenesis of PD (Theodore *et al*., 2008; Brochard *et al*., 2009; Kannarkat *et al*., 2013; Papachroni *et al*., 2007). However, early findings were disjointed, and unable to recapitulate the entire cascade of the adaptive immune events that elicit an antibody response to dopaminergic antigens.

IFN-γ is more than a potent proinflammatory cytokine. It also primes the adaptive immune system by enhancing Th1 cell expansion, potentiating secretion of antibodies by B cells, upregulating the expression of Fc receptor, and MHC class I and II on antigen presenting cells (Schoenborn *et al*, 2007). All these features form part of the adaptive immune system.

In brief, adaptive immunity provides the ability to recognize, remember, and generate immunity against specific antigens. It commences with the presentation of an antigen, on macrophages, dendritic cells, or B cells – the three antigen presenting cells. Microglia are the biggest antigen presenting cells in the central nervous system. After engulfing pathogens, debris and dying cells, they digest and display their peptides on major histocompatibility complex class II (MHC II). If the immune system interprets a peptide to be antigenic (not 'self'), it will launch an immunological attack to get rid of any cell displaying the antigen. MHC class I molecules display digested cytolosic protiens only to cytotoxic T cells, and therefore do not participate in an antibody immune response.

A peptide is deemed antigenic if it engages a specific T cell receptor on MHC class II. Subsequently, CD80/CD86 receptors on the antigen presenting cell must bind CD28 receptors on T cells. It is worth noting that astroglia do not express CD80/CD86,

and therefore do not act in antigen presentation. Specific cytokines, known as lymphokines, are secreted by the antigen presenting cells instructing the naïve CD4 T cell to mature into a specific T cell (Waldmann, 2006; Murphy *et al*., 2002)). The T cell consequently undergoes clonal expansion, and secretes cytokines that bind specific B cell receptors (Guyton *et al*, 2006). These B cells become activated, developing in plasma B cells and memory cells, which produce antibodies with high affinity to the antigen.

Antibodies destroy cells displaying antigens using three distinct mechanisms. They can neutralize the antigen and interfere with its normal intracellular trafficking. They can also recruit the complement system. Made up of over 20 proteins, the complement system perforate holes in the membrane of cells tagged by antibodies, causing them to swell and burst. Additionally, antibodies can tag the cell for phagocytosis or cytotoxicity. In a process known as opsonization, antibodies bound to the antigen displaying cell engage immune cell's Fc receptors, and thereby trigger antibody-mediated phagocytosis. Alternatively, the engagement of antibodies to Fc receptors can cause antibody-dependent cell-mediated cytotoxicity to get rid of the antigen.

The central nervous system is immunosensitive, possessing no lymphatic system and low MHC expression (Janeway *et al*, 2005). In fact, the brain was once thought to be an immune privileged organ, due to the tightly regulated blood brain barrier that is not permeable to lymphocytes under normal conditions (Ziv *et al*, 2006). However, during inflammation the perivascular space develops, and lymphocytes are capable of crossing all 3 layers of the blood brain barrier to infiltrate the brain. To do this, activated T cells

must undergo adhesion, attraction, invasion, and reactivation – a highly orchestrated chain of events with the macrophages and dendritic cells of the perivascular space.

Animals treated with DA neurotoxins have demonstrated blood-brain-barrier disruptions (Monahan *et al.,* 2008). No models of PD have documented the adaptive immune response in its entirety, instead fragments of its different pathways have been observed to participate in DA cell death (Han *et al*., 2012; He *et al*., 2002; Orr *et al*., 2005; Chen *et al*., 1998; Carvey *et al*., 1991). This underscores the experimental difficulty and time sensitive nature of establishing such models. Nonetheless, these experimental obstacles have not stopped countless researchers from inching closer.

Various neurodegenerative models, including MPTP intoxication and traumatic brain injury, have been shown to activate the adaptive immune system. Recently, Brochard *et al* found helper T cells in the SN*pc* of postmortem PD brains. Likewise, after injecting mice with MPTP, Kurkowska-Jastrzebska *et al* (1999a) observed infiltration of T cells into the SN*pc* and striatum, as well as an increase in microglial MHC class II antigen expression.

Furthermore, antibodies to dopamine neuron have been detected. Carvey *et al* (1991) discovered an antibody in the cerebral spinal fluid of PD patients that reacted immunocytochemically with DA neurons of the SN. It was detected in 78% of patients with clinical PD, versus 3% of control patients. Scientists are attempting to employ these antibodies as diagnostic markers for PD progression.

Given that PD is best managed when diagnosed early, there is an impetus to identify immune biomarkers (Sharma *et al*., 2013). Such warnings signs permit medical

intervention at an early stage when most dopamine neurons are still present. Immune biomarkers can facilitate an early diagnosis and buy time and therapeutic intervention for the remaining live DA cells in the SN*pc* to stave off a neurotoxic and inflammatory environment (Sharma *et al*., 2013). Effective biomarkers could therefore preserve the SN*pc* and prevent physical symptoms from ever arising.

Immune biomarkers are an attractive candidate for biomarkers because they arise well in advance of clinical signs of DA neurodegeneration, and can often be detected by a simple blood test or sampling of cerebrospinal fluid (Sharma *et al*., 2013; Mosley *et al*., 2012). Cytokine levels, such as IL-1beta, IL-6, and TNF-alpha, are increased in serum and cerebrospinal fluid of PD patients (Hirsch *et al*., 2009). We propose IFN-γ as a biomarker of PD, given it was expressed in high amounts in the serum of PD patients, compared to age-matched control patients (Mount *et al*., 2007). DA neuron and alpha-synuclein autoantibodies have been proposed biomarkers of PD for two decades (Papachroni *et al*., 2007; Han *et al*., 2012; Kunas *et al*., 1995; Carvey *et al*., 1991). Additional suggested biomarkers include lymphocyte brain infiltration (Brochard *et al*., 2009), blood brain barrier disruption (Kortekaas *et al*., 2005), and Fcγ receptor levels (He *et al*., 2002; Lira *et al*., 2011).

In 2008, Theodore *et al* (2008) overexpressed alpha-synuclein in mice, and found T and B cells infiltrates in the SN*pc* remained present for several months. Moreover, they discovered IgG expression in the SN*pc* and upregulation of the Fc receptor. MPTP administration has also been shown to increase the expression of Fc receptors (Kurkowska-Jastrzebska *et al*, 1999a; Kurkowska-Jastrzebska *et al*, 1999b; Hunot *et al*,

1999). Interestingly, the expression of CD23, a type of Fc receptor, was detected in the SN and striatum of PD patients but not in control patients (Hunot *et al.,* 1999).

Fc receptors are found in a variety of immune cells, including microglia, and play a critical role in the adaptive immune response. Upon engaging antibodies in the central nervous system, Fc receptors will activate microglia and stimulate phagocytosis or cytotoxicity. In this manner, we predict Fc receptors are important participants in dopaminergic cell death in PD, yet also bearing in mind that antibodies could mediate damage in different ways.

The initial data supporting the role an antibody response in PD models came from Dr. Stanley Appel's research. After isolating IgGs from PD patients and injecting them into the SN*pc* of mice, he discovered they bound to dopamine neurons, causing microglia activation and dopaminergic neurodegeneration. Fc receptors mediated this effect since mice deficient in the Fc receptors exhibited neuroprotection and less inflammation (He *et al.,* 2002). Given PD IgGs show preferential association with dopaminergic neurons of the SN*pc*, it is postulated that significantly modified dopaminergic antigens or neopeptides generated an antibody response.

Neopeptides may arise from dopaminergic neuron's inherent vulnerability to oxidative damage, which is attributed from having a low antioxidant capacity, and high concentration of oxidation-prone dopamine and lipids (Jenner *et al.,* 1998; Greenamyre *et al.,* 1999). DA neurons have high iron levels, and iron-loaded cells are more sensitive to IFN-gamma toxicity. Furthermore, the most abundant area of microglia is in the midbrain. The "neopeptide theory" states that with ageing and long-term exposure to

oxidative stress, DA neurons develop modification recognized as neopeptides or antigens by the immune system.

Aggregating excessively in Lewy bodies, a good candidate for a protein incurring sufficient modifications to become antigenic is alpha-synuclein. In a 2008 study, Benner *et al* (2008) reported MPTP treatment causes nitrosine-modified alpha-synuclein accumulation in cervical lymph nodes. Consequently, mice produce antibodies to native and nitrated alpha-synuclein. This insightful research demonstrates how dopaminergic injury can elicit an adaptive immune response to exacerbate injury and death. In this context, as an immunological target alpha-synuclein becomes yet even more culpable for progressive death of DA neurons. The scientific community makes a strong argument for this.

The ability for nitrosine-modified alpha-synuclein to bypass immunological barriers and alert T cells has been previously reported (Birnboim *et al.,* 2003). In squirrel monkeys, a single injection of MPTP was sufficient to cause a buildup of alpha-synuclein in DA neurons (McCormack *et al.,* 2008). Consequentially, antibodies against nitrated and phosphorylated alpha-synuclein were discovered to bind midbrain DA neurons. Likewise, researchers using an overexpression model of alpha-synuclein detected an increase in B cells, Fc receptors and IgG expression in the SN. This adaptive immunological reaction was followed by dopamine neuron death (Theodore *et al*, 2008).

We hypothesize the adaptive immune system becomes involved in response to ageing, possibly after DA neurons begin showing ubiquitin-protesome deficits. An unwanted buildup of proteins, particularly alpha-synuclein, combined with an increase in

oxidative load, may elicit protein modifications in DA neurons to invoke an antigenic response.

The ability of plasma or memory cells to remember antigens, delivering a faster and stronger immunological attack would speed up degeneration of dopamine neurons tagged with modified alpha-synuclein. Healthy DA neurons that do not develop antigenic neopeptides can still succumb to antibody-dependent cell-mediated cytotoxicity, which activates iNOS and cytokine production, by virtue of being in close proximity to injured or dying DA neurons that are targeted for displaying antigenic modifications.

The adaptive immune system can take approximately a week to mount a response. In order to better observe an adaptive immunity in PD models, a suitable dopamine neuron injury paradigm must be tailored to allow time for dopaminergic modifications to arise and adaptive immune response to fully develop. We aimed at recapitulating the adaptive response similarly observed in the aforementioned studies, by invoking low-grade damage to dopaminergic cells. Employing low concentrations of the neurotoxin MPTP, protracted over an extended period, is a novel approach to elicit low-grade dopaminergic injury, allowing for the full adaptive immune system. In this way, we believe our dopamine neuron death paradigm is best suited to study how dopaminergic injury stimulates adaptive immunity.

Brochard *et al* (2009) observed T cell infiltration in the SN*pc* and DA cell death, as early as 2 days after MPTP treatment. However they employed an acute death paradigm that is not ideal for studying the adaptive immune response. Their neurotoxic paradigm was not a low dose, protracted regiment like we used.

Traditional acute MPTP paradigms do not reflect PD pathogenesis as effectively, given that rapid onset and progression of neurodegeneration. We therefore subjected wild-type mice to biweekly intraperitoneal injections of MPTP (10mg/kg) or saline over 4 weeks. On the fifth week after the start of injections, the mice were sacrificed and their brains sectioned to examine for signs of DA cell loss.

The protracted MPTP regimen we developed has never been done, and is better suited for studying adaptive immunity, both in that a lower more frequent dose is given, over a longer time frame that allows for the full activation of an antibody response to target dopaminergic cells displaying sufficiently modified proteins.

We predict our protracted, low dose MPTP paradigm is best tailored to elicit dopaminergic injury and antigenic modifications capable of being phagocytosed and displayed on microglial major histocompatibility complexes. This antigen presentation will drive the humoral response to target and destroy a significant amount of DA neurons in the SN*pc*. A midpoint group of mice were subjected to the protracted MPTP paradigm but sacrificed at day 14. Assessing DA neuron death in this group indicate if degeneration is occurring early or late in the paradigm. Given a considerable amount of time is required to elicit dopaminergic modifications and the adaptive immune response, we hypothesis DA cell death will be low in this group of mice that are sacrificed 14 days after the start of MPTP administration.

To examine the participation of the adaptive immune response in DA cell death, we subjected two types of mutant mice to our specialized, protracted MPTP paradigm. Rag2 -/-mice have a disruption in the recombination activating gene 2. This gene produces an enzyme critical in the generation of T and B cell receptors, and therefore

these mice are devoid of T and B cells and are unable to produce antibodies. If adaptive immunity is participating in dopaminergic neuro death, we anticipate significant neuroprotection in the Rag 2 deficient mice.

Additionally, we employed Fcγ receptor knockout mice in our *in vivo* mouse model of PD.The function of Fc receptors differs among its subtypes. Fcγ receptors bind IgGs, the most common class of antibody, whereas Fc epsilon receptors bind IgEs, and Fc alpha receptors bind IgAs. The molecular structure of each Fc receptor governs its binding affinity (Indik *et al*., 1995). Low affinity receptors prevent binding without the antigens being present, and as such lower the risk of immune activation in the absence of infection.

Fc receptors bind the Fc stalk of antibodies (Swanson *et al*., 2004), and in doing so stimulates activation of the cell carrying the Fc receptor (Raghavan *et al*., 1996). Upon engaging antibodies, Fc receptors activate their respective phagocytic or cytotoxic cells to kill microbes, or infected cells via antibody-dependent phagocytosis or antibody-dependent cell –mediated cytotoxicity (Sun, 2003). A phagocytic cell undergoes an active process of binding and releasing Fc stalk/Fc receptor complex in order to completely engulf a pathogen (Joshi *et al*., 2006). The most important receptors involved in phagocytosis are the Fcγ receptors (Swanson *et al.,* 2004; Fridman *et al*., 1991). Members of the Fcγ receptor family include Fcγ receptor I, Fcγ receptor IIA, Fcγ receptor IIB, Fcγ receptor IIIA, and Fcγ receptor IIIB.

The Fcγ receptor deficient mice employed in our experiments lack the γ chain subunit of the Fcγ receptor I, Fcγ receptor III, and Fc epsilon receptor I (Takai *et al*., 1994). This γ accessory chain possesses an ITAM motif required for signal transduction

and cellular activation; it is also responsible for the cell surface expression of these receptors in macrophages, mast cells, NK cells, neutrophils and basophils, rendering them functionally impaired in our knockout mice (Nimmerjahn *et al*., 2006; Takai *et al*., 1994). Accordingly, we evaluated the absence of IgG and IgE triggered effector pathways (Takai *et al*., 1994) in our mouse model of PD.We anticipated a reduction of DA cell death in our Fcγ receptor deficient mice treated with MPTP, compared to the wild-type control mice. Antibodies can promote degeneration independently of Fc receptor stimulation; therefore we expect Fcγ receptor knockout mice to exhibit more DA cell death than the Rag 2 deficient mice.

To compare mechanisms and temporal degenerative profile of DA neurons, we conducted an acute MPTP dosing paradigm. In this paradigm, higher concentrations of MPTP are given over a shorter time frame. Expecting more direct MPTP-induced neurotoxicity with the acute paradigm, we predict the immune system participates far less than with the protracted dosing model. This is because the time for immune activation is drastically shortened. Also in the acute paradigm, the neurotoxin dosages are much higher, which probably elicit profound cell death as opposed to dopaminergic injury that allows immune system recognition of modified neopeptides. As such, we do not anticipate Rag 2 deficient and Fcγ receptor deficient mice to show significant protect against acute MPTP treatment.

Our assessment of the SN*pc* is corroborated with striatal immunocytochemical analysis. Since DA neurons degenerate in a retrograde manner, the loss of dopaminergic innervation should be more evident in the striatum.

Lastly, the nigrostriatal axis is functionally assessed with behavioural studies of the motor system. We anticipate that a significant loss of DA neurons in our protracted MPTP paradigm will translate into motor movement deficits. Both the adaptive immune system mutant mice, we predict will confer histological and behavioural protection against MPTP. Behavioural examinations including the pole test, micromax and water stress test, were given to the mice each week. These different motor tests are designed to examine the motor movement of mice under different conditions.

The micromax is a cage where mice are placed for 24 hours, and every time they move an infrared beam is broken and recorded by a computer. The water stress is accomplished by dropping mice in a 4-liter beaker of water and letting them swim for 1 minute. The mice subsequently are placed in the micromax and their movements are recorded for 2 hours. The purpose of stressing the mice is to reveal any underlying motor movement impairments that may not arise under normal conditions. Considering in humans the majority of the DA cells in the SN*pc* die before physical symptoms precipitate, we do not expect a significant decline in motor function to be apparent in mice with a modest SN*pc* lesion.

In the pole test, mice are placed near the top of a pole, and because mice have the tendency of avoiding heights, their turn latency and descend to the ground is a measure of their motor movement capabilities. This behavioural experiment is strenuous, physically demanding, and requires significantly more motor coordination than the other two tests. In this context, a smaller basal ganglia lesion would be most evident in the pole test, compared to the other two motor exams.

In our novel experimental paradigm, protracted MPTP administration will indicate whether damaged DA neurons can invoke the adaptive immune response to produce IgGs against them and exacerbate neurodegeneration of the nigrostriatal tract. Furthermore, our study will determine if Fcγ receptors are an important part of the way the adaptive immune system degenerates the SN*pc* – an important question that has not been answered.

We are the first to test the Fcγ receptor's involvement using a specialized protracted MPTP mouse model of PD. Our research widens the current understanding of humoral responses affecting DA cells, and provides novel therapeutic targets to safeguard the nigrostriatal tract.

# Chapter 2

# Involvement of Interferon-γ in Microglial-Mediated Loss of Dopaminergic Neurons

Journal of Neuroscience. 2007 21; 27(12):3328-37. Neurobiology of Disease

Matthew P. Mount[1], **Arman Lira[1]**, David Grimes[1], Patrice D. Smith[1], Sylvie Faucher[2], Ruth Slack[1], Hymie Anisman[3], Shawn Hayley[1],[3],* and David S. Park[1],*

± Author Affiliations

1. [1]*Ottawa Health Research Institute, Neuroscience Group, Ottawa, Ontario, Canada K1H 8M5,*
2. [2]*National Human Immunodeficiency Virus Immunology Laboratory, Centre for Infectious Disease Prevention and Control, Ottawa, Ontario, Canada K1A 0K9, and*
3. [3]*Institute of Neuroscience, Carleton University, Ottawa, Ontario, Canada K1S 5B6*

± Author Notes

S. Hayley's present address: Institute of Neuroscience, Carleton University, Ottawa, Ontario, Canada K1S 5B6.

## Statement of author contribution

All the *in vitro* experiments were conducted by Arman Lira, including the immunocytochemistry, RT PCR, data analysis and figure preparation. The *in vivo* work was carried out predominantly by Matthew Mount. Both he and Arman Lira wrote the manuscript with the assistance of Dr. David Park.

# Abstract

Growing evidence implicates microglia in the loss of dopaminergic neurons in Parkinson's disease (PD). However, factors mediating microglial activation in PD are poorly understood. Proinflammatory cytokines, such as interferon-γ (IFN-γ), orchestrate the actions of microglia. We report here that PD patients express significantly elevated levels of IFN-γ in their blood plasma. After this initial finding, we found that *IFN*-γ-deficient mice displayed attenuated 1-methyl-4-phenyl-1,2,3,6-tetrahydropyridine (MPTP)-induced substantia nigra pars compacta dopaminergic cell loss along with reduced loss of striatal tyrosine hydroxylase and dopamine transporter fiber density. MPTP-induced depletion of striatal dopamine and its metabolite DOPAC (3,4-dihydroxyphenylacetic acid), as well as ΔFosB, a marker of postsynaptic dysfunction, were also attenuated in these knock-out mice. Consistent with the role for IFN-γ in microglial activation, MPTP-induced morphological activation of microglia was abrogated compared with wild-type mice. To examine more mechanistically the role of IFN-γ in microglial activation, we evaluated the interactions between microglia and dopaminergic neurons in an *in vitro* mixed microglia/midbrain neuron rotenone-induced death paradigm. In this *in vitro* paradigm, dopaminergic neurons are selectively damaged by rotenone. Exogenous IFN-γ ligand alone and without rotenone resulted in dopaminergic cell loss, but only in the presence of microglia. The addition of an IFN-γ neutralizing antibody attenuated neuronal loss as a result of rotenone treatment. The presence of only wild-type microglia and not those deficient in IFN-γ receptor elicited significant dopaminergic cell loss when exposed to rotenone. Neurons deficient in IFN-γ receptor, however, did not display increased resistance to death. Finally, levels of IFN-γ

message increased in microglia in response to rotenone. Together, these data suggest that IFN-γ participates in death of dopaminergic neurons by regulating microglial activity.

# Introduction

Parkinson's disease (PD) is a neurodegenerative condition characterized by progressive motor deficits including tremor, bradykinesia, rigidity, and postural instabilities (Przedborski et al., 2001). Many of the cardinal symptoms of PD are attributed to depletion of dopamine (DA) in the brain resulting from the loss of dopaminergic neurons of the substantia nigra pars compacta (SNc) (Smeyne and Jackson-Lewis, 2005). Current therapies, such as L-DOPA (L-3,4-dihydroxyphenylalanine), are mainly directed toward replacing DA levels in the brain and, as such, provide only symptomatic relief. These drugs do not modify the progressive neurodegenerative cell loss process associated with PD that, in many cases, results in debilitating side effects (Kostic et al., 1991). Attenuation of the underlying degeneration in PD may provide opportunities for more effective therapeutic intervention. However, the mechanism(s) controlling dopaminergic loss is not completely clear.

Administration of 1-methyl-4-phenyl-1,2,3,6-tetrahydropyridine (MPTP) produces a syndrome in mice and primates resembling that of clinical PD (Langston et al., 2000; Fukuda, 2001). Similar to the histopathological features of PD, MPTP treatment provokes a selective loss of dopaminergic neurons in the SNc coupled with a profound reduction in striatal DA with little alteration in other monoamine neurotransmitter systems (Smeyne and Jackson-Lewis, 2005). This model is frequently used to examine dopaminergic cell loss in an *in vivo* setting.

A common characteristic of PD and the MPTP model of degeneration is increased microglial activation (Czlonkowska et al., 1996; Gao et al., 2002b; Barcia et al., 2004).

Several lines of evidence support the importance of this activation in the deterioration of dopaminergic neurons. The use of the pharmacological anti-inflammatory agent minocycline attenuates activation of microglia as well as MPTP-induced dopaminergic cell loss (Du et al., 2001; Wu et al., 2002). Direct administration of lipopolysaccharide (LPS) induces microgliosis and has been correlated with the loss of dopaminergic neurons *in vivo* (Arai et al., 2004; De Pablos et al., 2005). Activation of this innate immunity has also been implicated in neurodegeneration with the specific triggering of Toll-like receptor-4-dependent pathways (Lehnardt et al., 2003). Furthermore, low concentrations of rotenone require microglia to induce death of dopaminergic neurons (Gao et al., 2002a). One potential mechanism underlying the pro-death effects of microglia on dopaminergic neurons involves increased oxidative insult. For example, microglia are known to activate proteins that increase oxidative load, including NADPH oxidase and inducible nitric oxide synthase (iNOS) (Almer et al., 1999; Liberatore et al., 1999; Wu et al., 2003). Indeed, mice deficient in both of these signals display attenuated MPTP-induced loss of dopaminergic neurons. Although this evidence implicates microglial activation, the functional relevance of microgliosis is still controversial. Specifically, it is unclear, particularly *in vivo*, whether microglial activation is causative or correlative to dopaminergic neuron loss. In addition, other types of glial activation (i.e., astrocytes) might also be important in dopaminergic cell death (Suzumura et al., 2006). Accordingly, questions of (1) whether microglia may only be a secondary effect to initial dopaminergic degeneration and (2) how important microglial activation may be to dopaminergic degeneration *in vivo* remain. For example, agents such as minocycline may protect by means other than microglial activation (Wu et al., 2002; Yang et al., 2003).

Inflammatory mediators are central to microglial activation (McGeer and McGeer, 2002). However, the required nature of the inflammatory response, as it relates to microglia and dopaminergic death, is not completely clear. Various cytokines including interleukin (IL)-1β, IL-2, IL-4, IL-6, transforming growth factor-β, and tumor necrosis factor-α (TNF-α) are increased in the brains of PD patients (Nagatsu et al., 2000). Likewise, cDNA microarray revealed that MPTP-treated mice displayed alterations in genes for numerous proinflammatory cytokines (IL-1, IL-6, and TNF-α) as well as the anti-inflammatory cytokine IL-10 (Mandel et al., 2000). However, the function of these cytokines in dopaminergic neuronal loss is less clear.

There is recent evidence that another critical inflammatory cytokine, interferon-γ (IFN-γ), may be important in PD. IFN-γ is believed to play an important role in early immunological responses to viral and tumor insults, as well as slow developing adaptive responses to infections (Mamane et al., 1999). In the brain, IFN-γ is produced by microglia (De Simone et al., 1998) and can be a strong activator of microglia *in vitro* (Badie et al., 2000). IFN-γ, through the Janus kinase/signal transducers and activators of transcription-1 (Jak/STAT1) pathway, mediates the induction of iNOS (Delgado, 2003). Recently, Ciesielska et al. (2003) have shown IFN-γ transcripts increase after MPTP treatment in mice. Evidence for a relationship between IFN-γ and PD is suggested by the fact that allelic differences between early- and late-onset PD patients were reported for the *IFN*-γ gene (Mizuta et al., 2001). However, to date, there is no clear evidence to indicate that IFN-γ is central to dopaminergic cell loss. Consequently, we examined whether IFN-γ may be required in the loss of dopaminergic neurons in both *in vivo* and *in vitro* models of PD. We present evidence for the importance of IFN-γ in the death of

dopaminergic neurons induced by MPTP (*in vivo*) and rotenone (*in vitro*). We also provide evidence that IFN-γ can act through microglia to promote dopaminergic loss and suggest that this may be critical in the pathogenesis of PD.

# Materials and Methods

### Patient IFN-γ plasma analysis.

Human plasma was examined using a multiplex bead-based immunoassaying system as described previously (Hulse et al., 2004). The patients' sera were diluted fourfold in PBS containing 1% BSA and 0.05% $NaN_3$. Fifty microliters of each sample were incubated for 2 h at room temperature with the antibody-coupled beads in a filter-bottomed 96-well plate (Nunc, Naperville, IL; VWR International, West Chester, PA). The biotinylated anti-cytokine antibody conjugate (1:500) was added to the well and incubated for 1 h at room temperature. Bound antibodies were revealed with a streptavidin–phycoerythrin conjugate. After washing and resuspension in 2% paraformaldehyde in PBS, the beads were analyzed on a luminex-100 system (Luminex, Austin, TX) equipped with Luminex Data Collector software, version 1.7, using the median fluorescence intensity as the read out. Standard curves were established using recombinant IFN-γ, and sample IFN-γ concentrations were derived from the linear portion of the curve. Patient diagnosis was assessed by David Grimes after clinical history and examination. Blood samples from 13 PD patients and 7 disease control patients were analyzed in this study (supplemental Table 1, available at www.jneurosci.org as supplemental material). The Ottawa Hospital Research Ethics Board sanctioned approval for this study. Samples were drawn and immediately centrifuged with serum drawn off and frozen. Patient confidentiality was maintained using number coding, and samples were blinded to condition. The mean age of the PD patients was 66 years (range, 44–77 years), the duration of the disease was 7.5 ± 1.3 years, and all patients had been medicated as specified (supplemental Table 1,

available at www.jneurosci.org as supplemental material). The mean age of the disease control patients was 66 years (range, 61–76 years).

**Experimental animals.**

Male *IFN*-γ −/− knock-out (KO), *IFN*-γ receptor −/− KO, and +/+ wild-type (WT) mice (all on a C57BK/6J background; 12 generations of KO mice) were obtained from The Jackson Laboratory (Bar Harbor, ME). The animals were maintained on a 12 h light/dark cycle with lights on at 6:00 A.M., the room temperature was maintained at 21°C, and the mice were permitted an *ad libitum* diet of Ralston Purina (St. Louis, MO) mouse chow. For the *in vivo* experiments, two separate groups of animals were analyzed. In the first, *IFN*-γ KO and WT mice were treated with both MPTP and saline. To corroborate data from these findings, the *IFN*-γ KO and WT mice were interbred for two generations to produce littermate controls, which were then used in a second set of experiments. All experimental procedures were approved by the University of Ottawa Committee for Animal Care and met the guidelines set out by the Canadian Council on Animal Care.

**MPTP administration.**

*N*-methyl-4-phenyl-1,2,3,6-tetrahydropyridine (MPTP-HCl; 25 mg/kg, i.p., measured as free base; Sigma, St. Louis, MO) was administered to mice (8–10 weeks old) intraperitoneally once per day for 5 consecutive days (Crocker et al., 2003). Mice used as controls received an equivalent volume of saline (0.9%). Mice were killed 14 d after initial MPTP/saline treatment.

**Immunohistochemistry.**

After overnight postfixation in 4% paraformaldehyde, brains were cryoprotected in 10% sucrose before cryosectioning into 14 or 40 μm (used for stereology) free-floating sections, obtained as described previously (Smith et al., 2003). Immunostaining was performed as described previously using mouse anti-tyrosine hydroxylase (TH; 1:10,000; ImmunoStar, Hudson, WI), rat anti-DA transporter (DAT; 1:2000; Millipore, Bedford, MA), rat anti-CD11b (1:200; Serotec, Oxford, UK), or rabbit anti-ΔFosB (1:1000; Santa Cruz Biotechnology, Santa Cruz, CA). Primary antibodies were visualized using diaminobenzidine, as described previously (Crocker et al., 2003).

**Assessment of neuronal survival.**

Dopaminergic neurons in the SNc of treated mice were assessed for survival using the dopaminergic cell marker TH. Assessment of survival was performed using two different counting methodologies. In the first set of animals, dopaminergic neurons in the SNc of WT and *IFN*-γ KO mice were determined by serial section analysis of the total number of TH-positive (TH+) neurons as described previously (Crocker et al., 2003; Smith et al., 2003) at 14 d after initial MPTP treatment. Briefly, midbrain tissue sections were stained for TH. At least two sections were obtained from each animal representing each of five levels from −2.92 to −3.52 relative to bregma. Sections from each level and animal were averaged for the number of TH+ neurons. A total of six to eight animals per group were analyzed. Estimates of total TH+-stained neurons in the SNc were calculated using Abercrombie's correction for the previously stated bregma levels, centering on the central region of the SNc, the medial terminal nucleus (MTN) (Hayley et al., 2004). Adjacent tissue was also stained using anatomical stain, cresyl violet, to validate survival as assessed by TH analysis. These results were subsequently corroborated, by examining a

second group of animals interbred to produce littermate controls, as described above. The SNc region of this second group of animals was analyzed by unbiased stereological estimates. The total number of TH+ neurons in the SNc was obtained by applying optical fractionation (Gundersen et al., 1988) using Stereo Investigator (version 6; MicroBrightField, Williston, VT), as described previously (Rymar et al., 2004). In brief, 40 μm brain sections were examined within the rostal and caudal limits of the SNc (bregma −2.54 to −3.88) (Paxinos and Franklin, 2001). For each brain, six coronal sections were examined. After immunohistochemistry, mounting, defatting, and coverslipping, the mean section thickness, as measured with a *z*-axis microcator, was 16 μm. Sections were analyzed using a 100× lens. Total number of TH+ neurons was determined using the optical fractionator.

**Quantification of striatal immunohistochemistry.**

Quantification of striatal dopaminergic density fiber staining and striatal ΔFosB-positive nuclei were analyzed using Eclipse densitometry analysis (Crocker et al., 2003). In all cases of immunohistochemical quantification, analyses were performed by an individual unaware of the experimental treatments. Each tissue quantified was compared relative to its own nonstained background.

N-*methyl-4-phenylpyridinium ion measurements*. Striatal concentrations of *N*-methyl-4-phenylpyridinium ion ($MPP^+$) were measured 90 min after a single dose of MPTP using HPLC measurements, as described previously (Crocker et al., 2003).

**Neurochemical analyses.**

After decapitation, brains were sectioned into a series of coronal slices using a dissecting block with adjacent slots spaced 2 mm apart. The SNc and striatum were obtained by micropunch using a 1-mm-diameter biopsy needle. Brain punches were taken according to the mouse brain atlas of Paxinos and Franklin (Paxinos and Franklin, 2001; Smith et al., 2003). HPLC analysis was performed 14 d after initial MPTP treatment. Levels of DA and its metabolite 3,4-dihydroxyphenylacetic acid (DOPAC) were determined by HPLC using methods described previously (Seegal et al., 1986; Smith et al., 2003).

**Primary neuron-enriched mesencephalic cultures.**

The entire midbrain, without meninges and blood vessels, was collected from the brains of embryonic day 13.5 (E13.5) mice, as described previously (Liu et al., 2000). The midbrain tissue was removed and subjected to trypsin (T-4549; 1 mg/ml; Sigma) for 25 min at 37°C. After dissociation, the cells were treated with trypsin inhibitor (0.92 mg/ml dissolved in 1 mM HCl; catalog #10137100; Roche, Indianapolis, IN) and DNase (1 mg/ml; catalog #1284-932; Roche) and were counted using a hemacytometer (Bright-Line; Hausser Scientific, Horsham, PA). Midbrain cells were seeded ($5 \times 10^5$ per well) in 24-well culture plates precoated for 1 h with poly-D-lysine (20 μg/ml). Cultures were maintained in 0.5 ml per well of Neurobasal medium supplemented with 2% B27, 1% N2, 416 μM L-glutamine, 41.6 U/ml penicillin, and 41.6 μg/ml streptomycin and kept in a 37°C incubator-humidified atmosphere of 5% $CO_2$ and 95% air.

**Microglia harvest.**

Postnatal day 2–3 mice were used for mixed glia cultures. Brains were dissociated using a tissue grinder kit and plated in minimum essential medium supplemented with 5% heat-

inactivated fetal bovine plasma, 5% heat-inactivated horse plasma, and 0.05 mg/ml gentamycin. Two days later, the medium was replenished, and the culture reached confluency ~8 d later. Confluent mixed-glia cultures were shaken for 5 h at 180 rpm at 37°C to separate microglia from astrocytes. This produces a yield of >94% enriched microglia and is comparable with similar harvesting protocols (Gao et al., 2003a).

**Coculturing.**

Harvested microglia were added ($5 \times 10^4$ per well) to 7-d-old neuron-enriched mesencephalic cultures. The following day, rotenone was added (20–25 nM), and 7 d later the cultures were fixed and stained for TH (1:2500) and Hoescht (0.24 μg/ml; Sigma). TH immunoreactivity was quantified by counting the total number of all live cells (assessed by Hoescht staining) that stained positive for TH. All live cells typically appear intact with uncondensed nuclei, whereas dead cells displayed fragmented with a condensed morphology. Rotenone treatment has been shown previously to diminish the total number of TH+ live cells in this culture model (Gao et al., 2002a). The results were performed in triplicate and show the average total number of live TH-immunoreactive cells per well. This was compared with untreated control wells that were plated identically and obtained from the same neuronal culture preparation as the experimental wells. For neutralizing antibody studies, IFN-γ-neutralizing IgG (rIFN-γ-purified goat IgG; R & D Systems, Minneapolis, MN) or control nonspecific IgG (normal goat IgG; R & D Systems) was added (15 μg/ml) 30 min before rotenone application. In our ligand application studies, IFN-γ ligand (recombinant mouse IFN-y; R & D Systems) was added 24 h after coculturing, and the cultures were fixed 7 d later. IFN-γ receptor KO neurons and microglia were cultured in the same way as WT cells.

**Detection of IFN-γ mRNA using reverse transcription-PCR.**

One day after plating, WT microglia-enriched cultures were treated with rotenone (20 nM) for 0, 1, or 3 d. RNA was extracted using Trizol (Invitrogen, San Diego, CA). After RNA purification and determination of RNA concentration, reverse transcription (RT)-PCR analysis for IFN-γ mRNA was conducted using the following primers: forward, ACT GGC AAA AGG ATG GTG AC; reverse, GAC CTG TGG GTT GTT GAC CT. As an internal control, S12 RNA was amplified using the following primers: forward, GGA AGG CAT AGC TGC TGG; reverse, CCT CGA TGA CAT CCT TGG. Cycle conditions were as follows: 94°C (30 s), 59°C (30 s), and 72°C (1 min). Positive control samples were extracted from CD4+ T-cells after being stimulated in the presence of $T_H1$ (T helper cell 1) cytokines for 6 d. After amplification, the PCR products were run on a 2.25% agarose electrophoretic gel in 1× Tris–acetate–EDTA buffer for 30 min and visualized by ethidium bromide staining. Densitometry analysis revealed an increase in IFN-γ mRNA after exposure with rotenone for 1 and 3 d.

**Statistical analysis.**

All data analyses were performed by using one-way ANOVA, followed by the Newman–Keuls *post hoc* test (unless otherwise stated).

# Results

### Elevated levels of plasma IFN-γ in PD patients

We initially examined the levels of several cytokines [IL-2, IL-4, IL-5, IL-6, IL-10, IL-12, granulocyte-macrophage colony-stimulating factor (GM-CSF), IFN-γ, and TNF-α] by multiplex bead-based immunoassaying analyses in blood plasma from 13 PD patients compared with 7 normal control individuals. As shown in the Figure 1 dot plot, immunoassay analysis revealed a significant elevation of IFN-γ in blood plasma from PD patients over that in control subjects (33.0 ± 4.1% increase; $p < 0.01$), as was revealed previously by Gribova et al. (2003). Other cytokines, including GM-CSF, TNF-α, IL-2, IL-4, and IL-5, were not detectable, whereas no significant differences in IL-6 and IL-10 were detected (supplemental Table 2, available at www.jneurosci.org as supplemental material). Accordingly, combined with results by Ciesielska et al. (2003), displaying elevated IFN-γ transcripts in the SNc of mice treated with MPTP, we hypothesized that IFN-γ may be central to dopaminergic loss occurring in PD and MPTP-induced neurotoxicity. Accordingly, we proceeded to examine whether IFN-γ may be important in an *in vivo* animal model of dopaminergic loss.

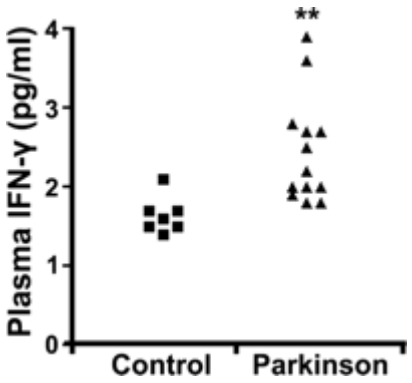

**Figure 1.**

PD patients display elevated IFN-γ plasma levels relative to non-PD patients. Blood plasma from 13 PD and 7 control patients was analyzed by a multiplex bead assay system for several cytokines. Results for IFN-γ concentrations are provided here in dot plot representation (two-tailed *t* test, $^{**}p < 0.01$).

**IFN-γ-deficient mice exhibit attenuated MPTP-induced degeneration of dopaminergic cell bodies in the SNc**

We first assessed dopaminergic neuron survival after saline or MPTP treatment of separate groups of WT and *IFN*-γ KO mice on a C57BK/6J background (Fig. 2*A–C*). No statistical difference in the number of TH+ neurons in the SNc could be detected between saline-treated WT and *IFN*-γ KO mice (Fig. 2*B*). Similarly, no statistical difference in striatal TH or DAT fiber density was detected by immunohistochemistry (Fig. 2*D–G*). DAT is critical for the reuptake of DA and $MPP^+$, the active MPTP metabolite in dopaminergic neurons (Meissner et al., 2003). Finally, no differences in levels of striatal DA or its metabolite DOPAC were detected in these mutant mice under basal conditions (Fig. 3*C*,*D*). After MPTP administration, there was a significant reduction (42%; $p < 0.01$) in TH+ SNc neurons in WT mice (Fig. 2*E*). Interestingly, *IFN*-γ-deficient mice displayed significantly more TH+ cells than WT mice treated with MPTP ($p < 0.05$).

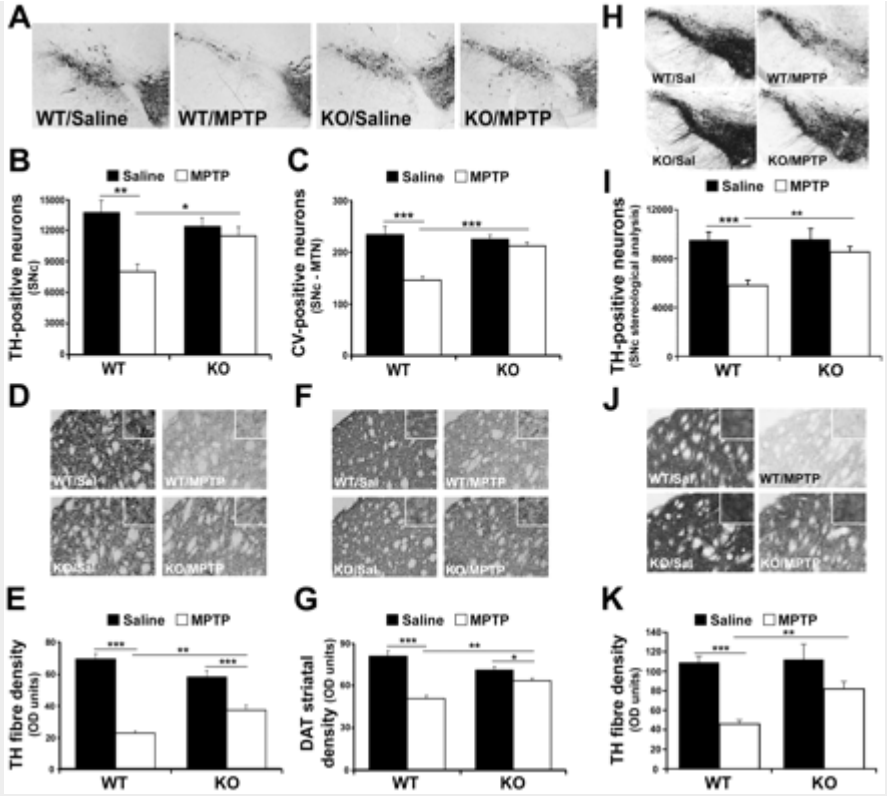


**Figure 2.**

IFN-γ-deficient mice display protection of dopaminergic cell bodies and striatal terminals of MPTP-induced degeneration of SNc dopaminergic neurons. ***A***, Representative photomicrographs illustrating TH immunoreactivity in the ventral midbrain SNc of the indicated non-littermate treatment groups, as indicated in Materials and Methods. ***B***, Quantification of TH+ neurons using Abercrombie correction, as described in Materials and Methods. ***C***, Quantification of cresyl violet-stained cells of the SNc (MTN level). ***D***, Representative photomicrographs of striatal sections stained with TH from the animal groups as described in ***A***. Magnified images are included in the insets of ***D–J***. ***E***, Quantification of optical density of TH striatal fibers. ***F***, Representative photomicrographs illustrating DAT immunoreactivity in the striatum of indicated treatment groups as in ***A***. ***G***, Quantification of optical density of striatal DAT-stained

fiber density. ***H***, Representative photomicrographs illustrating TH immunoreactivity in the SNc of the indicated littermate treatment animal groups. Staining is more intense here than in ***A*** because of increased section thickness required for stereological analyses. ***I***, Quantification of TH+ neurons, in littermate animals by stereology, as described in Materials and Methods. ***J***, Representative photomicrographs of striatal TH fiber density of indicated littermate treatment groups. ***K***, Quantification of OD of striatal TH-stained fiber density of indicated littermates. Error bars represent mean ± SEM. ANOVA, *$p <$ 0.05, **$p < 0.01$, ***$p < 0.001$; $n = 6–8$ animals per group. OD, Optical density; Sal, saline.

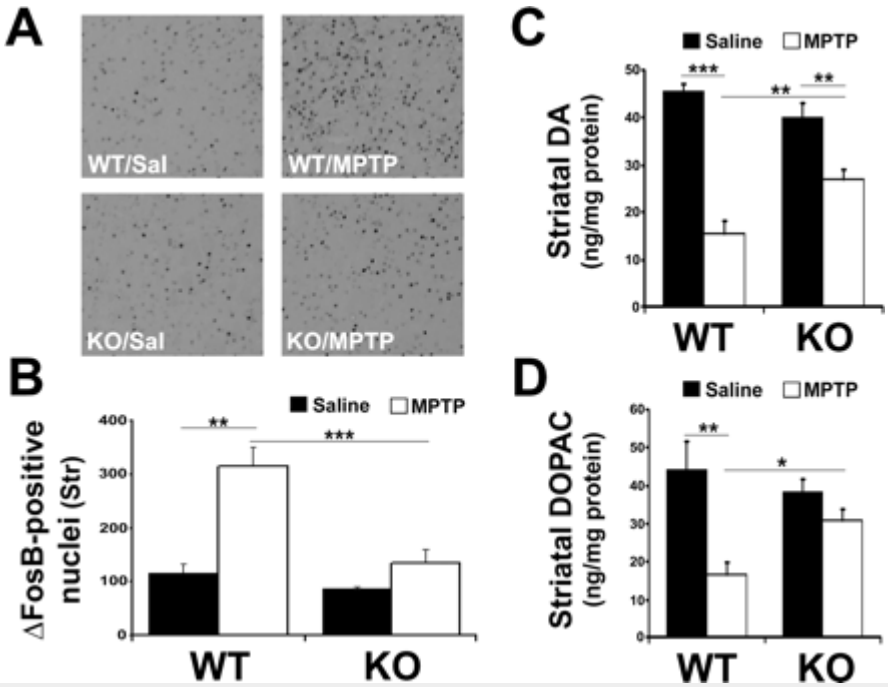


**Figure 3.**

IFN-γ KO mice display reduced striatal ΔFosB, a marker for postsynaptic changes in the denervated striatum, as well as attenuated DA and DOPAC. ***A***, Representative photomicrographs showing ΔFosB staining in the striatum of mice treated as indicated.

Sal, Saline. ***B***, Quantification of ΔFosB-positive cells/nuclei. Str, striatum. ***C***, ***D***, Levels of DA (***C***) and its metabolite DOPAC (***D***) in the striatum were analyzed using HPLC on 14-d-old tissue after saline/MPTP injection. Error bars represent mean ± SEM. ANOVA, $*p < 0.05$, $**p < 0.01$, $***p < 0.001$; $n = 6$ animals per group.

To further substantiate these findings, we repeated the experiment using WT and *IFN*-γ KO mice interbred to produce littermate controls. These animals were analyzed by stereological assessment for surviving TH+ neurons over the entire nigral region. Identical results were obtained in comparison to the initial dopaminergic cell survival experiment (Fig. 2*A–C*). MPTP-treated *IFN*-γ KO mice exhibited a significant dopaminergic cell-body survival ($p < 0.001$) compared with WT littermate control animals also treated with MPTP (Fig. 2*H*,*I*).

To corroborate TH analysis of dopaminergic neuron survival, the number of neurons at the level of the MTN (bregma −3.16) within the SNc of all groups was determined using cresyl violet staining (Fig. 2*C*). Analysis was consistent with that of TH survival, showing no difference between saline-treated groups, a significant loss of TH+ neurons in WT MPTP-treated mice ($p < 0.001$), and a significant reduction in cells lost in IFN-γ-deficient MPTP-treated animals compared with WT mice ($p < 0.001$).

MPTP derives its toxic effects once it crosses the blood–brain barrier (BBB) and is converted to $MPP^+$, the active dopaminergic neural toxin, by monoamine oxidase-B. The protective effects observed in *IFN*-γ-deficient animals may be attributed to altered MPTP metabolism and therefore reduced $MPP^+$. To examine this possibility, striatal tissue was evaluated from mice 90 min after a single injection of MPTP, and levels of $MPP^+$ were

determined using HPLC. It was observed that $MPP^+$ levels did not significantly differ between WT and *IFN*-γ-deficient animals (data not shown), suggesting that the protection afforded by *IFN*-γ deficiency was not because of impaired MPTP metabolism.

**IFN-γ-deficient mice exhibit attenuated MPTP-induced degeneration of the DA axon terminal nigrostriatal dopaminergic pathway**

Previous results indicated that MPTP-induced loss of dopaminergic cell bodies in the SNc is attenuated by *IFN*-γ deficiency. To determine whether the striatal projections of the SNc neurons were also protected in *IFN*-γ-deficient mice, striatal dopaminergic terminal fiber density was assessed initially in non-littermate animals. This analysis is important because this is the region where dopaminergic neurons express their activity through DA release. Densitometry analysis of TH striatal fiber staining showed a significant reduction (68%; $p < 0.001$) in WT MPTP-treated animals compared with saline controls (Fig. 2*D*,*E*). Similar to that observed in the SNc, there was no statistical difference in the TH striatal density of saline-treated WT or *IFN*-γ-deficient mice. *IFN*-γ KO animals exhibited an attenuation of MPTP-induced reduction in striatal TH density compared with MPTP-treated WT animals (32 vs 68%). This suggests striatal terminal fibers were protected by *IFN*-γ deficiency similar to the dopaminergic cell bodies. Results using littermate control animals paralleled these findings, with *IFN*-γ KO mice displaying attenuation in TH-fiber density ($p < 0.01$) (Fig. 2*J*,*K*).

Additional corroboration of these findings included examining density levels of striatal DAT. Densitometric analysis of DAT staining of striatal fibers showed a significant reduction (38%; $p < 0.001$) in WT MPTP-treated animals compared with saline controls

(Fig. 2*F*,*G*). *IFN*-γ KO animals exhibited an attenuation of MPTP-induced reduction in striatal DAT density compared with WT treated mice ($p < 0.01$).

**Postsynaptic functional effects of IFN-γ deficiency**

Treatment with MPTP has been demonstrated previously to induce expression of the transcription factor ΔFosB within the striatum, which is thought to reflect postsynaptic changes (Smith et al., 2003). ΔFosB is suggested to mediate the supersensitivity of striatal DA receptors after denervation (Dragunow et al., 1995). Consistent with these reports, WT MPTP-treated mice displayed a significant increase in the number of ΔFosB-positive cells (Fig. 3*A*,*B*) compared with saline controls. Importantly, MPTP-treated *IFN*-γ-deficient mice showed a significantly reduced increase in FosB staining.

**Effect of *IFN*-γ deficiency on amine levels**

Finally, we examined how DA levels are affected in IFN-γ-deficient mice after MPTP treatment. Previous analyses report diminished DA and its metabolite, DOPAC, in the striatum 14 d after MPTP treatment (Crocker et al., 2003). The effects of *IFN*-γ deficiency parallel the dopaminergic cell survival results observed previously (Fig. 3*C*,*D*). In both the striatum and the SNc, MPTP significantly reduced the levels of DA and DOPAC in WT mice. However, there was a significant decrease in the loss of DA in the MPTP-treated *IFN*-γ KO mice.

***IFN*-γ-deficient mice display attenuated microglial activation in the SNc in response to MPTP**

In WT mice, MPTP has been shown to initiate microgliosis, the morphological and pathological activation of microglia, within the SNc where the highest concentration of microglia resides (Czlonkowska et al., 1996, 2002). Because IFN-γ has also been reported to activate microglia, we examined whether microgliosis was altered in *IFN*-γ-deficient mice treated with MPTP compared with WT animals. Microglia were stained for CD11b, the α-subunit of the $\alpha_M\beta_2$ integrin (CD11b/CD18, complement 3bi receptor) that plays an important role in leukocyte adhesion and whose expression in the brain is confined to microglial cells (Zeng et al., 2005). Activated microglia appear more compact and rounded with cellular thickening and complexing (Fig. 4*A*, WT/MPTP, arrow) (Soltys et al., 2001). Although normal resident microglia express basal levels of CD11b, they appear smaller and have a ramified shape with thin processes (Fig. 4*A*, WT/Sal, arrow). Quantification of microgliosis yielded a significant difference ($p < 0.01$) with twice the number of activated microglia in MPTP WT mice than in saline-treated mice (Fig. 4*B*). Basal activity of microglia in *IFN*-γ KO mice treated with saline displayed no difference in microgliosis compared with WT saline-treated mice (Fig. 4*B*). The increase in microgliosis exhibited with MPTP treatment, as seen in WT mice, was not observed in *IFN*-γ-deficient mice. There was no significant difference in active microglia between *IFN*-γ-deficient saline- versus MPTP-treated mice. However, there was a significant difference between WT and *IFN*-γ KO mice treated with MPTP ($p < 0.01$) (Fig. 4*B*).

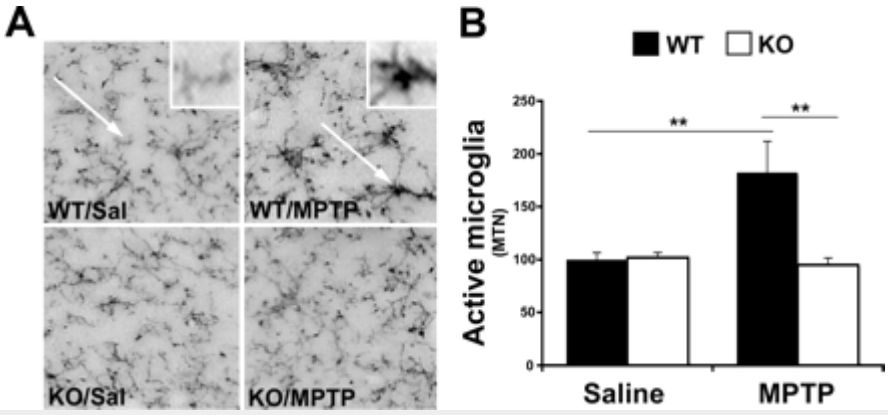


**Figure 4.**

Analysis of active microglia using anti-CD11b. ***A***, Representative photomicrographs illustrating CD11b immunoreactivity in the SNc (MTN) of WT and KO animals treated with either saline (Sal) or MPTP. Arrows indicate resting CD11b-positive microglia (WT/Sal) and activated microglia (WT/MPTP). ***B***, Quantification of morphologically active microglia. Magnified images of each are provided in the insets of ***A*** (WT/Sal and WT/MPTP). Error bars represent mean ± SEM (ANOVA, $^{**}p < 0.01$; $n = 6$ animals per group).

**Role of IFN-γ in dopaminergic cell loss in an *in vitro* microglia/neuron coculture system**

Our *in vivo* results indicate that IFN-γ is important in MPTP-induced dopaminergic cell death. The protection associated with *IFN*-γ deficiency is accompanied with reduced microglial activation. However, the mechanism by which IFN-γ deficiency may be protective and whether it involves microglial activation is difficult to assess in an *in vivo* setting. This is particularly true in this present situation in which reduced microglial activation could be a secondary effect of reduced neuronal loss. Accordingly, we used an *in vitro* model of dopaminergic cell loss in which effects of microglia on dopaminergic

neurons can be studied more directly. Therefore, to address whether IFN-γ may promote dopaminergic loss through activation of microglia and to more closely study the interaction between these two populations of cells, we used a microglia/midbrain neuron coculture system, similar to that reported previously (Gao et al., 2002a). In this system, midbrain cultures enriched for neurons, obtained from E13.5 embryos, are cultured in defined Neurobasal medium. In these cultures, dopaminergic neurons constitute <1% of all the neurons in culture. All neurons, including TH+ cells, in these cultures are resistant to 20–25 nM rotenone, another complex I inhibitor similar to $MPP^+$ (Kotake and Ohta, 2003). No dopaminergic cell death is observed even after 7 d of rotenone treatment in the absence of microglia (Fig. 5*A*). The addition of microglia to these cultures alone, in the absence of rotenone, does not significantly affect survival of total neurons or the more sensitive dopaminergic neurons. However, with the addition of 20–25 nM rotenone, a significant loss of TH+ neurons is observed only in the presence of microglia (Fig. 5*A*). These findings indicate that death of TH+ neurons in this system, at a defined rotenone concentration, is dependent on microglia. It is important to note that this effect is concentration specific; at higher concentrations, rotenone will begin to kill nondopaminergic cell types as well, even in the absence of microglia (data not shown).

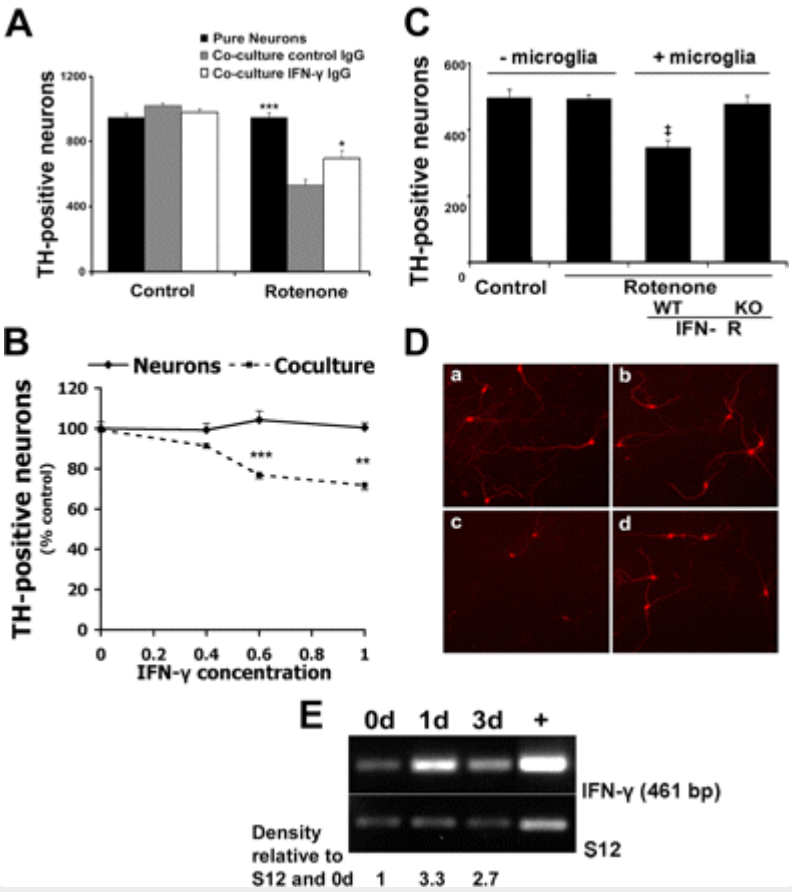


**Figure 5.**

IFN-γ requirement in a coculture model of dopaminergic cell loss induced by rotenone *in vitro*. ***A***, Neutralizing IFN-γ antibody protects dopaminergic neurons from rotenone-induced death in the presence of microglia. Seven-day-old WT neuron-enriched midbrain cultures were cocultured with and without WT microglia in the presence or absence of rotenone and with control or IFN-γ neutralizing antibody, as described in Materials and Methods and as shown. The number of live TH+ neurons was assessed as described in Materials and Methods. *$p < 0.05$, ***$p < 0.001$ relative to coculture with control IgG (two-tailed *t* test). ***B***, Seven-day-old neuron-enriched midbrain cultures supplemented with or without microglia were subjected to IFN-γ ligand (nanograms per milliliter) applications. The cultures were fixed 7 d later and stained with TH and Hoechst. ***$p <$

0.001 compared with control, $^{**}p < 0.01$ (two-tailed *t* test; $n = 3$). ***C***, Dopaminergic neurons treated with rotenone are resistant to death in the presence of microglia lacking IFN-γ receptor. Dopaminergic neurons used were similar to those in ***A***, except WT neurons were cultured in the presence of either WT or IFN-γ receptor (IFN- R)-deficient microglia. $^{‡}p < 0.05$ relative to IFN-γ receptor KO (two-tailed *t* test; $n = 3$). ***D***, Representative immunofluorescence of cocultures quantified in ***C***, stained with TH antibody are as follows: ***a***, WT mesencephalic neurons; ***b***, WT mesencephalic neurons treated with rotenone; ***c***, WT mesencephalic neurons and microglia treated with rotenone; ***d***, WT mesencephalic neurons and IFN-γ receptor KO microglia treated with rotenone. ***E***, WT microglia-enriched cultures were treated with rotenone for 0, 1, and 3 d. One week after plating, microglia were collected, RNA was extracted, and RT-PCR was performed for IFN-γ and S12 control. Densitometric analysis was performed with values normalized to each respective S12 signal and further normalized to 0 d value. +, IFN-γ-positive RNA control sample obtained from CD4+ T-cells. Error bars represent mean ± SEM.

Using this system, we first asked whether inhibition of IFN-γ would affect rotenone-induced dopaminergic death as was observed *in vivo*. As shown in Figure 5*A*, a neutralizing antibody to IFN-γ but not control IgG significantly improved dopaminergic survival. This indicates that IFN-γ can modulate the rotenone-induced dopaminergic cell death, which occurs only in the presence of microglia. To further support the importance of IFN-γ in microglia-induced sensitivity of dopaminergic neurons, we exposed midbrain neurons with and without cocultured microglia to varying concentrations of exogenous IFN-γ ligand. As shown in Figure 5*B*, 0.6 and 1 ng/ml concentrations of exogenous IFN-γ caused significant loss of dopaminergic neurons. This, however, only occurred in the

presence of microglia and not in their absence. This indicates that IFN-γ is an important mediator of dopaminergic neuron loss, but only in the presence of microglia.

To determine more clearly whether IFN-γ may act on microglia to control rotenone-induced dopaminergic cell loss in this system, we cultured microglia from *IFN*-γ receptor KO or WT control mice. These WT or *IFN*-γ receptor-deficient microglia were then cocultured with normal neurons with or without rotenone treatment. Death of dopaminergic neurons only occurred in the presence of WT microglia with rotenone treatment (Fig. 5*C*,*D*). Cultures treated with rotenone but containing IFN-γ receptor-deficient microglia displayed no death. Conversely, we also examined whether midbrain neurons cultured from *IFN*-γ receptor-deficient animals were resistant to rotenone in the presence of WT microglia. There was no difference in death of IFN-γ receptor-deficient neurons compared with WT neurons exposed to rotenone in the presence of WT microglia (data not shown). Finally, if rotenone-mediated death of dopaminergic neurons occurs through IFN-γ, we would predict that IFN-γ should be present in microglia. Accordingly, we isolated microglia, exposed them to rotenone, and determined the IFN-γ message at certain times after treatment by RT-PCR. As shown in Figure 5*E*, there was a basal level of IFN-γ message present in untreated microglia that increased on exposure to rotenone. Together, these results indicate that IFN-γ plays a crucial role in modulating microglial responses *in vitro*. In addition, it suggests that IFN-γ may promote MPTP-induced dopaminergic loss *in vivo*, at least partially through activation of microglia.

# Discussion

Previous work has suggested the importance of the inflammatory response and microglial activation in dopaminergic loss in animal models of PD as well as in PD patients (McGeer et al., 1988; Banati et al., 1998; Wu et al., 2002; Barcia et al., 2004). However, the required nature of the inflammatory mediators or their mechanisms of action in PD is not fully understood. Our findings are of significance because they directly demonstrate that a central inflammatory mediator, IFN-γ, plays a critical role in dopaminergic loss, both *in vitro* and *in vivo*. We found that (1) levels of IFN-γ are elevated in the serum of PD patients, (2) *IFN*-γ deficiency attenuates the degeneration of the nigrostriatal system and significantly reduces microgliosis in a model of *in vivo* dopaminergic loss, and (3) IFN-γ is involved in microglial-mediating dopaminergic neurodegeneration.

Our analysis of human blood serum for possible elevated cytokines yielded results with only levels of IFN-γ displaying a significant increase from those of control patients. It must be noted that cytokine detection in this assay may be hampered because of a lack in cytokine stability (Noguchi et al., 1996). In addition, it should also be stressed that cytokine blood levels do not necessarily reflect actions in the CNS. However, systemic IFN-γ-producing inflammatory cells have been reported to infiltrate the brain (Perry, 2004). In addition, Banks (2005) has recently suggested that cytokines circulating in the blood may cross into the CNS through direct cytokine transport across the BBB. Therefore, we also examined the role of IFN-γ in dopaminergic neuronal loss.

Our results, in an *in vivo* mouse model of dopaminergic neurodegeneration, reveal that mice deficient in *IFN*-γ show reduced loss of dopaminergic cell bodies and striatal

terminals compared with WT animals treated with MPTP. Germline loss of *IFN*-γ did not appear to grossly perturb the dopaminergic system, including possible postsynaptic signaling changes (FosB), as assessed in saline-treated animals. In addition, DA and DOPAC levels, as well as markers of postsynaptic function (FosB), are significantly attenuated in *IFN*-γ-deficient animals treated with MPTP. Interestingly, microglial activation is also reduced in these deficient mice.

Consistent with our *in vivo* findings, we observed that IFN-γ is required for the death of dopaminergic neurons cultured in the presence of microglia with rotenone. Importantly, reduced cell loss was only observed when microglia deficient in IFN-γ receptor, but not WT microglia, were added to the dopaminergic neurons. In contrast, deficiency of IFN-γ receptors in dopaminergic neurons did not result in protection in our coculture death paradigm. IFN-γ was also detected in cultured microglia that increased on rotenone exposure. Together, the data not only provide evidence for direct relevance of the microglial response in dopaminergic cell loss induced by mitochondrial toxins but also define IFN-γ as a critical inflammatory mediator in this process.

Our results are consistent with the view that IFN-γ is a primary mediator of microglial activation (Moss and Bates, 2001; Platten et al., 2001; Abbas et al., 2002; Delgado, 2003). There are a number of possible effects of IFN-γ on microglia that may contribute to dopaminergic loss, both *in vivo* and *in vitro*. First, IFN-γ, through binding to its receptor and activation of the Jak/STAT pathway, can activate iNOS. Alternatively, IFN-γ has also been shown to upregulate the death receptor Fas and its ligand, FasL (Badie et al., 2000). Accordingly, IFN-γ could mediate its effects on microglia through direct activation of the death receptor on dopaminergic neurons. Indeed, Fas has been shown to

be localized to dopaminergic neurons and is implicated in MPTP-induced dopaminergic cell death (Hayley et al., 2004).

Our model that IFN-γ promotes dopaminergic cell death through the activation of microglia is consistent with growing evidence that the inflammatory pathway is central to dopaminergic loss in *in vivo* and in *in vitro* models. Indeed, microglial activation has been noted in PD animal models and postmortem brains (McGeer et al., 1988; Banati et al., 1998). Direct activation of microglia through administration of the endotoxin LPS was found to induce loss of dopaminergic neurons in mice (Arai et al., 2004), while also stimulating the production of iNOS and subsequent reactive oxygen species (ROS) (Li et al., 2005). In fact, the nigra appears to be exquisitely sensitive to microglia activation because equivalent LPS injections in alternate brain regions (hippocampus, cortex) did not have the same pattern of degeneration (Xie et al., 2003). Finally, LPS and MPTP can synergistically increase dopaminergic death (Gao et al., 2003b).

However, most functional evidence implicating microglia as a direct cause of dopaminergic cell degeneration is controversial. Minocycline, a tetracycline derivative known to inhibit microglia activation/inflammation and protect dopaminergic neurons in an MPTP model of PD, can also inhibit classic death molecules, such as caspases (Chen et al., 2000; Wei et al., 2005). Moreover, others have reported that minocycline can exacerbate MPTP-induced toxicity (Yang et al., 2003). In addition, the role of microglia may also be dependent on the mode of activation. For example, activation of microglia in the hippocampus by IL-4- and IFN-γ-expressing T-cells is neuroprotective (Butovsky et al., 2005). Our evidence presented here is important because it provides clear evidence for the central death-promoting nature of the inflammatory response in dopaminergic

neuronal loss. Finally, it is important to note that microglial activation is likely a graded response, and the degree of activation may depend on the type and severity of insult.

Although our evidence indicates the important nature of IFN-γ activation of microglia *in vitro*, the exact mechanism by which IFN-γ promotes dopaminergic death *in vivo* and whether this is strictly reliant on microglial activation is unclear. Indeed, IFN-γ receptors are expressed ubiquitously (Blanck, 2002). In addition, it is important to note that our results do not imply that inflammatory processes are the exclusive mediators of neuronal damage. Indeed, although IFN-γ deficiency effectively blocks microglial activation, it does not completely eliminate the reduction in striatal DA/DOPAC. This is an interesting observation that suggests that microglial activation, although important, is not the only mechanisms by which dopaminergic neuron damage occurs. This notion is supported by the fact that MPTP ($MPP^+$ metabolite) can directly target mitochondria in neurons and lead to increased ROS and damage (Liberatore et al., 1999; Dehmer et al., 2000; Gonzalez-Polo et al., 2004; Chen et al., 2006).

There are some intriguing links with our present IFN-γ studies to that of human PD. First, microglial activation in PD patients is well characterized (Ouchi et al., 2005). Second, we and others have shown that plasma levels of IFN-γ are elevated in PD patients (Nakamura et al., 1992). The exact significance of this is unknown, particularly because the relationship, if any, between peripheral events and events in the CNS is unclear. However, increased plasma IFN-γ levels could reflect a systemic increase in IFN-γ production by lymphocytes and infiltrates capable of entering the CNS. In support of this, T-cells are known to circulate in the brain with lymphocyte infiltration, and release of proinflammatory cytokines, such as TNF-α and IFN-γ, have been shown at the site of

injury (Raivich et al., 2003). Third, IFN-γ levels have also been shown to be increased in CSF and in the substantia nigra of PD patients (Widner et al., 2002). Fourth, IFN-γ has been shown to upregulate iNOS, by binding the IFN-γ receptor and by upregulating expression of astrocyte CD23 (Okuno et al., 2005). Interestingly, CD23 is found in glia from the SNc of PD patients, yet it is not detected in control subjects (Hunot et al., 1999). Finally, genetic studies have linked a dinucleotide CA repeat polymorphism within the first intron of the *IFN*-γ gene of patients with late onset of PD (Hakansson et al., 2005). This polymorphism leads to a higher production of IFN-γ. Together, this evidence suggests the potential importance of IFN-γ in PD pathogenesis and provides a link to our animal studies presented here.

In conclusion, we have shown that mice deficient in *IFN*-γ display an attenuation of MPTP-induced dopaminergic cell death and maintenance of DA functional activity. Our data suggest that one mechanism by which this is observed involves the activation of microglia, aiding in the damage to dopaminergic neurons. Accordingly, targeting microgliosis by modulating levels of IFN-γ may be a candidate therapeutic strategy for treatment of PD.

**Footnotes**

↵*S.H. and D.S.P. are co-corresponding senior authors.

This work was supported by grants from the Canadian Institutes of Health Research (D.S.P., H.A.), Parkinson's Society Canada, the Parkinson's Disease Foundation (USA), the United States Department of National Defense, the Michael J. Fox Foundation and Parkinson's Research Consortium, Heart and Stroke

Foundation Ontario (D.S.P.), and the Natural Sciences and Engineering Research Council (S.H.). H.A. and S.H. have Canadian Research Chairs in Neuroscience. We thank the technical staff at Roger Guindon Hall Animal Care Veterinary Services (University of Ottawa, Ottawa, Ontario, Canada) for their assistance with our animals, Fraser Scott and David Lefebvre for reagents, Abbas Sadikot and Vladimir Rymar for their assistance with stereological analysis, and Yasmilde Rodriguez Gonzalez for her technical assistance.

Correspondence should be addressed to Dr. David S. Park.

# Chapter 3:

# Involvement of the Fcγ Receptor in a Chronic *N*-Methyl-4-phenyl-1,2,3,6-tetrahydropyridine Mouse Model of Dopaminergic Loss*

The Journal of Biological Chemistry (2011)
vol. 286, no. 33, pp. 28783–28793

**Arman Lira**[‡], Jerzy Kulczycki[§], Ruth Slack[‡], Hymie Anisman[§] and David S. Park[‡¶,1]

*From the [‡]Department of Cellular Molecular Medicine, University of Ottawa, Ottawa, Ontario K1H 8M5, Canada, the [§]Institute of Neuroscience, Carleton University, Ottawa, Ontario K1S 5B6, Canada, and the [¶]Department of Cogno-Mechatronics Engineering, Pusan National University, Korea*

1. To whom correspondence should be addressed: Department of Cellular and Molecular Medicine, University of Ottawa

# Statement of author contibution

All the experiment s in this manuscript were performed by Arman Lira. The biopsy brain tissue samples were obtained by Arman Lira and subsequent HPLC analysis was conducted by Dr. Jerzy Kulczycki. All figures and texts in this manuscript were prepared by Arman Lira under the assistance of Dr. David Park.

# Abstract

Although there is growing evidence for a role of the innate immune response in Parkinson's disease, the nature of any humoral response in dopaminergic degeneration is uncertain. Here we report on a protracted N-methyl-4-phenyl-1,2,3,6-tetrahydropyridine model of dopaminergic death that potentially allows a more full adaptive humoral response to develop. Rag2 mutant mice that lack the full adaptive response (deficient in both T and B cells) are resistant to dopaminergic death and behavioral deficiencies in this model. These mice are resensitized after reconstitution with WT splenocytes. To more directly provide evidence for humoral/IgG involvement, we show that deficiency of Fcγ receptors, which are critical for activation of macrophages/microglia by binding to IgGs, is also protective in this protracted model. FcγR-deficient mice display improved behavior and impaired microglial activation. Interestingly, however, Rag2 mutant but not FcγR-deficient mice are resistant to a more standard N-methyl-4-phenyl-1,2,3,6-tetrahydropyridine paradigm where death is more rapid. Taken together, these data indicate that, provided sufficient time, the humoral arm of the adaptive immune system can play a critical functional role in modulating the microglial response to dopaminergic degeneration and suggest that this humoral component may participate in degeneration in Parkinson's disease.

# Introduction

Degeneration of dopamine (DA)[2] neurons of the substancia nigra pars compacta (SN*pc*) is a key hallmark of Parkinson's disease (PD). However, the mechanism by which this death occurs is not completely clear (1,–,3). Growing evidence indicates that oxidative stress, mitochondrial damage, and ubiquitin-proteasomal dysfunction participate in the degenerative process of DA neurons (4). Interestingly, an increasing number of observations also indicate the importance of the immune response in PD and models of PD. Most of this evidence, however, has centered around the innate neuroinflammatory response. For example, microgliosis-mediated DA cell death, particularly via oxidative insult, has been reported in different models of PD (5). NADPH oxidase, the largest superoxide-producing enzyme in microglia, and inducible nitric oxide synthase are involved in N-methyl-4-phenyl-1,2,3,6-tetrahydropyridine -induced death of DA neurons (6,–,8). Moreover, the classic inflammagen lipopolysaccharide causes neurodegeneration of DA neurons through Toll-like receptor 4-dependent pathways (9,–,11). More recently, however, increasing evidence also suggests a role for the adaptive immune response in models of PD.

The first correlative evidence suggesting a role for a cellular adaptive response was the observations of infiltrating T cells in a number of PD-related contexts. For example, a substantial number of T cells were detected in the SN*pc* of PD patients (12, 13). Similarly, MPTP treatment results in infiltration of T cells to the SN*pc* and striatum as well as an increase in expression of microglial MHC class II antigen (14, 15). The required role of T cells, in particular CD4-positive T helper cells, was highlighted by

studies that show that Rag, Scid, and CD4-negative mice are resistant to dopaminergic loss induced by MPTP (2, 13). The role of the humoral response, however, is unclear. Antibodies to DA neurons have been detected in the cerebral spinal fluid of PD patients. These antibodies were found in 78% of patients with clinical PD *versus* 3% of control patients (16). In addition, the expression of CD23, a type of Fc receptor, is detected in the substancia nigra and striatum of PD patients but not in control patients (17). Likewise, MPTP has been shown to increase Fcγ receptor expression (14, 15, 17). However, the role/participation of FcγR and the humoral response in DA degeneration is unknown.

Here we report a novel protracted degeneration paradigm to study the adaptive immunopathogenic mechanisms in a mouse model of dopaminergic loss. With this model, we provide evidence that the adaptive immune response, in particular the FcγRs, can play a critical role in DA loss in *vivo*.

# EXPERIMENTAL PROCEDURES

## Experimental Animals

The following strains were obtained from Taconic Laboratory (Germantown, NY): Black $6^{+/+}$ (C57BL/6Ntac), $Rag2^{-/-}$ (B6.129S6-$Rag2^{tm1Fwa}$N12), and $Fcer1g^{-/-}$ (B6.129P2-$Fcer1g^{tmRav}$N12) mice. All mice were backcrossed with C57BL/6 mice for 12 generations and intercrossed to homozygosity. Animals were housed in a barrier facility specialized for immunocompromised mice because of their high susceptibility to infection. Mice were maintained on a 12-h light/dark cycle with lights on at 6 am and a room temperature of 21 °C. Animals had *ad libitum* access to slightly acidified water and mouse chow from Ralston Purina (St. Louis, MO). KO and WT mice were interbred to produce littermate controls. All experimental procedures met the Canadian Council on Animal Care guidelines and were approved by the University of Ottawa Committee for Animal Care.

## Immunohistochemistry

Mice were anesthetized and intracardially perfused with 4% paraformaldehyde. Brains were removed, fixed overnight with 4% paraformaldehyde and subsequently cryoprotected in 10% sucrose before cryosectioning into 14- to 40-µm free-floating sections. Striatal and substancia nigra sections were immunostained with rat anti-CD11b (1:200, Serotec, Oxford, UK), rat anti-dopamine transporters (DAT, 1:2000; Millipore, Bedford, MA), rat anti-ΔFosB (1:1000, Santa Cruz Biotechnology, Inc., Santa Cruz, CA), or mouse anti-tyrosine hydroxylase (TH, 1:10,000, Immunostar, Hudson, WI). Primary antibodies were visualized with diaminobenzidine or cy3.

**Neurochemical Analysis**

Mice were decapitated, and their striatum was obtained through micropunches with a 1-mm-diameter biopsy needle and immediately stored in a freezer (−80 °C). Measurements of DA and its metabolite (HVA) were determined using HPLC methods.

**N-Methyl-4-phenylpyridinium Ion (MPP+) Measurements**

HPLC analysis was used to measure the MPP+ ion 90 min after MPTP administration as described previously (18).

**MPTP Administration**

Seven- to ten-week old mice were used for injections. All animals were injected in the regular animal care facility with extra precautions to prevent infection, such as using a portable fume hood during injections and handling these mice first during all wellness assessments. MPTP (Sigma) was administered intraperitoneally using the standard subchronic or more protracted paradigm. The subchronic standard paradigm consists of injecting 30 mg/kg of MPTP once daily for 5 consecutive days and sacrificing 14 days after the start of injections. For the protracted treatment, we injected 10 mg/kg of MPTP on the first and third day of each week for 4 consecutive weeks. These mice were sacrificed 5 weeks after the start of injections. Control mice received an equal volume of saline (0.9%).

**Passive Transfer**

Single-cell suspensions were prepared from spleens of MPTP-treated WT mice. Recipient $Rag2^{-/-}$ mice received two i.v. injections, 4 h apart, of $10^7$ total splenocytes in

0.2 ml of phosphate buffered saline solution. After a 4-week reconstitution period, mice were treated with the protracted MPTP paradigm or received an equal volume of saline (0.9%) solution, as described above.

**Pole Test**

The time of descend to the ground was recorded after mice were individually placed upright near the top of a 2-foot pole. The pole test was administered on the sixth day of every week during chronic MPTP treatment. Mice have a natural tendency to avoid heights, and their descend to the ground offers a unique perspective into motor output.

**Quantification of Neuronal Survival**

DA neurons in the SNc were assessed for survival using the dopaminergic cell marker TH. A minimum of two sections from each of five levels around the medial terminal nucleus region of the SNc (from −2.92 to −3.52 relative to the bregma) were estimated for the number of TH-positive neurons. The average total number of TH-positive neurons was determined by Abercrombie's correction. Quantification of TH immunoreactivity was substantiated by a second group of mice interbred to produce littermate controls. The average total number of TH-positive neurons was estimated using Stereo investigator (version 6, MicrobrightField, Williston, VT) and applying optical fractionation to 40-μm sections from the entire SNc (-2.54 to −3.88 relative to the bregma).

**Quantification of Striatal Immunohistochemistry**

Density of striatal DA fiber, DAT, and ΔFosB was quantified using an Eclipse densitometry analysis (18). Each tissue density was compared relative to its own background.

**Statistical Analysis**

All data are expressed as mean ± S.E. Analyses of all values were performed using one-way ANOVA followed by Tukey's post-hoc test, to determine differences among normal distribution of means.

# RESULTS

## A More Protracted Model of MPTP-induced Degeneration

We examined dopaminergic loss induced by the neurotoxin MPTP as a prototypical toxin model of degeneration (19). In this paradigm, the metabolite of MPTP, MPP+, is selectively taken up by dopamine neurons and targets complex 1 of the mitochondria, resulting in increased oxidative stress and eventual dopaminergic loss (4, 20,–,22). It is a widely utilized model of DA loss, made even more relevant because genetic depletion of known PD genes do not yet result in substantial dopamine death in mice (23). It is important to note, however, that the MPTP model has obvious caveats in its relevance to PD. However, it likely provides important insights into how DA neurons may die *in vivo*. To test the potential role of the adaptive response, in particular the FcγR in dopaminergic loss, we reasoned that we required a more protracted model of dopamine loss to allow time for a humoral response to develop. Typical acute (20 mg × 4 in 1 day) or subchronic (30 mg/kg × 5 days) lead to significant dopaminergic loss within 1 week of treatment (13, 24). We chose a more protracted dosing paradigm consisting of an intraperitoneal injection (10 mg/kg) twice a week for a month and sacrificing 5 weeks after the start of MPTP injections. Fig. 1 illustrates the timing of DA neuron loss with this latter dosage. To ensure that the bulk of dopamine loss did not occur early, we examined degeneration at the 2-week time point. No significant loss was observed at this time, whereas a significant loss (43.93%) was detected after 5 weeks of MPTP treatment. These results indicate a more protracted time frame of loss that would potentially allow time for the humoral component of the immune response to participate in the degeneration of MPTP-treated mice.

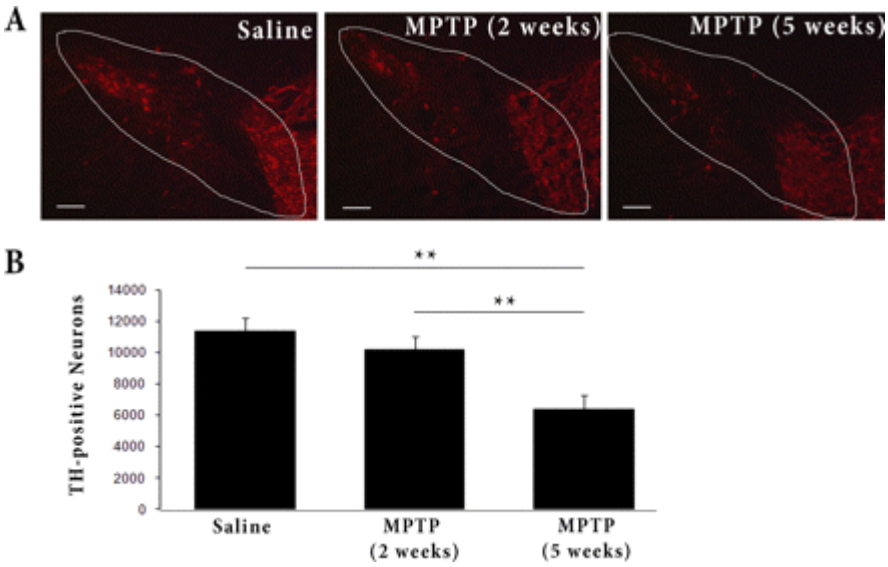


**FIGURE 1.**

**Chronic MPTP elicits DAergic neuron death.** *A*, representative photomicrographs of TH+ cells in the SN*pc* of the indicated non-littermate treatment groups. The SNc is demarcated. *B*, quantification of dopaminergic cell bodies 2 or 5 weeks after the start of chronic MPTP intoxication. *Scale bars* = 250 μm. *Error bars* represent mean ± S.E. ANOVA, **, $p < 0.01$; $n$ = five to seven animals per group.

**The Rag2-deficient Mice Are Resistant to Chronic MPTP**

We first tested whether any aspects of the adaptive immune response might play a role in the observed dopaminergic loss in this more protracted model of loss. We examined the contribution of both T cells and B cells to death by evaluating $Rag2^{-/-}$ mice in our chronic paradigm. Chronic MPTP induces significantly less DA neurodegeneration in $Rag2^{-/-}$ mice compared with their $Rag2^{+/+}$ littermates (12.83% *versus* 35.94%) (Fig. 2). To ensure that these differences were not due to differences in the production of MPP+, the active metabolite of MPTP, we measured MPP+ production by HPLC analyses. There was no detectable difference in MPP+ levels in WT and Rag2-deficient mice (data not

shown). We also performed a rescue experiment whereby we passively transferred splenocytes from Rag2$^{+/+}$ mice treated with MPTP to Rag2$^{-/-}$ mice. One month later, we looked for resensitization in reconstituted Rag2$^{-/-}$ mice. Indeed, reconstituted Rag2$^{-/-}$ mice are more susceptible to MPTP-induced DA neuron death compared with non-reconstituted littermates (Fig. 2), further supporting the importance of the immune system in dopaminergic loss.

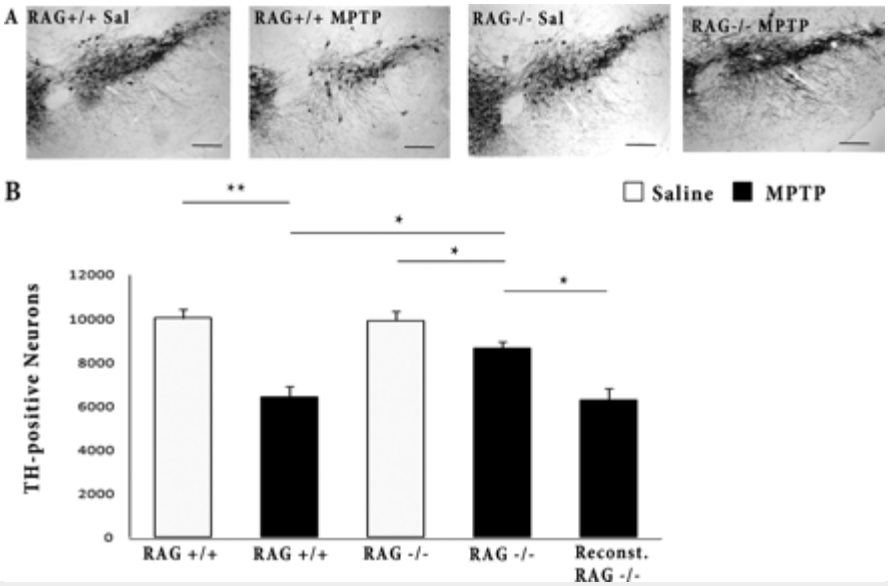


**FIGURE 2.**

**Rag2$^{-/-}$ mice display attenuated TH+ cell loss after chronic MPTP administration.**

*A*, representative photomicrographs of TH+ cells in the SN*pc* of the indicated littermate treatment groups. *B*, quantification of dopaminergic cell bodies 5 weeks after the start of saline (*Sal*) or chronic MPTP intoxication by stereology, as described under "Experimental Procedures". *Scale bars* = 250 μm. *Error bars* represent mean ± S.E. ANOVA, *, $p < 0.05$; **, $p < 0.01$; $n$ = five to seven animals per group.

We next examined the effects of Rag2 deficiency in the target region of the SNc, the striatum that contains the terminals from the dopamine neurons in the SNc. We analyzed

for the expression of TH and DAT as markers for these terminals. Chronic MPTP induced greater TH-reactive nerve terminal loss in Rag2$^{+/+}$ mice compared with Rag2$^{-/-}$ littermates (Fig. 3). Likewise, the DAT expression profile mirrors that of DA fiber density. DAT density is less in RAG$^{+/+}$ mice treated with MPTP than in RAG$^{-/-}$ littermates (Fig. 3). Finally, we examined levels of DA and its metabolite HVA in striatal punches by HPLC analyses. There was a dramatic loss in both DA and HVA levels following chronic MPTP treatment at 5 weeks in the Rag 2$^{+/+}$ mice, 73.1% and 82.1%, respectively (Fig. 4). These reductions were ameliorated in the Rag2$^{-/-}$ mice (47.2% and 43.1%, respectively).

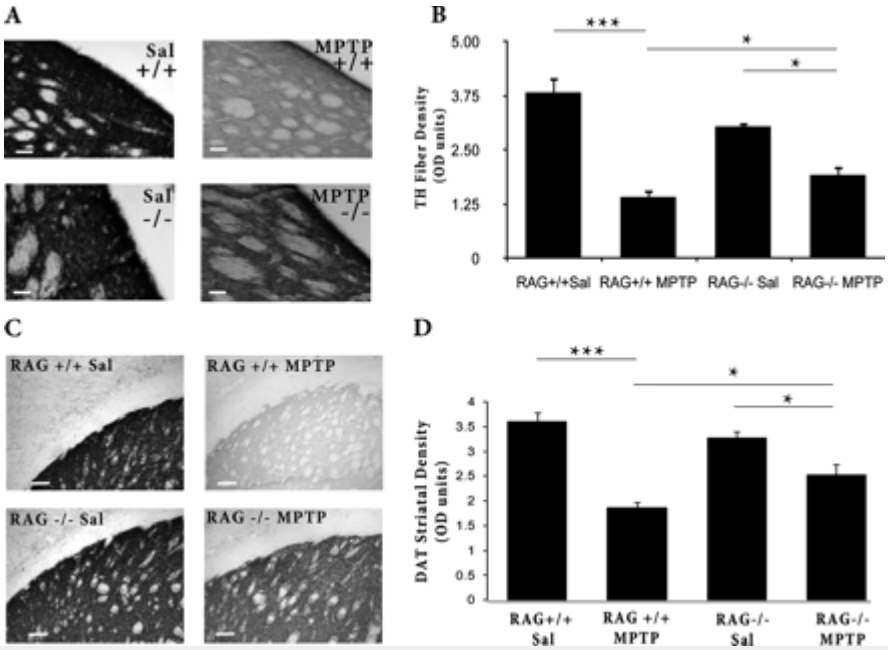


**FIGURE 3.**

**Dopamine nerve terminals are protected in Rag2$^{-/-}$ mice treated with chronic MPTP.** *A*, representative photomicrographs showing TH immunoreactivity from the striatum of indicated littermate treatment groups. *Sal*, saline. *B*, optical density quantification of striatal TH+ fiber density. *C*, representative photomicrographs of striatal

sections stained for DATs from indicated littermate groups. *D*, optical density quantification of striatal DATs. *Scale bars* = 50 μm (*A*) and 200 μm (*C*). *Error bars* represent mean ± S.E. ANOVA, *, $p < 0.05$; ***, $p < 0.001$; $n$ = six to eight animals per group.

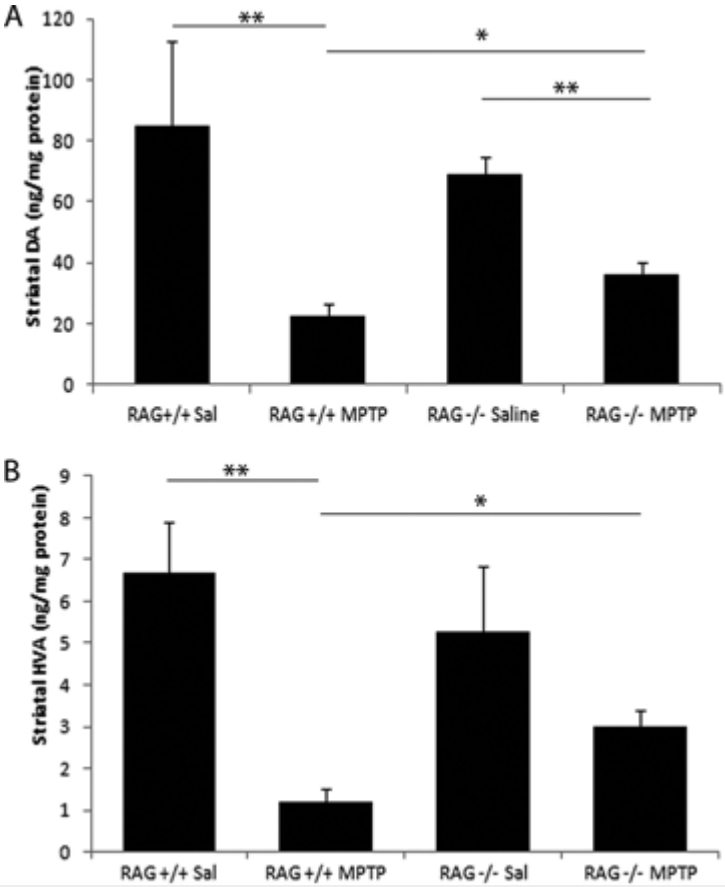


**FIGURE 4.**

**DA and HVA levels in striatum of Rag2$^{-/-}$ mice.** Levels of DA and HVA were measured using HPLC from striatal punch biopsies of the indicated littermate treatment groups. *Sal*, saline. *Error bars* represent mean ± S.E. ANOVA, *, $p < 0.05$; **, $p < 0.01$; $n$ = five to six animals per group.

Previous work from a number of groups indicates that damage to the nigrostriatal dopaminergic pathway results in compensatory responses in the postsynaptic neurons of the striatum. Although this response is complex, we have shown one marker that changes is ΔFosB, which is induced postsynaptically, presumably as an indication of hyperactivation mediated by denervation of the dopaminergic tracts, to compensate for reduced dopaminergic neurotransmission. We have used this measure as an indication of altered basal ganglion circuitry (25,–,27). As shown in Fig. 5, $Rag2^{+/+}$ mice intoxicated with MPTP display a significantly higher density in striatal ΔFosB expression, suggesting that nigrostriatal tract degeneration sufficiently alters basal ganglia function. In $Rag2^{-/-}$ mice, in contrast, this response is blunted.

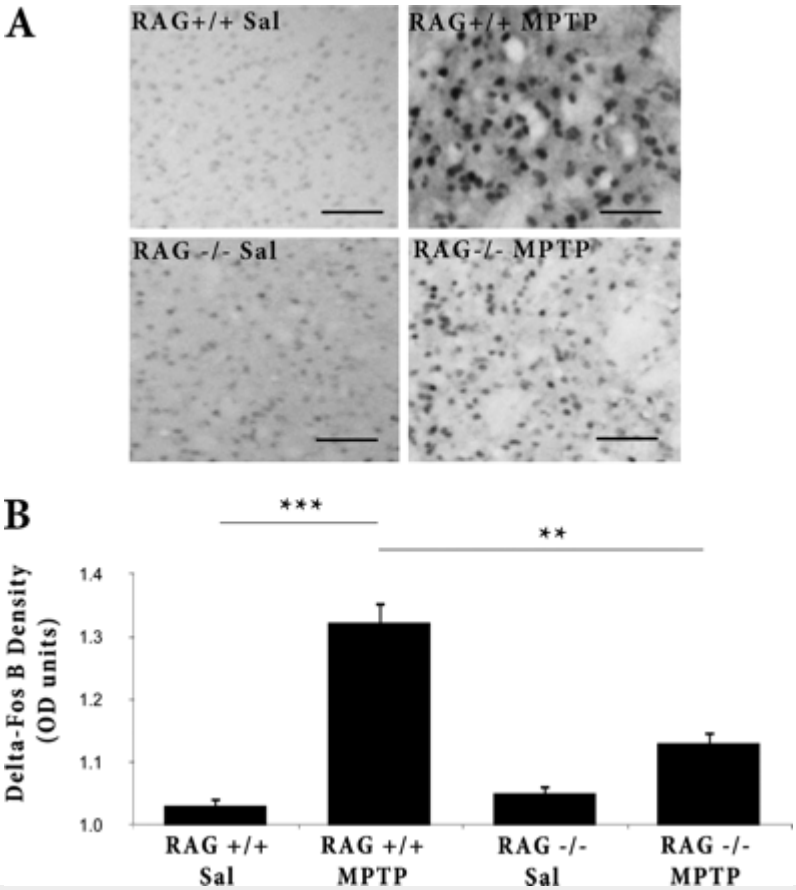


**FIGURE 5.**

**Rag2$^{-/-}$ mice treated with chronic MPTP exhibit reduced expression of striatal Δ-Fos B, a marker for postsynaptic changes in the denervated striatum.** *A*, representative photomicrographs illustrating ΔFosB immunoreactivity in the striatum. *B*, quantification of striatal Δ-Fos B optical density. *Sal*, saline. *Scale bars* = 100 μm. *Error bars* represent mean ± S.E. ANOVA, **, $p < 0.01$; ***, $p < 0.001$; $n$ = six to eight animals per group.

Microgliosis plays an important process in the adaptive immune response. Alongside DA neuron death, we examined for markers of neuroinflammation using the microglia-specific CD11b receptor, which is up-regulated upon microgliosis (28). Rag2$^{+/+}$ mice treated with chronic MPTP display significantly higher CD11b expression within the MTN region of the SN*pc* (Fig. 6). However, in the Rag2-deficient mice, MPTP did not elicit any notable microglial activation.

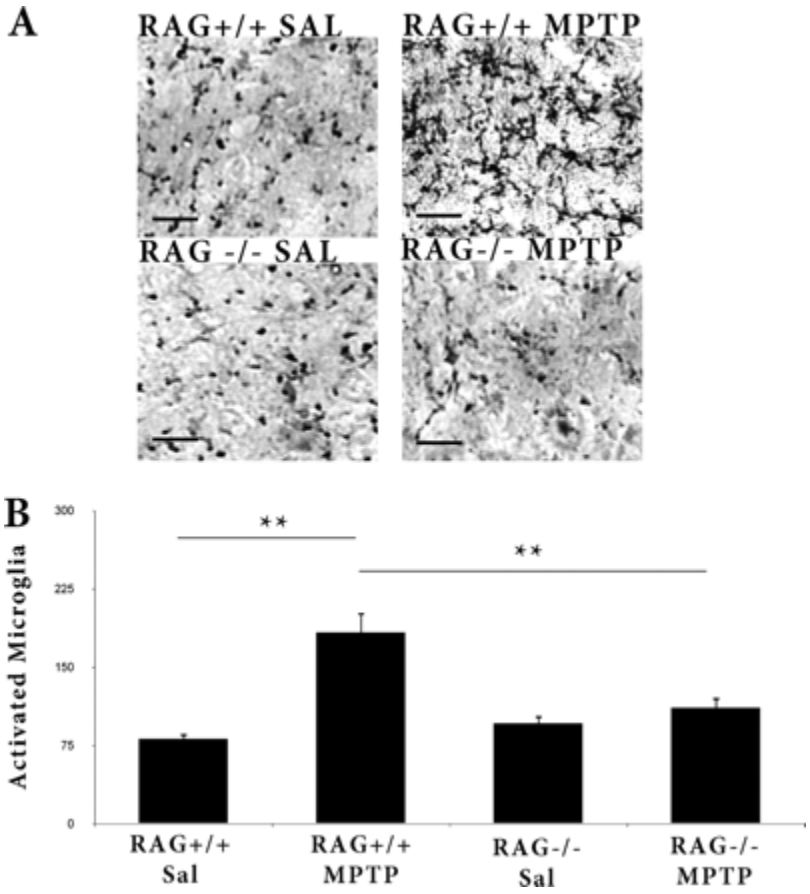


**FIGURE 6.**

**Rag2$^{-/-}$ mice exhibit less neuroinflammation.** *A*, representative photomicrographs of microglia stained with anti-CD 11b. *B*, quantification of morphologically activated microglia around the MT nucleus of the ventral SN*pc*. *Sal*, saline. *Scale bars* = 100 μm. *Error bars* represent mean ± S.E. ANOVA, **, $p < 0.01$; $n$ = six to eight animals per group.

Finally, we evaluated the behavioral consequences of chronic MPTP toxicity and DA loss in WT and Rag2-deficient littermate controls. Initially, we examined for any changes in general locomotor activity using beam break cages. However, no reproducible changes in locomotor behavior could be detected (data not shown). We hypothesized that perhaps a

more challenging test was required to unmask deficits brought on by the observed dopaminergic loss because typically more than a 60–80% loss is required to see major differences in general locomotion. The pole test measures the time it takes for mice to descend a 2-foot pole. The first 2 weeks of testing after initiation of the MPTP challenge did not show any detectable differences in any groups. However, at week 3, differences between WT non-treated and MPTP-treated mice could start to be detected. At 4 and 5 weeks, these differences became accentuated. This time course of the motor deficit is consistent with the observed destruction of the nigrostriatal axis. Importantly, Rag2-deficient mice displayed significantly improved behavior when compared with WT MPTP- treated counterpart. $Rag2^{-/-}$ mice do not develop impairments when compared with its untreated counterpart even after 5 weeks of starting chronic MPTP treatment (Fig. 7). This evidence suggests that neuroprotection afforded by Rag2 deficiency translates into motor movement preservation and that surviving DA neurons are indeed functional.

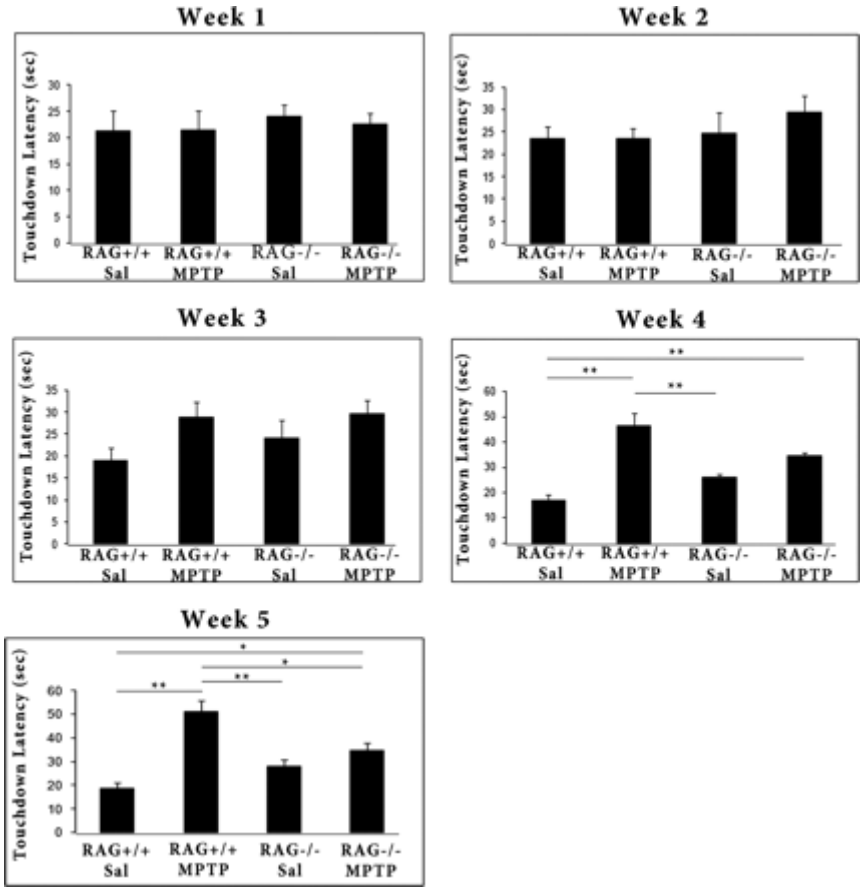


**FIGURE 7.**

**Rag2$^{-/-}$ mice are resistant against MPTP-induced motor movement impairments, unlike Rag2$^{+/+}$ littermate mice.** The pole test was given to mice throughout the dosing paradigm, as described under "Experimental Procedures." The time of descend to the ground was recorded after mice were individually placed upright near the top of a 2-foot pole. *Sal*, saline. *Error bars* represent mean ± S.E. ANOVA, *, $p < 0.05$; **, $p < 0.01$; *n* = six to eight animals per group.

**Fcγ Receptors Play a Role in the Protracted Paradigm of MPTP Induced Loss**

The evidence above supports a role for the adaptive immune system. However, the contribution of any humoral response cannot be ascertained using Rag mice because both T and B cells are affected. To more carefully evaluate the potential role of the humoral response, we next examined the role of FcγRs in our protracted MPTP paradigm. Importantly, chronic MPTP treatment induces less DA cell body degeneration in $Fc\gamma R^{-/-}$ mice compared with their $Fc\gamma R^{+/+}$ littermates (Fig. 8). However, this protection was less than that afforded by Rag2 deficiency (Fig. 2).

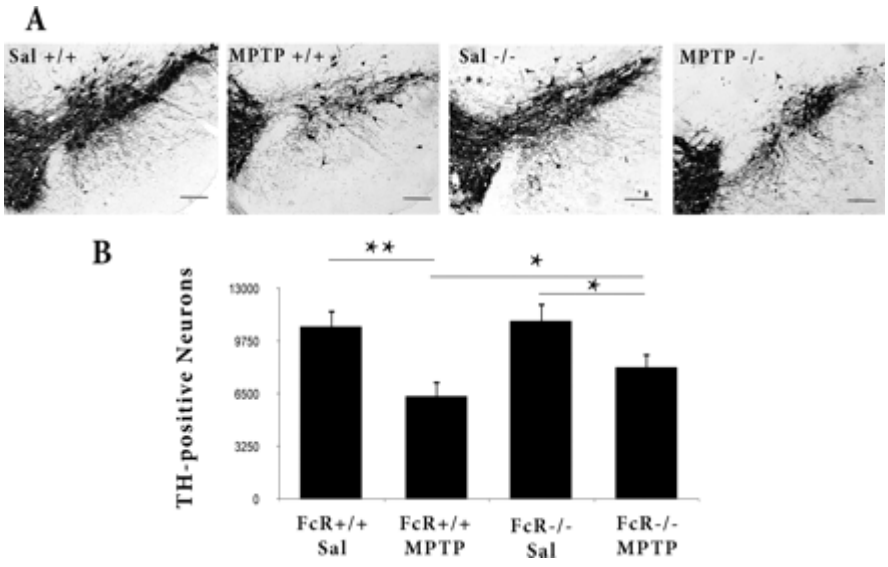


**FIGURE 8.**

**$Fc\gamma R^{-/-}$ mice exhibit attenuated DA cell loss after chronic MPTP treatment.** *A*, representative photomicrographs of TH+ cells in the SN*pc* of the indicated littermate treatment groups. *B*, quantification of dopaminergic cell bodies 5 weeks after the start of saline (*Sal*) or chronic MPTP intoxication by stereology, as described under "Experimental Procedures." *Scale bars* = 250 μm. *Error bars* represent mean ± S.E. ANOVA, *, $p < 0.05$; **, $p < 0.01$; $n$ = five to seven animals per group.

This partial neuroprotection afforded in the SN*pc* extends down the nigrostriatal axis, as demonstrated by our immunohistochemical analysis of the striatum for dopamine terminal loss. Striatal density of both TH and DAT were significantly increased in FcγR$^{-/-}$ mice when compared with WT littermate controls (Fig. 9). Similarly, improvements in both dopamine and HVA levels as measured by HPLC were observed in the FcγR-deficient mice (Fig. 10). This protection, particularly with the dopamine, was relatively mild, however. Striatal ΔFosB staining was also attenuated in FcγR-deficient mice treated with chronic MPTP when compared with WT MPTP-treated controls (Fig. 11). Finally, CD11b expression was also attenuated with FcγR deficiency in response to chronic MPTP when compared with WT controls (Fig. 12).

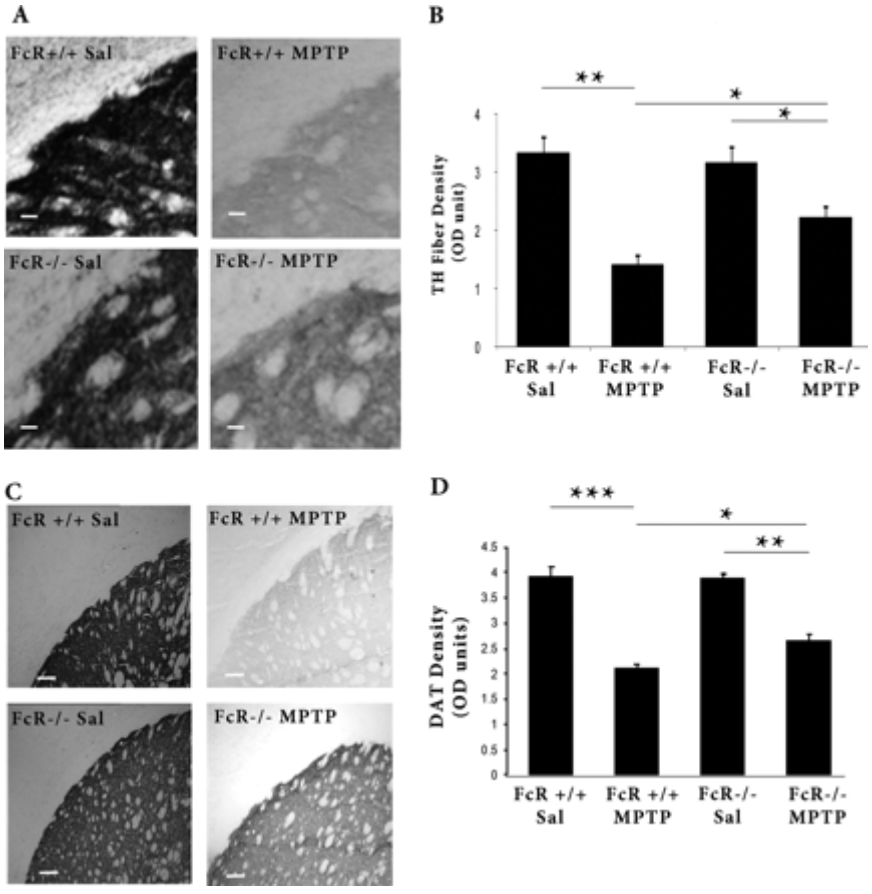

**FIGURE 9.**

**Dopamine nerve terminals are protected in FcγR$^{-/-}$ mice treated with chronic MPTP.** *A*, representative photomicrographs showing TH+ fiber density from the striatum of indicated littermate treatment groups. *Sal*, saline. *B*, optical density quantification of striatal TH+ fiber density. *C*, representative photomicrographs of striatal sections stained for DATs from indicated littermate groups. *D*, optical density quantification of striatal DATs. *Scale bars* = 50 μm in (*A*) and 200 μm (*C*). *Error bars* represent mean ± S.E. ANOVA, *, $p < 0.05$; **, $p < 0.01$; ***, $p < 0.001$; $n$ = six to eight animals per group.

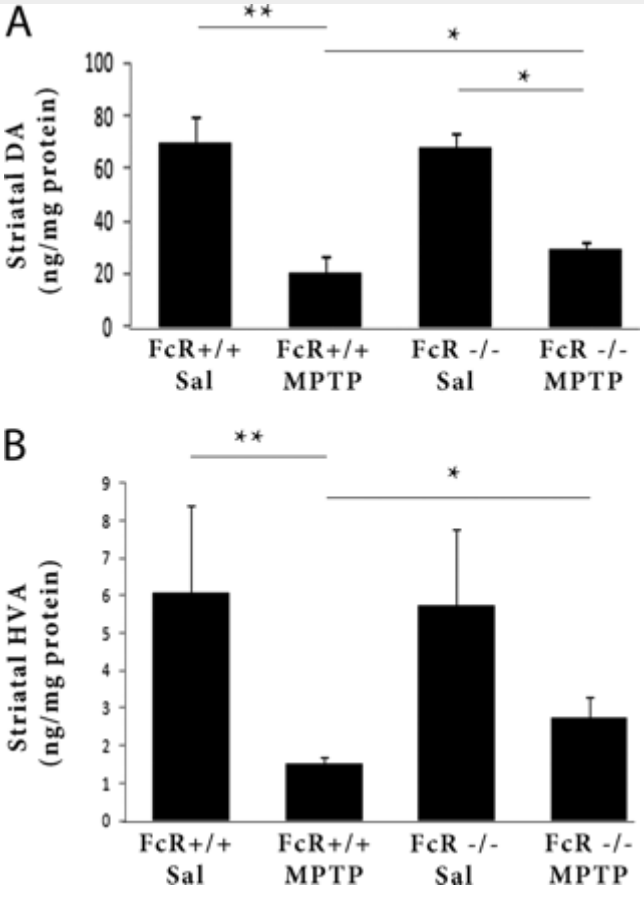


**FIGURE 10.**

**DA and HVA levels in striatum of FcγR$^{-/-}$ mice.** Levels of DA and HVA were measured using HPLC from striatal punch biopsies of the indicated littermate treatment groups. *Sal*, saline. *Error bars* represent mean ± S.E. ANOVA, *, $p < 0.05$; **, $p < 0.01$; $n$ = five to six animals per group.

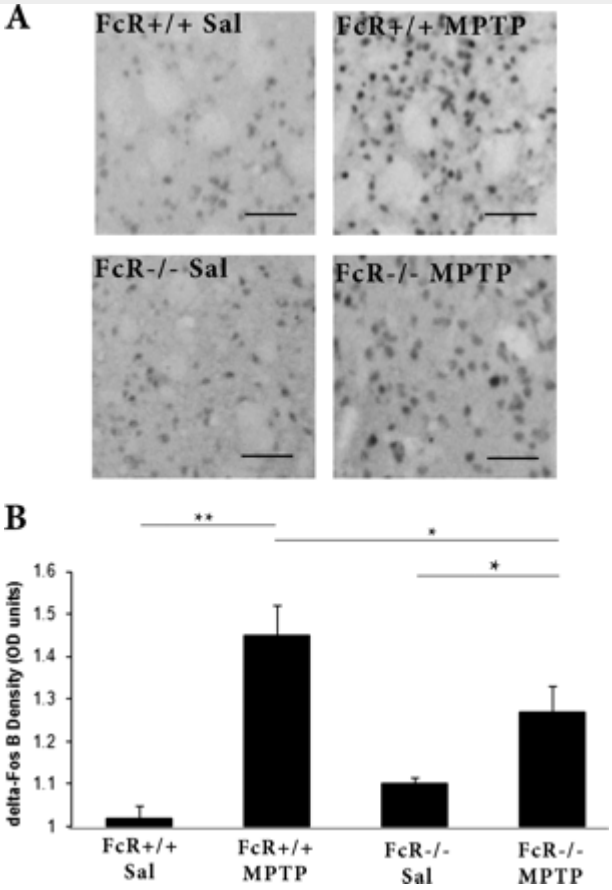


**FIGURE 11.**

**FcγR$^{-/-}$ mice treated with chronic MPTP exhibit reduced expression of striatal Δ-Fos B.** *A*, representative photomicrographs illustrating ΔFosB immunoreactivity in the striatum. *Sal*, saline. *B*, quantification of striatal ΔFosB optical density. *Scale bars* = 100 μm. *Error bars* represent mean ± S.E. ANOVA, *, $p < 0.05$; **, $p < 0.01$; $n$ = six to eight animals per group.

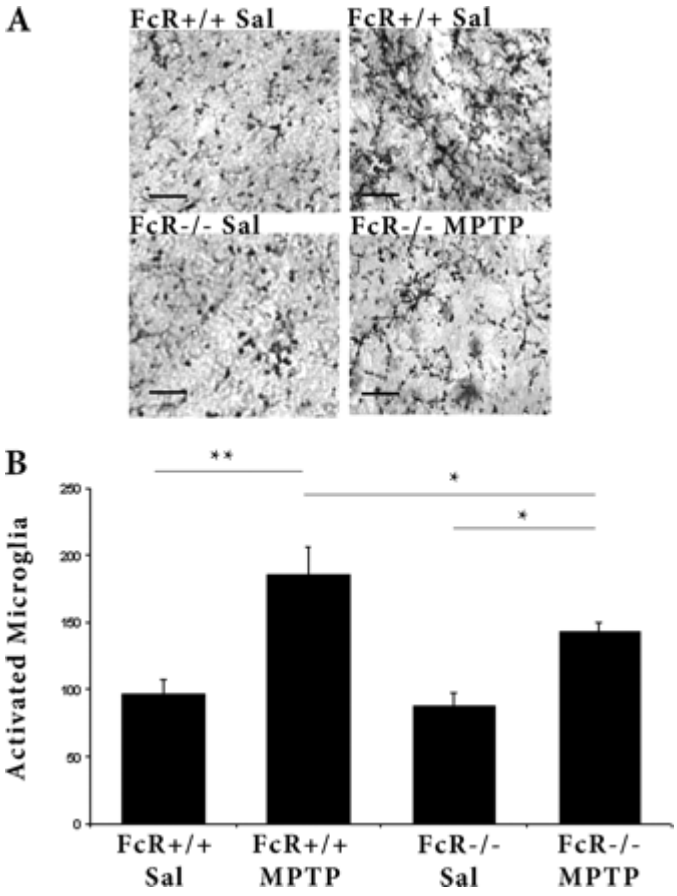


**FIGURE 12.**

**FcγR$^{-/-}$ mice exhibit less neuroinflammation.** *A*, representative photomicrographs of microglia stained with anti-CD11b. *Sal*, saline. *B*, quantification of morphologically activated microglia around the MT nucleus of the ventral SN*pc*. *Scale bars* = 100 μm. *Error bars* represent mean ± S.E. Representative photomicrographs of TH+ cells in the SN*pc* of the indicated littermate treatment groups. ANOVA, *, $p < 0.05$; **, $p < 0.01$; $n$ = six to eight animals per group.

The pole test was administered to the FcγR mice throughout the dosing paradigm to corroborate the histological findings. After 3 to 5 weeks of chronic MPTP administration, FcγR$^{+/+}$ mice developed motor movement deficits (Fig. 13). Consistent with our

histological protection and ΔFosB results, FcγR$^{-/-}$ mice were significantly protected from these deficits at weeks 3 and 4. However, the behavioral improvement was transient because the deficit was again observed at week 5. Other tests, such as the 24-h beam break locomotion test, showed no difference in any groups as described with the Rag2 mice above (data not shown).

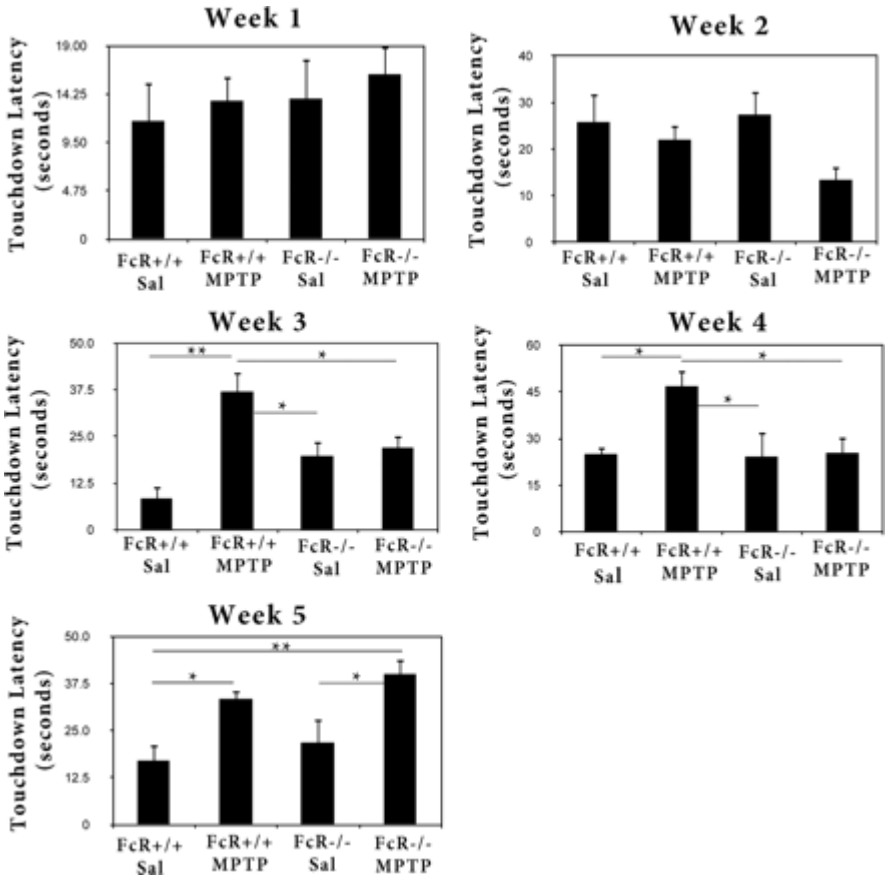


**FIGURE 13.**

**FcγR$^{-/-}$ mice are resistant against early MPTP-induced motor movement impairments, unlike FcγR$^{+/+}$ littermates mice.** Pole test analysis of mice treated with saline (*Sal*) or MPTP during the 5-week paradigm. *Error bars* represent mean ± S.E. ANOVA, *, $p < 0.05$; **, $p < 0.01$; $n$ = six to eight animals per group.

**Rag2- but Not FcγR-deficient Mice Are Resistant to More Acute MPTP Toxicity**

Our results above with the FcγR$^{-/-}$ mice support a role of the humoral arm of the adaptive immune response in chronic MPTP-induced loss. To further support this notion, we reasoned that the FcγR under a more acute MPTP paradigm of death will not functionally participate in DA neuron death. Consistent with this model, FcγR$^{+/+}$ mice and their FcγR$^{-/-}$ littermates exhibit equal DA neurotoxicity after acute MPTP treatment (Fig. 14). Note that this is not to imply that the more acute MPTP paradigm does not activate the humoral response. Indeed, acute MPTP treatment has been reported to elicit antibody generation to selective epitopes (2). However, the functional consequences of such activation are diminished likely because of the more rapid onset of DA loss.

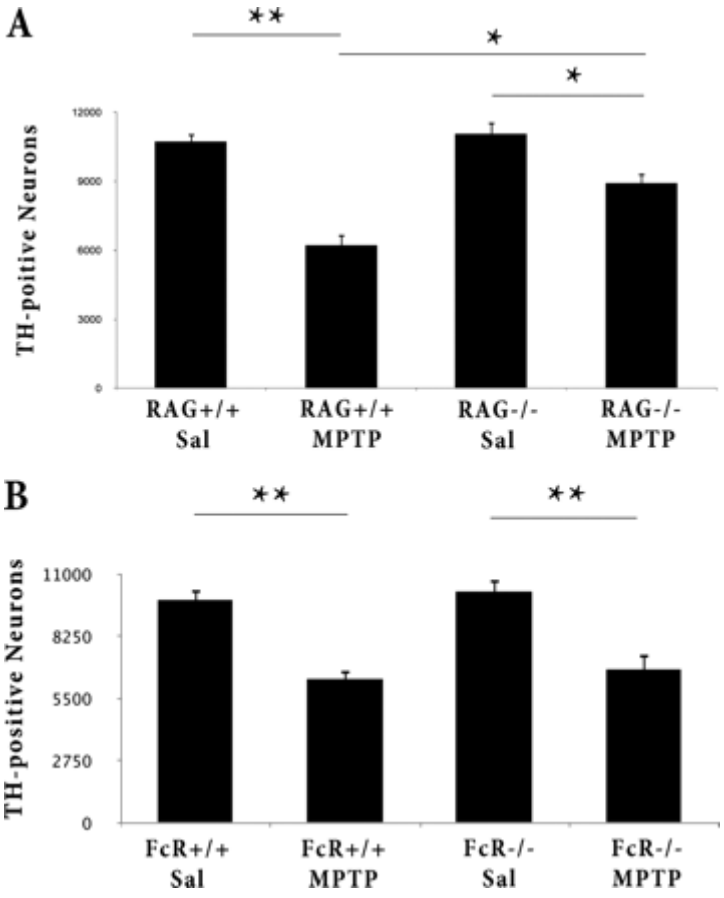

**FIGURE 14.**

**Rag2$^{-/-}$ mice but not FcγR$^{-/-}$ mice display attenuated TH+ cell loss after acute MPTP administration.** Quantification of dopaminergic cell bodies in the SN*pc* of Rag2 mice (*A*) and FcγR mice (*B*) after acute MPTP intoxication by stereology, as described under "Experimental Procedures." *Error bars* represent mean ± S.E. ANOVA, **, $p < 0.01$; $n$ = five to six animals per group.

We also tested Rag2-deficient mice in this acute paradigm. Consistent with previous reports of T- and B cell-deficient mice (2, 13), these Rag2$^{-/-}$ mice were also significantly protected from acute MPTP induced loss, similar to our more chronic paradigm (Fig. 14).

# DISCUSSION

Growing evidence suggested the participation of the humoral response in PD. These data include the observations of IgGs from PD patients reacting with dopamine neurons (16) and IgG deposition in lewy bodies (29). Altered peripheral humoral function has also been reported in PD patients, and elevated levels of IgGs to heat shock proteins were described (30). B cell and T cell infiltrates have also been demonstrated in an α-synuclein overexpression model of PD (31). We set out to provide more functional data on the required nature of this response as well as shed light on which antibody effector function may promote dopaminergic degeneration. To achieve this, we developed a more protracted/chronic MPTP model potentially more conducive to participation of a humoral response in DA degeneration. Histological analysis of wild-type mice indicates that 1 month of protracted MPTP treatment elicits significant DA neuron loss in the SN*pc*. DA neuron injury is observed later in the dosing paradigm. The loss of DA cell bodies was accompanied by nerve terminal degeneration and compensatory changes in postsynaptic striatal neurons. Moreover, mice incur motor movement impairments late in the MPTP dosing paradigm. This delayed and progressive neurodegenerative nature is consistent with the temporal expression of the adaptive immune response. Likewise, it more closely resembles PD pathogenesis than traditional acute MPTP treatment, which elicits more rapid neurotoxicity.

Using this model, we first detected $Rag2^{-/-}$ mice to have less dopaminergic death than littermate WT controls. Rag2-deficient mice have a disruption in the recombination activating gene 2. This gene produces an enzyme critical in the generation of T and B cell

receptors. Therefore, these mice are devoid of mature T and B cells (the major cellular components of the adaptive immune response) and are unable to produce antibodies (32, 33). In addition, this protection was associated with reduced terminal loss, significant preservation of dopamine levels, improvement in markers of postsynaptic function, and improved behavioral outcomes. These results are consistent with previous reports of protection mediated by a number of immune-compromised mice following more acute paradigms of MPTP exposure (2, 13).

After confirming lymphocytic involvement in our chronic model, we next looked at potential downstream effectors, in particular FcγR function, because of its involvement in antibody-microglia interactions and its importance in adaptive immunity (1). The FcγR$^{-/-}$ mice we used are deficient in a γ chain that is required for receptor assembly and signal transduction of FcγRIII and FcεRI receptors (34). Accordingly, FcγR deficiency leads to a functional impairment of macrophages/microglia, neutrophils, mast cells, basophils, and NK cell binding capabilities for IgGs (34). As with the Rag mice, FcγR-deficient mice also showed significant protection in all the parameters examined. However, the protection observed in FcγR$^{-/-}$ mice was qualitatively less than that observed with Rag2$^{-/-}$ mice. For example, although behavioral improvements were observed with FcγR deficiency, this protection was transient. The potential reasons for this are several. Rag2 deficiency eliminates multiple arms of the adaptive immune response, whereas FcγR deficiency is obviously more limited in this respect. Relevant to this, FcγR involvement does not occur in more acute paradigms of MPTP, whereas Rag2 deficiency is protective in both acute and chronic models. Nonetheless, our results clearly demonstrate the

involvement of FcγR in dopaminergic loss induced in a system where the adaptive immune system is allowed to develop fully.

Our observations of FcγR involvement in MPTP-induced toxicity is consistent with other reports that FcγR is up-regulated in postmortem PD brains (35) and following MPTP treatment in experimental animal models (14, 15, 17). IgGs produced against DA neurons could promote neurodegeneration via the FcγR (31, 35, 36). Upon engaging antibodies in the CNS, FcγR causes the activation of immune cells, secretion of neurotoxic and neuroinflammatory factors, and stimulates phagocytosis in processes termed antibody-dependent cell-mediated cytotoxicity and antibody-mediated phagocytosis, respectively (37, 38). The role of FcγRs on microglia activation are a particularly interesting possibility, provided the large number of resident immune cells in the nigral region and a large number of reports suggesting the importance of these cells in nigral degeneration (39). An initial microglial response as part of the innate immune response is consistent with a role of inflammation in PD. However, the humoral immune response may interact with the innate inflammatory system, leading to a more sustained response (1, 40). Consistent with this view, we showed that FcγR$^{-/-}$ mice demonstrate less microglial activation when compared with their control littermates.

Our results, as well as those of others with a variety of immune-compromised animal models, clearly suggest the importance of the cellular adaptive immune response following MPTP treatment. Helper T cells likely play a major role in this degeneration because CD4-deleted mice specifically show decreased degeneration (13). How T cells are activated in the context of MPTP is unclear. MPTP treatment has been shown to not only elicit lymphocytic infiltration but also to increase expression of microglial MHC

class II antigen (14, 15). The nature of potential antigens eliciting an adaptive response is unclear. However, there have been numerous proposals of "neopeptide" generation initiated by oxidative stress. For example, microglia generate superoxide and nitric oxide that can rapidly interact to form the peroxynitrite (ONOO-), a highly reactive oxidative species capable of traversing cell membranes and causing lipid peroxidation, DNA damage, mitochondrial inhibition, and nitrotyrosine formation (41, 42). DA quinine has also been shown to be equally reactive. These oxidized molecules may serve as epitopes stimulating an adaptive response.

One proposed neopeptide is nitrosine-modified synuclein. A single injection of MPTP in squirrel monkeys was sufficient to cause a buildup of α-synuclein in midbrain DA neurons, which stained positive for nitratred and phosphorylated α-synuclein (43). MPTP treatment also causes nitrosine-modified α-synuclein buildup in cervical lymph nodes of mice (2). These mice also mice generate antibodies to native and nitrated α-synuclein. We propose that the generation of the humoral response such as that observed above and consequent activation of Fcγ receptor complexes is critical to mediate both the microglial response and dopaminergic degeneration in more chronic models of MPTP toxicity.

Taken together, these data further support the critical nature of the adaptive immune system in DA neuron injury in a mouse model of PD. The discovery of this role has profound implications for how we view PD as a neurodegenerative disease that relies, at least in part, on both the innate and adaptive immune response to mediate degeneration.

## Acknowledgments

We thank Dr. Harry Atkins and Dr. Serge Przedborski for help in editing this manuscript.

**Footnotes**

↵* This work was supported by grants from the Canadian Institutes of Health Research (CIHR), the Heart and Stroke Foundation of Ontario (HSFO), the Parkinson's Disease Foundation (PDF), the Parkinson's Society of Canada (PSC), Michael J. Fox Foundation, Neuroscience Canada, the Centre for Stroke Recovery (CSR) Canadian Stroke Network, and World Class University program through the National Research Foundation of Korea funded by the Ministry of Education, Science and Technology, South Korea Grant R31-2008-000-20004-0.

# CHAPTER 4

## General Discussion.

## Interferon-γ and Microglia Neurotoxicity:

We established a comprehensive *in vitro* PD model to study microglia neurotoxicity. Firstly we determined the dose response concentrations of rotenone that will elicit significant and selective DA cell death. Concentrations of rotenone below 25nM selectively killed dopamine neurons and no other midbrain cells. This toxicity was evident only in co-cultures supplemented with microglia, not neuron-enriched midbrain cells. Selective DA neurotoxicity was confirmed by a marked reduction in TH immunoreactivity, while Hoechst staining remained unchanged. Increasing the concentration of rotenone caused non-specific neurodegeneration.

This co-culture paradigm has advantages over traditional *in vitro* models, given that the neurodegeneration elicited is selective for dopaminergic cells and better mimics PD. In addition, the dependence of dopaminergic cell loss on microglia is desirable for studying innate immune pathways, which in recent years have become a pathological feature of PD.

Our laboratory detected elevated levels of the IFN-γ in the blood plasma of PD patients, which piqued our curiosity. Its elevation was highest out of all the cytokines tested, even more than TNF-alpha, which was previously shown to mediate LPS-induced damage of DA neurons. Prior to this point in time, little was known about IFN-γ's involvement in dopamine neuron loss. Furthermore, it was not known if the blood plasma levels of the proinflammatory cytokine correlated with those in the brain, and no reports had previously documented IFN-γ production in the central nervous system. We sought to answer all these questions using our inflammatory co-culture model. Given that microglia are macrophages, we hypothesized they would produce IFN-γ when

activated by rotenone. Moreover, IFN-γ is a potent proinflammatory, thuswe predicted it would drive microglial neurotoxicity.

Rotenone-induced dopamine neurodegeneration was prevented in co-cultures by administering a neutralizing antibody for IFN-γ. A control, non-specific antibody was not protective under the same conditions. Moreover, the addition of exogenous IFN-γ ligand alone to the co-cultures, without rotenone, triggered a selective loss of DA neurons. This neurotoxicity was only evident in neurons-enriched midbrain cultures that were supplemented with microglia. By the use of neutralizing antibodies or exogenous ligands in our co-culture system, we determined IFN-γ mediates microglial neurotoxicity. This fits in line with our hypothesis, and sheds light on its signaling dynamic, given that microglia are required for IFN-γ toxicity. Furthermore, it highlights a potential therapeutic approach to attenuate DA neuron death. Highlighting IFN-γ's involvement is a big accomplishment, in view of the lack of pre-existing evidence implicating it in DA cell death.

Another significant discovery was the detection of IFN-γ messenger transcripts from microglia-enriched cultures. Using RT-PCR analysis, we confirmed microglia treated with rotenone produce IFN-γ mRNA. Production of IFN-γ messenger transcripts increased when microglia were given higher doses of rotenone. IFN-γ was not thought to be produced in the CNS, making us the first group to discover this important finding. This broadens neuroimmunologist's perspective of this proinflammatory cytokine in the CNS, not only for PD but any neurological condition that interacts with the immune system. Additionally, this finding may partially account for the elevated levels of IFN-gamma in the blood.

We further delineated IFN-γ's involvement in DA cell loss by studying its signaling mechanism. Neuron-enriched midbrain cultures were supplemented with IFN-γ receptor deficient microglia, and in the alternative experiment we added wild-type microglia to IFN- γ receptor deficient neuron-enriched midbrain cultures. In doing so, we discovered IFN-γ receptor deficient microglia protect dopamine neurons against rotenone; however neuron-enriched midbrain cells lacking the IFN-γ receptor did not protect. These experiments show IFN-γ receptors on microglia, not neurons, participate in our model of dopamine neuron death, and serve as a valuable analytical tool in delineating IFN-γ's mode of signaling during microglia neurotoxicity.

The *in vitro* data underscore the role of IFN-γ in rotenone induced-dopaminergic cell loss. Our research findings elucidate upon a proinflammatory cytokine that was not well understood in the context of PD pathology. We discovered rotenone activated microglia produce IFN-γ, which consequently acts in an autocrine manner to drive microglial neurotoxicity. Together, our *in vitro* data reveals IFN-y's involvement in DA cell by regulating microglial activity. Highlighting its signaling mechanism elucidates upon potential therapeutic targets that can be utilized to protect DA neurons in PD.

## The Adaptive Immune Response:

IFN-γ and microglial activity are not limited to the innate neuroinflammatory reaction, they are also critical for the adaptive immune response in the CNS. Microglia,the most efficient antigen presenting cells in the brain, also possess Fcγ receptors, which are important mediators of the antibody response. IFN-γ performs several functions to prime adaptive immune reactions (Schoenborn *et al*., 2007). Having studied microglia neurotoxicity in vitro, we broadened our scope to examine the response of the adaptive immune system in a specialized *in vivo* mouse model of PD.

Despite growing evidence implicating adaptive immunity in DA cell death, it remains unclear whether it has a definite role in the pathogenesis of PD. Early findings implicating the adaptive immune system in the pathogenesis of PD were disjointed and unable to experimentally observe the full response (Han *et al*., 2012; He *et al*., 2002; Orr *et al*., 2005; Chen *et al*., 1998; Carvey *et al*., 1991). Our research goal was to observe the full adaptive immune system in a specialized model where injury or modifications to DA neurons would invoke an antibody response against them. Mechanistically, we followed the entire adaptive immune system to determine which of its key players are involved in DA neuron death.

We hypothesize a protracted, low dose MPTP paradigm will elicit the adaptive immune response by making antigenic dopaminergic modifications. Moreover, we predict interfering with lymphocytes or Fcγ receptors will disrupt the adaptive immune system's ability to synthesize antibodies and kill DA neurons of the SN*pc* via antibody-mediated phagocytosis and antibody-dependent cell–mediated cytotoxicity, respectively.

By administering low doses of MPTP over a 4 week period, we created a novel *in vivo* model of PD, specially tailored to invoke the adaptive immune system. The use of this new paradigm generated several key findings. WT mice treated with our protracted MPTP paradigm exhibit a significant loss of dopaminergic cells in the SN*pc* (Figure 1 and 2). This is marked by a dramatic reduction of dopamine fiber density in the striatum (Figure 3). The loss of DA neurons is also reflected in the striatum by a marked reduction in DAT staining (Figure 3), and an increased delta-Fos B expression (Figure 5). Additionally at the end of the protracted MPTP paradigm, microglia activation was detected in the SN*pc,* compared to mice treated with saline (Figure 6).

A midpoint group of mice treated with MPTP and sacrificed 14 days after the start of injections did not to incur significant DA neuron loss (Figure 1). This implies dopaminergic neurodegeneration occurs late in the paradigm, and is in line with the time required for the adaptive immune response to detect antigens and synthesize antibodies against them. According to this temporal relationship between MPTP intoxication and DA cell loss, our novel death paradigm is suited to study a more developed, full adaptive humoral response. Also, the delayed and progressive neuron death better mimics the progressive degenerative nature in PD, rendering it advantageous over conventional acute MPTP treatment that elicits more immediate neurotoxicity.

Our novel protracted MPTP paradigm is a significant contribution to PD research. Given DA neuron death is delayed, progressive and allows for the full manifestation of the immune system, our protracted MPTP paradigm is superior to traditional acute MPTP treatment.

To assess the involvement of the humoral immune response, we used our protracted MPTP paradigm to intoxicate two types of mice with mutations affecting their adaptive immune system. The first objective was to determine the contribution of T and B cells in DA neuron death. Whereas WT mice treated with MPTP incur a dramatic loss of DA cells, Rag2 -/- mice (devoid of T and B) cells suffered significantly less neurodegeneration (Figure 2). Alongside examining dopamine cell body loss in the SN*pc*, we looked at the caudate and putamen for signs of dopaminergic denervation. We found significant protection in the levels of dopamine transporters and dopamine fiber density from Rag2 -/- mice compared to wild-type controls treated with MPTP (Figure 3). Concurrently, Rag2 -/- mice exhibited improved levels of striatal delta-Fos B (Figure 5). Neuroinflammation was also reduced in Rag2-/- mice, as indicated by reduced cd-11b staining within the SN*pc* (Figure 6). Upon reconstituting with wild-type splenocytes, Rag2 -/- mice regained sensitization to MPTP (Figure 2). Therefore our data suggests T and B cells are involved in protracted MPTP-induced dopamine neuron death.

Previously Rag2 -/- mice intoxicated with an acute MPTP paradigm and showed involvement of cytotoxic T cells (Brochard *et al*., 2009). Different MPTP paradigms will elicit different mechanism of neuron death. Our experimental set-up is arguably superior in terms of neurotoxin dosage and allowing sufficient time for the full activation of the adaptive immune response. For these reasons, we contend the protracted MPTP paradigm is advantageous over traditional models and elicits neuron death pathways that are more clinically relevant in the context of PD.

To further investigate the mechanism by which lymphocytes exacerbate DA neuron loss, we looked downstream at the involvement of the Fcγ receptor. We

hypothesized IgGs are involved in DA cell loss, and hence treated Fcγ receptor deficient mice to our protracted MPTP paradigm. These mice demonstrated significant dopaminergic neuroprotection in the SN*pc* and striatum after 5 weeks of MPTP administration (Figure 8). This was marked by reduced DA cell loss and improved DAT, DA fiber density (Figure 9) and delta-FosB levels (Figure 11). Neuroprotection was also accompanied with attenuated microgliosis in the SN*pc* (Figure 12). These findings reinforce our hypothesis that antibodies against DA neurons are engaging Fcγ receptors to trigger neurodegeneration.

This is the first time the Fcγ receptor's contribution to DA cell loss has been observed using an *in vivo* MPTP model of PD. As proposed in our model, microglial Fcγ receptor engage antibodies targeting DA neurons, in turn invoking antibody-mediated phagocytosis or antibody-dependent cell–mediated cytotoxicity. We anticipate this to be a significant cause of DA cell death, and acknowledge some degree of direct MPTP neurotoxicity. Likewise, neurodegeneration may stem from antibodies directly binding and interfering with the normal trafficking properties of DA neurons, or antibodies recruiting the complement system. This indeed may be the case, given the partial protection afforded by the absence of the Fcγ receptors is not as significant as that observed in Rag2 -/- mice.

Previous scientists had shown an anecdotal connection concerning Fcγ receptors and DA cell death (Kurkowska-Jastrzebska *et al*., 1999a; Kurkowska-Jastrzebska *et al*., 1999b; Hunot *et al*., 1999). However, we are the first to show the causal relationship between dopamine neuron injuries triggering an antibody response that hinges on Fcγ

receptors. Accordingly, our research findings render our Fc receptor study more comprehensive and relevant to PD pathology.

Our histological data were corroborated with biochemical measurements of DA and its metabolite homovallinic acid from striatal biopsies. Whereas wild-type mice intoxicated with MPTP incurred a profound reduction in DA and HVA levels, both Rag2 -/- and Fcγ receptor deficient mice exhibited less of a deficit (Figure 4 and 10).

The biochemical data is important to assess the functionality of SN*pc*. Likewise, behavioural tests were conducted to ascertain nigrostriatal axis function. Every week throughout the dosing paradigm, the groups of mice performed three behavioural exams. The pole test is a more physically demanding probe of the motor system and coordination. It demonstrated wild-type mice treated with MPTP became slower the more intoxicated they became with MPTP. Particularly they required more time to descend the pole to the ground, after 3-4 weeks of MPTP intoxication (Figure 7 and 13). This motor deficit is consistent with the observed reduction of dopaminergic neurons in the SN*pc* of mice treated with our MPTP paradigm. Motor system impairments were delayed and progressive, similar to the neurodegenerative profile of dopaminergic neurons. This physical debilitation also mimics the motor decline of PD patients, further validating the superiority of our protracted MPTP paradigm over traditional acute PD models.

Conversely, Rag2 -/- mice did not incur such motor movement impairments, compared to their wild-type littermates (Figure 7). After four weeks of MPTP treatment, Rag2 -/- mice did not take longer to climb down the pole than saline treated control mice. This finding suggests the surviving DA neurons in Rag2 -/- mice treated with MPTP are

indeed functional. Exactly how long the histological and behavioural protection lasts remains to be determined, however it is a clear indication that lymphocytes are contributing to PD-like syndrome in mice.

In the same pole test, Fcγ receptor deficient mice exhibited resistance against MPTP-induced motor deficits, compared to WT controls (Figure 13). However this behavioural protection was observed early in the MPTP paradigm, and did not persist in the final week of dosing. Again suggesting the antibody response eventually mediates DA degeneration through alternative mechanisms besides the Fcγ receptor.

Further behavioural examinations included the micromax beam break experiment and water stress test. Each exam is designed to monitor the motor activity of mice. The micromax is a cage where mice are placed for 24 hours. Every time they move an infrared beam is broken and recorded by a computer. The water stress is accomplished by dropping mice in a 4-liter beaker of water and letting them swim for 1 minute. Subsequently, the mice are placed in the micromax and their movements are recorded for 2 hours. The purpose of stressing the mice is to reveal any underlying motor movement impairments that may not arise under normal conditions. The micromax beam break and water stressor behavioural test did not reveal a motor deficit in mice treated with MPTP. This is likely because the SN*pc* lesion is relatively small, does not manifest physical symptoms at rest. Thus the more strenuous pole test was capable of revealing a smaller lesion, given it requires more basal ganglia function.

In humans, the majority of DA neurons in the SN*pc* degenerate before clinical manifestation of PD symptoms. Also, stress tends to bring out these physical symptoms.

Similarly in rodents, a relatively small lesion in the SN*pc* will not become noticeable without challenging the motor movement and coordination.

The pole test is more physically demanding and requires more basal ganglia function than the other two behavioural exams. This explains how a relatively small SN*pc* lesion can be detected using the pole test and not the less rigorous behaviour tests. Understanding how different behavioural test detect basal ganglia lesions, is a useful tool in validating models of PD. More taxing behavioural analyses, like the pole test, should be used to more carefully assess the integrity of the motor circuit. The histological and behavioural protection observed in the Fcγ receptor deficient mice warrants a closer look at the nature of the gamma chain of this receptor.

The FcRγ chain is the signal generating subunit of Fc gamma receptors, Fc alpha receptors, and Fc epsilon receptors (Otten *et al*., 2004; Suzuki *et al*., 1998). It is required in the cell surface expression of the high affinity FcγRI (Hulett *et al*., 1998), low affinity FcγRIIIA, and the high affinity Fc epsilon RI (Suzuki *et al*., 1998).

FcγRI is found on macrophages, dendritic cells, eosinophils, and neutrophils. It contains a signal peptide for transport to the cell membrane, 3 extracellular C2-type immunoglobulin domains for high affintity binding IgG-type antibodies, a hydrophobic transmembrane domain, and lastly a cytoplasmic tail (Ernst *et al*., 1998). Upon binding IgG, FcγRI interacts with the immunoreceptor tyrosine-based activation motif (ITAM) of its γ chain (Szalai *et al*., 2005). This is the signal generating interaction required for cellular activation, phagocytosis and induction of the respiratory burst (Nimmerjahn *et*

*al*., 2006). Macrophages from mice lacking the γ subunit cannot phagocytose antibody-covered particles (Takai *et al*., 1994).

ITAM is made up of a tyrosine residue separated by any two amino acids from either a leucine or isoleucine residue (Pan *et al*., 2003). Two ITAMs are separated in the cytoplasmic tail by 6-8 amino acids. When FcγRIIA engages its ligand, tyrosine kinases add phosphate groups to the tyrosine residues triggering an intracellular signalling cascade. Intracellular activation includes influx of calcium, phagocytosis, antigen presentation, and interleukin-2 production (Van den Herik-Oudijk *et al*., 1995). If only one YXXL sequence is present, it is not sufficient to activate the cell; rather it generates an inhibitory signal. This motif is called ITIM, immunoreceptor tyrosine-based inhibitory motif and is found in the FcγRIIB1 and FcγRIIB2. The inhibitory signal is mediated by the phosphatases SHP-1 and SHIP-1, which remove phosphates from tyrosine residues (Huang *et al*., 2003).

The FcγRIIB transduces an inhibitory signal through the immunoreceptor tyrosine-based inhibition motif (Szalai *et al*., 2005). The cell surface expression of the FcγRII is unaffected in mice lacking the γ chain (Cao *et al*., 2012). Negative signaling by FcγRIIB is primarily observed in regulation of activated B lymphocytes and mast cells (Takai *et al*., 1996; Van den Herik-Oudijk *et al*., 1995).

The FcγRIIIA is expressed on NK cells and macrophages. It is involved in antibody-dependent cell-meditated cytotoxicity and macrophage induction of cytokine release, including TNF-alpha and IFN-γ (Dhanji *et al*., 2005). The cytokine release by these cells promotes the adaptive immune response (Dhanji *et al*., 2005). Indeed IFN-γ has been shown to bridge the innate and adaptive immune system (Palucka *et al*., 1999).

The Fc epsilon receptor I is formed by a tetrameric complex consisting of an alpha subunit acting as a binding site, a beta subunit that amplifies the downstream signal, and two γ chains connected by a disulphide bridge. Upon binding IgE-type antibodies, they stimulate cellular activation and degranulation associated with allergic responses. The Fc epsilon receptor I is expressed on mast cells and basophils, and it is inducible in eosinophils (Pawankar *et al*., 2001).

The Fc receptor γ subunit deficiency affects the functional expression of Fcγ receptor I, Fcγ receptor IIIA and Fc epsilon receptor I, however we did not distinguish in our study the effects mediated by each individual receptor, rather the deficiency of all three. Also, the γ chain is not only expressed in Fc receptors, but also the TCR/CD3 complex, alpha/beta and γ/delta T cells (Szalai *et al*., 2005; Hayes *et al*., 2003). CD3 is a T cell co-receptor composed of 4 chains, namely a CD gamma chain, a CD delta chain, and two CD epsilon chains. ITAM is common to these four chains in their cytoplasmic tails. Since the γ subunit is expressed in these receptors, it is possible that impairing their function also attributes to the observed protection in our Fcγ receptor deficient mice. This effect is likely a minimal given that mice deficient in the γ chain do not show impaired T cell function (Takai *et al*., 1994).

Likewise, for the interpretation of our results we must consider Fcγ receptors can also bind non-IgG ligands, including C-reactive proteins and complement receptors (Galon *et al*., 1996; Stein *et al*., 2000; Okun *et al*., 2010). As such it is possible that they contribute in some degree to the DA cell loss exhibited in our protracted MPTP model. Our novel protracted MPTP paradigm differs from traditional acute MPTP paradigms in

that it triggers different death pathways. To test whether the adaptive humoral response is involved early after dopamine neuron injury, we subjected Rag 2-/- and Fcγ receptor deficient mice to an acute MPTP paradigm. We did not expect the Fcγ receptor deficient mice to exhibit neuroprotection against acute MPTP, since it triggers a more rapid cell death mechanism that we believe to be antibody independent.

Rag2 -/- mice showed reduced DA cell loss after acute MPTP treatment, but not Fcγ receptor deficient mice. This novel finding highlights the temporal expression of the humoral arm of the adaptive immune system. In the acute MPTP paradigm, the loss of DA cells occurred at a faster rate than the adaptive immune system manifests itself. Our protracted cell death paradigm allows antibody synthesis to dopaminergic antigens, eliciting significant neurodegeneration. This is consistent with recent findings that early DA cell injury can expose alpha-synuclein modifications, which become antigenic and trigger the immune system to exacerbate PD pathology (Benner *et al*., 2008).

Conducting the acute MPTP paradigm was a useful analysis enabling the comparison of neuron death pathways. We determined acute MPTP toxicity is mediated in part by lymphocytes, but not an Fcγ receptor/IgG interaction. This data matches our hypothesis, and is consistent with Brochard's *et al* findings that cytotoxic T cells induced death after acute MPTP treatment. Conversely, protracted MPTP treatment invokes the antibody response. Therefore, employing the appropriate neurotoxin paradigm is critical for studying particular neuron death pathways. Our results validate the advent of a new model of PD to study adaptive immune responses.Taken together our *in vivo* data indicate that given ample time after MPTP-induced DA cell loss, the humoral arm of the adaptive immune systems is triggered, whereby Fcγ receptors play a critical role. Our data

highlight novel therapeutic targets that warrant further clinical investigation, such as receptors for IFN-γ and Fcγ on microglia, which were not previously thought to be involved in the pathogenesis of PD. We bring to light key innate and adaptive immunpathogenic responses contributing to DA neurons death, both of which are promoted by IFN-γ and contingent on microglial activity. Our data underscore the importance of controlling microglial activity as a therapeutic strategy to protect DA cells of the SN*pc*.

# REFERENCES:

Abbas N, Bednar I, Mix E, Marie S, Paterson D, Ljungberg A, Morris C,Winblad B, Nordberg A, Zhu J(2002) Up-regulation of the inflammatory cytokines IFN-gamma and IL-12 and down-regulation of IL-4 in cerebral cortex regions of APP(SWE) transgenic mice. J Neuroimmunol 126:50–57.

Adler, CH (2005) Nonmotor complications in Parkinson's disease. Movement Disorders 20: Suppl 11:23–9.

Aguzzi A, Barres BA, Bennett ML (2013) Microglia: scapegoat, saboteur, or something else? Science. 11;339(6116):156-61.

Aleyasin H, Rousseaux MW, Marcogliese PC, Hewitt SJ, Irrcher I, Joselin AP, Parsanejad M, Kim RH, Rizzu P, Callaghan SM, Slack RS, Mak TW, Park DS (2010) DJ-1 protects the nigrostriatal axis from the neurotoxin MPTP by modulation of the AKT pathway. Proc Natl Acad Sci 16;107(7):3186-91.

Aloisi F (2001) Immune function of microglia. Glia. 36(2):165-79.

Almer G, Vukosavic S, Romero N, Przedborski S(1999) Inducible nitric oxide synthase up-regulation in a transgenic mouse model of familial amyotrophic lateral sclerosis. J Neurochem 72:2415–2425.

Appel, S. H., Beers, D. R., and Henkel, J. S. (2010) T cell-microglial dialogue in Parkinson's disease and amyotrophic lateral sclerosis: are we listening? Trends Immunol. 31, 7–17.

Arai H, Furuya T, Yasuda T, Miura M, Mizuno Y, Mochizuki H (2004) Neurotoxic effects of lipopolysaccharide on nigral dopaminergic neurons are mediated by microglial activation, interleukin-1beta, and expression of caspase-11 in mice. J Biol Chem 279:51647–51653.

Arima K, Uéda K, Sunohara N, Arakawa K, Hirai S, Nakamura M, Tonozuka-Uehara H, Kawai M (1998a) NACP/alpha-synuclein immunoreactivity in fibrillary components of neuronal and oligodendroglial cytoplasmic inclusions in the pontine nuclei in multiple system atrophy. Acta Neuropathol. 96 (5): 439–44.

Arima K, Uéda K, Sunohara N, Hirai S, Izumiyama Y, Tonozuka-Uehara H, Kawai M (1998b) Immunoelectron-microscopic demonstration of NACP/alpha-synuclein-epitopes on the filamentous component of Lewy bodies in Parkinson's disease and in dementia with Lewy bodies. Brain Res. 808 (1): 93–100.

Badie B, Schartner J, Vorpahl J, Preston K (2000) Interferon-gamma induces apoptosis and augments the expression of Fas and Fas ligand by Microglia in vitro. Exp Neurol 162:290–296.

Banati RB, Daniel SE, Blunt SB (1998) Glial pathology but absence of apoptotic nigral neurons in long-standing Parkinson’s disease. Mov Disord 13:221–227.

Banerjee, R., Starkov, A. A., Beal, M. F., and Thomas, B. (2009) Mitochondrial dysfunction in the limelight of Parkinson's disease pathogenesis. Biochim. Biophys. Acta1792, 651–663.

Banks WA (2005) Blood-brain barrier transport of cytokines: a mechanism for neuropathology. Curr Pharm Des 11:973–984.

Barcia C, Sanchez Bahillo A, Fernandez-Villalba E, Bautista V, Poza YPM,Fernandez-Barreiro A, Hirsch EC, Herrero MT (2004) Evidence of active microglia in substantia nigra pars compacta of parkinsonian monkeys 1 year after MPTP exposure. Glia 46:402–409.

Beckman JS (1994) Peroxynitrite versus hydroxyl radical: the role of nitric oxide in superoxide-dependent cerebral injury. Ann N Y Acad Sci. 17;738:69-75.

Benner EJ. Banerjee R, Reynolds A, Sherman S, Pisarev V, Tsiperson V ,Nemachek C, Ciborowski P, Przedborski S., Mosley R., Gendelman H (2008) Nitrated alpha-synuclein immunity accelerates degeneration of nigral dopaminergic neurons. PLoS ONE 3(1):e1376.

Birnboim H., Lemay AM., Lam D., Goldstein R., Webb J (2003) Cutting edge: MHC class II-restricted peptides containing the inflammation-associated marker 3-nitrotyrosine evade central tolerance and elicit a robust cell-mediated immune response. J Immunol;171:528–532.

Blackinton J, Ahmad R, Miller DW, van der Brug MP, Canet-Avilés RM, Hague SM, Kaleem M, Cookson MR (2005) Effects of DJ-1 mutations and polymorphisms on protein stability and subcellular localization. Brain Res Mol Brain Res. 24;134(1):76-83.

Blaylock RL (2013) Immunology primer for neurosurgeons and neurologists part 2: Innate brain immunity. Surg Neurol Int.18;4:118.

Blanck G (2002) Components of the IFN-gamma signaling pathway in tumorigenesis. Arch Immunol Ther Exp (Warsz) 50:151–158.

Block ML, Hong JS (2007a) Chronic microglial activation and progressive dopaminergic neurotoxicity. Biochem Soc Trans 2007;35:1127-32.

Block ML, Zecca L, Hong JS (2007b) Microglia-mediated neurotoxicity: uncovering the molecular mechanisms. Nat Rev Neurosci;8:57-69.

Bonifati V, Meco G (1999) New, selective catechol-O-methyltransferase inhibitors as therapeutic agents in Parkinson's disease. Pharmacology and Therapeutics 81(1):1–36.

Bower JH, Maraganore DM, Peterson BJ, McDonnell SK, Ahlskog JE, Rocca WA (2003) Head trauma preceding PD: a case-control study. Neurology 27; 60(10):1610-5.

Bredesen DE, Rao RV, Mehlen P (2006) Cell death in the nervous system. Nature; 443:796-802.

Bredesen DE, Rao RV, Mehlen P (2006) Cell death in the nervous system. Nature. 2006 443(7113):796-802.

Brey RL (2006) Muhammad Ali's Message: Keep Moving Forward. Neurology Now (American Academy of Neurology) 2 (2): 8.

Brochard V, Combadière B, Prigent A, Laouar Y, Perrin A, Beray-Berthat V, Bonduelle O, Alvarez-Fischer D,Callebert J, Launay JM, Duyckaerts C, Flavell RA, Hirsch EC, Hunot S (2009) Infiltration of CD4+ lymphocytes into the brain contributes to neurodegeneration in a mouse model of Parkinson disease. J Clin Invest.; 119(1):182-92.

Bronstein JM, Tagliati M, Alterman RL, Lozano AM, Volkmann J, Stefani A, Horak FB, Okun MS, Foote KD, Krack P, Pahwa R, Henderson JM, Hariz MI, Bakay RA,Rezai A, Marks WJ Jr, Moro E, Vitek JL, Weaver FM, Gross RE, DeLong MR (2010) Deep Brain Stimulation for Parkinson Disease: An Expert Consensus and Review of Key Issues. Arch Neurol 68 (2): 165–165.

Brown TP, Rumsby PC, Capleton AC, Rushton L, Levy LS (2006) Pesticides and Parkinson's disease—is there a link? Environ Health Perspect. 114:156–164.

Burd C (2011) Physiology and Pathology of Endosome-to-Golgi Retrograde Sorting. 12(8): 948–955.

Butovsky O, Talpalar AE, Ben-Yaakov K, Schwartz M (2005) Activation of microglia by aggregated beta-amyloid or lipopolysaccharide impairs MHC-II expression and renders them cytotoxic whereas IFN-gamma and IL-4 render them protective. Mol Cell Neurosci 29:381–393.

Burkhardt H, Kalden JR, Schulze-Koops H (2001) Chicken and egg in autoimmunity and joint inflammation. Trends Immunol.; 22(6):291-3.

Cambier, J. C. (1997). Inhibitory receptors abound? Proc. Natl. Acad. Sci. U.S.A. 94 (12): 5993–5.

Canet-Avilés RM, Wilson MA, Miller DW, Ahmad R, McLendon C, Bandyopadhyay S, Baptista MJ, Ringe D, Petsko GA, Cookson MR (2004) The Parkinson's disease protein DJ-1 is neuroprotective due to cysteine-sulfinic acid-driven mitochondrial localization. Proc Natl Acad Sci U S A.15; 101(24):9103-8.

Cao S, Standaert DG, Harma A (2012) The gamma chain subunit of Fc receptors is required for alpha-synuclein-induced pro-inflammatory signaling in microglia. Journal of Neuroinflammation 9:259.

Cao S, Theodore S, Standaert DG (2010) Fcγ receptors are required for NF-κB signaling, microglial activation and dopaminergic neurodegeneration in an AAV-synuclein mouse model of Parkinson's disease. Mol Neurodegener. 26;5:42.

Cardona A, Pioro E, Sasse M, Kostenko V, Cardona S, Dijkstra I, Huang D, Kidd G, Dombrowski S, Dutta R, Lee J, Cook D, Jung S, Lira S, Littman D, Ransohof R (2006) Control of microglial neurotoxicity by the fractalkine receptor. Nature Neuroscience 9, 917 – 924.

Carvey PM, McRae A, Lint TF, Ptak LR, Lo ES, Goetz CG, Klawans HL (1991) The potential use of a dopamine neuron antibody and a striatal-derived neurotrophic factor as diagnostic markers in Parkinson's disease. Neurology ;41(5 Suppl 2):53-8; discussion 59-60.

Chang C, Wu G, Gao P, Yang L, Liu W, Zuo J (2013) Upregulated Parkin expression protects mitochondrial homeostasis in DJ-1 konckdown cells and cells overexpressing the DJ-1 L166P mutation. Mol Cell Biochem.

Chen H, Jacobs E, Schwarzschild MA, McCullough ML, Calle EE, Thun MJ, Ascherio A (2005) Nonsteroidal antiinflammatory drug use and the risk for Parkinson's disease. Ann Neurol 58(6):963-7.

Chen J, Tang XQ, Zhi JL, Cui Y, Yu HM, Tang EH, Sun SN, Feng JQ, Chen PX (2006) Curcumin protects PC12 cells against 1-methyl-4-phenylpyridinium ion-induced apoptosis by bcl-2-mitochondria-ROS- iNOS pathway. Apoptosis 11:943–953.

Chen M, Ona VO, Li M, Ferrante RJ, Fink KB, Zhu S, Bian J, Guo L, Farrell LA, Hersch SM, Hobbs W, Vonsattel JP, Cha JH, Friedlander RM (2000) Minocycline inhibits caspase-1 and caspase-3 expression and delays mortality in a transgenic mouse model of Huntington disease. Nat Med 6:797–801.

Chen S, Le WD, Xie WJ, Alexianu ME, Engelhardt JI, Siklos L, & Appel SH (1998) Experimental destruction of substantia nigra initiated by Parkinson disease immunoglobulins. Arch Neurol 55, 1075-1080.

Christensen RN, Ha BK, Sun F, Bresnahan JC, Michael SB. (2006) Kainate Induces Rapid Redistribution of the Actin Cytoskeleton in Ameboid Microglia. *Journal of Neuroscience Research* **84** (1): 170–181.

Chuang R, Gitler A (2013) Parallel PARKing: Parkinson's Genes Function in Common Pathway. Neuron 77(3), 377-379.

Chinta SJ, Andersen JK (2005) Dopaminergic neurons. Int J Biochem Cell Biol. 37(5):942-6.

Cicchetti F, Brownell AL, Williams K, Chen YI, Livni E, Isacson O (2002) Neuroinflammation of the nigrostriatal pathway during progressive 6-OHDA dopamine degeneration in rats monitored by immunohistochemistry and PET imaging. Eur J Neurosci.15(6):991-8.

Ciesielska A, Joniec I, Przybylkowski A, Gromadzka G, Kurkowska-Jastrzebska I, Czlonkowska A, Czlonkowski A (2003) Dynamics of expression of the mRNA for cytokines and inducible nitric synthase in a murine model of the Parkinson's disease. Acta Neurobiol Exp (Wars)63:117–126.

Cookson MR (2009) Alpha-Synuclein and neuronal cell death. Mol Neurodegener 4: 9

Cookson M., Bandmann O. (2010) Parkinson's disease: insights from pathways. Hum Mol Genet. 15; 19(R1): R21–R27.

Cookson MR (2005) The biochemistry of Parkinson's disease. Annu Rev Biochem;74:29-52.

Corti O, Lesage S, Brice A (2011) What genetics tells us about the causes and mechanisms of Parkinson's disease. Physiol Rev. 91(4):1161-218

Crocker SJ, Smith PD, Jackson-Lewis V, Lamba WR, Hayley SP, Grimm E, Callaghan SM, Slack RS, Melloni E, Przedborski S, Robertson GS, Anisman H, Merali Z, Park DS (2003) Inhibition of calpains prevents neuronal and behavioral deficits in an MPTP mouse model of Parkinson's disease. J Neurosci 23:4081–4091.

Crosiers D., Pickut B.,Theuns J., Paul De Deyn P., Van Broeckhoven C., Martinez-Martin P., Ray Chaudhuri K., and Cras P., (2012) Non-motor symptoms in a Flanders-Belgian population of 215 Parkinson's disease patients as assessed by the Non-Motor Symptoms Questionnaire. Am J Neurodegener Dis. 1(2): 160–167.

Cruise J; Lewis R (2009). Illustrated dictionary of immunology. CRC Press. pp. 208–. ISBN 978-0-8493-7987-1.

Czlonkowska A, Kohutnicka M, Kurkowska-Jastrzebska I, Czlonkowski A (1996) Microglial reaction in MPTP (1-methyl-4-phenyl-1,2,3,6-tetrahydropyridine) induced Parkinson's disease mice model. Neurodegeneration 5:137–143.

Członkowska A, Kurkowska-Jastrzebska I, Członkowski A, Peter D, Stefano GB (2002) Immune processes in the pathogenesis on parkinons disease – a potential role for microglia and nitric oxide. Med Sci. Monit.8(8): RA 165-RA177.

Davie CA (2008) A review of Parkinson's disease. Br. Med. Bull. 86 (1): 109–27.

Dauer W, Przedborski S (2003) Parkinson's disease: mechanisms and models. Neuron 39:889-909.

Dawson TM, Dawson VL. (2010) The role of parkin in familial and sporadic Parkinson's disease. Mov Disord. 25 Suppl 1:S32-9.

Dawson, T. M., Ko, H. S., and Dawson, V. L. (2010) Genetic animal models of Parkinson's disease. Neuron 66, 646–661.

De Pablos RM, Herrera AJ, Villaran RF, Cano J, Machado A (2005) Dopamine-dependent neurotoxicity of lipopolysaccharide in substantia nigra. FASEB J 19:407–409.

de Carvalho Aguiar P, Sweadner KJ, Penniston JT, Zaremba J, Liu L, Caton M, Linazasoro G, Borg M, Tijssen M, Bressman S, Dobyns W, Brashear A, Ozelius L (2004) Mutations in the Na+/K+ -ATPase alpha3 gene ATP1A3 are associated with rapid-onset dystonia parkinsonism. Neuron;43:169-75.

de Lau M, Breteler M (2006) Epidemiology of Parkinson's disease. Lancet Neurology, 5(6): 525 – 535.

Dehmer T, Lindenau J, Haid S, Dichgans J, Schulz JB (2000) Deficiency of inducible nitric oxide synthase protects against MPTP toxicity in vivo. J Neurochem 74:2213–2216.

Denison SR, Callahan G, Becker NA, Phillips LA, Smith DI (2003a) Characterization of FRA6E and its potential role in autosomal recessive juvenile parkinsonism and ovarian cancer. Genes Chromosomes Cancer. 38(1):40-52.

Denison SR, Wang F, Becker NA, Schüle B, Kock N, Phillips LA, Klein C, Smith DI (2003b) Alterations in the common fragile site gene Parkin in ovarian and other cancers. Oncogene 13;22(51):8370-8.

Dentesano G, Straccia M, Ejarque-Ortiz A, Tusell JM, Serratosa J, Saura J, Solà C (2012) Inhibition of CD200R1 expression by C/EBP β in reactive microglial cells. J Neuroinflammation 9;9: 165

Delgado M (2003) Inhibition of interferon (IFN) gamma-induced Jak-STAT1 activation in microglia by vasoactive intestinal peptide: inhibitory effect on CD40, IFN-induced protein-10, and inducible nitric-oxide synthase expression. J Biol Chem 278:27620–27629.

De Pablos RM, Herrera AJ, Villaran RF, Cano J, Machado A (2005) Dopamine-dependent neurotoxicity of lipopolysaccharide in substantia
nigra. FASEB J 19:407–409.

De Simone R, Levi G, Aloisi F (1998) Interferon gamma gene expression in rat central nervous system glial cells. Cytokine 10:418–422.

Dhanji S, Tse K, Teh HS (2005) The low affinity Fc receptor for IgG functions as an effective cytolytic receptor for self-specific CD8 T cells. J Immunol 1; 174(3):1253-8

Ding Q, Keller JN (2001) Proteasome inhibition in oxidative stress neurotoxicity: implications for heat shock proteins. J Neurochem 77(4): 1010–7.

Dissing-Olesen L, Ladeby L, Nielsen HH, Toft-Hansen H, Dalmau I, Finsen B (2007) Axonal lesion-induced microglial proliferation and microglial cluster formation in the mouse. Neuroscience 149 (1): 112–122.

Doucet,J.P.,Nakabeppu,Y.,Bedard,P.J.,Hope,B.T.,Nestler,E.J.,Jasmin, B. J., Chen, J. S., Iadarola, M. J., St-Jean, M., Wigle, N., Blanchet, P., Grondin, R., and Robertson, G. S. (1996) Chronic alterations in dopaminergic neurotransmission produce a persistent elevation of deltaFosB-like protein(s) in both the rodent and primate striatum. Eur. J. Neurosci.8,365–381.

Dringen, R (2005) Oxidative and antioxidative potential of brain microglial cells. Antioxid Redox Signal;7:1223–1233.

Dragunow M, Butterworth N, Waldvogel H, Faull RL, Nicholson LF (1995)Prolonged expression of Fos-related antigens, Jun B and TrkB in dopamine-denervated striatal neurons. Brain Res Mol Brain Res 30:393–396.

Du Y, Ma Z, Lin S, Dodel RC, Gao F, Bales KR, Triarhou LC, Chernet E, Perry KW, Nelson DL, Luecke S, Phebus LA, Bymaster FP, Paul SM (2001) Minocycline prevents

nigrostriatal dopaminergic neurodegeneration in the MPTP model of Parkinson's disease. Proc Natl Acad Sci USA 98:14669–14674.

Duke DC, Moran LB, Kalaitzakis ME, Deprez M, Dexter DT, Pearce RK, Graeber M (2006) Transcriptome analysis reveals link between proteasomal and mitochondrial pathways in Parkinson's disease. Neurogenetics; 7:139-48.

Ealick SE, Cook WJ, Vijay-Kumar S, Carson M, Nagabhushan TL, Trotta PP, Bugg CE (1991) Three-dimensional structure of recombinant human interferon-gamma". Science 252 (5006): 698–702.

Engelender S (2008) Ubiquitination of alpha-synuclein and autophagy in Parkinson's disease. Autophagy 4 (3): 372–4.

Ernst L, Duchemin A, Miller K, Anderson C (1998) Molecular characterization of six variant Fcgamma receptor class I (CD64) transcripts. Mol Immunol 35 (14-15): 943–54.

Fahn S, Oakes D, Shoulson I, Kieburtz K, Rudolph A, Lang A, Olanow CW, Tanner C, Marek K; Parkinson Study Group (2004) Levodopa and the progression of Parkinson's disease. New England Journal of Medicine 351(24):2498–2508.

Fasano, S., and Brambilla, R. (2002) Cellular mechanisms of striatum-dependent behavioral plasticity and drug addiction. Curr. Mol. Med. 2,649–665.

Fearnley J. M., Lees, A. J. (1991) Ageing and Parkinson's disease: substantia nigra regional selectivity. Brain 114, 2283-305.

Ferrer I, Bernet E, Soriano E, Del Rio T, Fonseca M (1990) Naturally occurring cell death in the cerebral cortex of the rat and removal of dead cells by transitory phagocytes. *Neuroscience* **39** (2): 451–458.

Fiszer, U., Fredrikson, S., and Czlonkowska, A. (1996) Humoral response to hsp 65 and hsp 70 in cerebrospinal fluid in Parkinson's disease. J. Neurol. Sci.139, 66–70.

Fix, James D. (2008) Basal Ganglia and the Striatal Motor System. Neuroanatomy (Board Review Series) (4th ed.). Baltimore: Wulters Kluwer & Lippincott Wiliams & Wilkins. pp. 274–281.

Fukuda T (2001) Neurotoxicity of MPTP. Neuropathology 21:323–332.

Galon J, Gauchat JF, Mazieres N, Spagnoli R, Storkus W, Lotze M, Bonnefoy JY, Fridman WH, Sautes C (1996) Soluble Fcgamma receptor type III (FcgammaRIII, CD16) triggers cell activation through interaction with complement receptors. J Immunol. 157:1184–1192.

Gao F, Chen D, Hu Q, Wang G (2013) Rotenone directly induces BV2 cell activation via the p38 MAPK pathway. PLoS One. 2013 Aug 20;8(8).Gao HM, Hong JS, Zhang W, Liu B (2002a) Distinct Role for Microglia in Rotenone-Induced Degeneration of Dopaminergic Neurons. J Neurosci, 22(3):782–790.

Gao HM, Hong JS, Zhang W, Liu B (2003a) Synergistic dopaminergic neurotoxicity of the pesticide rotenone and inflammogen lipopolysaccharide: Relevance to the etiology of Parkinson's disease.JNeurosci23:1228–1236.

Gao HM, Jiang J, Wilson B, Zhang W, Hong JS, Liu B (2002b) Microglial activation-mediated delayed and progressive degeneration of rat nigral dopaminergic neurons: relevance to Parkinson's disease. J Neurochem 81:1285–1297.

Gao HM, Liu B, Zhang W, Hong JS (2003b) Synergistic dopaminergic neurotoxicity of MPTP and inflammogen lipopolysaccharide: relevance to the etiology of Parkinson's disease. FASEB J 17:1957–1959.

Gao HM, Liu B, Zhang W, Hong JS (2003c) Critical role of microglial NADPH oxidase-derived free radicals in the in vitro MPTP model of Parkinson's disease. Faseb J17:1954-6.

Gavett B.E., Stern R.A., McKee A.C. (2011) Chronic traumatic encephalopathy: a potential late effect of sport-related concussive and subconcussive head trauma. Clin Sports Med. 30(1):179–188.

Gayle DA, Ling Z, Tong C, Landers T, Lipton JW, Carvey PM (2002) Lipopolysaccharide (LPS)-induced dopamine cell loss in culture: roles of tumor necrosis factor-alpha, interleukin-1beta, and nitric oxide. Brain Res Dev Brain Res.133(1):27-35.

George JM, Jin H, Woods WS, Clayton DF (1995) Characterization of a novel protein regulated during the critical period for song learning in the zebra finch. Neuron 15 (2): 361–72.

Gehrmann J (1996) Microglia: a sensor to threats in the nervous system?. Research in Virology 147 (2–3): 79–88.

Gehrmann J, Matsumoto Y, Kreutzberg GW (1995) Microglia: intrinsic immuneffector cell of the brain. Brain Research Reviews 20 (3): 269–287.Gomez C, Bandez MJ,

Gonzalez-Polo RA, Soler G, Rodriguezmartin A, Moran JM, Fuentes JM (2004) Protection against MPP neurotoxicity in cerebellar granule cells by antioxidants. Cell Biol Int 28:373–380.

Greenamyre JT, MacKenzie G, Peng TI, Stephans SE (1999) Mitochondrial dysfunction in Parkinson's disease. Biochem Soc Symp 66:85–97.

Guyton, AC; Hall, JE (2006) Medical Physiology, Elsevier Saunders. 11th edition, pp.447.

Gribova IE, Gnedenko BB, Poleshchuk VV, Morozov SG (2003) [Level of interferon-gamma, tumor necrosis factor alpha, and antibodies to them in blood serum from Parkinson disease patients]. Biomed Khim 49:208–212.

Gundersen HJ, Bagger P, Bendtsen TF, Evans SM, Korbo L, Marcussen N,Moller A, Nielsen K, Nyengaard JR, Pakkenberg B, Sorensen FB, Vesterby A, West MJ (1988) The new stereological tools: disector, fractionator, nucleator and point sampled intercepts and their use in pathological research and diagnosis. APMIS 96:857–881.

Hakansson A, Westberg L, Nilsson S, Buervenich S, Carmine A, Holmberg B, Sydow O, Olson L, Johnels B, Eriksson E, Nissbrandt H (2005) Investigation of genes coding for inflammatory components in Parkinson's disease. Mov Disord 20:569–573.

Han M, Nagele E, DeMarshall C, Acharya N, & Nagele R (2012) Diagnosis of Parkinson's disease based on disease-specific autoantibody profiles in human sera. PLoS One 7, e32383.

Hayes, S. M., Shores, E. W. and Love, P. E. (2003) An architectural perspective on signaling by the pre-, alphabeta and gammadelta Tcell receptors. Immunol. Rev. 191: 28–37

Hayley S, Crocker SJ, Smith PD, Shree T, Jackson-Lewis V, Przedborski S, Mount M, Slack R, Anisman H, Park DS (2004) Regulation of dopaminergic loss by Fas in a 1-methyl-4-phenyl-1,2,3,6-tetrahydropyridine model of Parkinson's disease. J Neurosci 24:2045–2053.

He Y, Imam SZ, Dong Z, Jankovic J, Ali SF, Appel SH, Le W (2003) Role of nitric oxide in rotenone-induced nigro-striatal injury.J Neurochem.; 86(6):1338-45.

He Y, Le W, Appel S (2002) Role of Fcgamma receptors in nigral cell injury induced by Parkinson disease immunoglobulin injection into mouse substantia nigra. Exp Neurol.;176:322–327.

Hemmer K, Fransen L, Vanderstichele H, Vanmechelen E, Heuschling P (2001) An in vitro model for the study of microglia-induced neurodegeneration: involvement of nitric oxide and tumor necrosis factor-alpha. Neurochem Int. 38(7):557-65.

Hierro A, Rojas AL, Rojas R, Murthy N, Effantin G, Kajava AV, Steven AC, Bonifacino JS, Hurley JH (2007) Functional architecture of the retromer cargo-recognition complex". Nature 449 (7165): 1063–7.

Hirsch EC, Breidert T, Rousselet E, Hunot S, Hartmann A, Michel PP (2003) The role of glial reaction and inflammation in Parkinson's disease. Ann N Y Acad Sci 991:214-28.

Hirsch EC, Hunot S (2009) Neuroinflammation in Parkinson's disease: a target for neuroprotection? Lancet Neurol 8:382–397.

Huang Z, Hunter S, Kim M, Indik Z, Schreiber A (2003) The effect of phosphatases SHP-1 and SHIP-1 on signaling by the ITIM- and ITAM-containing Fcgamma receptors FcgammaRIIB and FcgammaRIIA. J Leukoc Biol 73 (6): 823–9.

Huh Y, Jung JW, Park C, Ryu JR, Shin CY, Kim WK, Ryu J (2003) Microglial activation and tyrosine hydroxylase immunoreactivity in the substantia nigral region following transient focal ischemia in rats. Neurosci Lett;349:63-7.

Hulett M, Hogarth P (1998) The second and third extracellular domains of FcgammaRI (CD64) confer the unique high affinity binding of IgG2a. Mol Immunol 35 (14-15): 989–96.

Hulse RE, Kunkler PE, Fedynyshyn JP, Kraig RP (2004) Optimization of multiplexed bead-based cytokine immunoassays for rat serum and brain tissue. J Neurosci Methods 136:87–98.

Hunot S, Dugas N, Faucheux B, Hartmann A, Tardieu M, Debré P, Agid Y, Dugas B, Hirsch EC (1999) FceRII/CD23 is expressed in Parkinson's disease and induces in vitro production of nitric oxide and tumor necrosis factor-alpha in glial cells. J Neurosci 19 (9):3440-3447.

Ischiropoulos, H; Beckman, JS (2003) Oxidative stress and nitration in neurodegeneration: cause, effect, or association? J Clin Invest; 111:163–169.

Ishizawa T, Matilla P, Davies P, Wang, D, Dickson DW (2003) Colocalization of Tau and Alpha-Synuclein Epitopes in Lewy Bodies. Journal of Neuropathology & Experimental Neurology 62 (4): 389–397.

Janeway, C. A.Jr., Travers, P., Walport, M., Shlomchik. M.J. (2005). ImmunoBiology, the immune system in health and disease 6th Edition. Garland Science.

Jenner P (1998) Oxidative mechanisms in nigral cell death in Parkinson's disease. Mov Disord 13:24 –34.

Jenner P (2001) Parkinson's disease, pesticides and mitochondrial dysfunction. Trends Neurosci 24: 245—247.

Junn E, Jang WH, Zhao X, Jeong BS, Mouradian MM (2009) Mitochondrial localization of DJ-1 leads to enhanced neuroprotection. J Neurosci Res. 87(1):123-9.

Kabuta T, Wada K (2008) Insights into links between familial and sporadic Parkinson's disease: physical relationship between UCH-L1variants and chaperone-mediated autophagy. Autophagy. 4(6):827-9.

Kannarkat G, Boss J, Tansey M (2013) The Role of Innate and Adaptive Immunity in Parkinson's Disease. Journal of Parkinson's Disease 3: 493–514.

Kay DM, Stevens CF, Hamza TH, Montimurro JS, Zabetian CP, Factor SA, Samii A, Griffith A, Roberts JW, Molho ES, Higgins DS, Gancher S, Moses L, Zareparsi S, Poorkaj P, Bird T, Nutt J, Schellenberg GD, Payami H (2010) A comprehensive analysis of deletions, multiplications, and copy number variations in PARK2. Neurology 28;75(13):1189-94.

Kim, W. G., Mohney, R. P., Wilson, B., Jeohn, G. H., Liu, B., and Hong, J. S. (2000) Regional Difference in Susceptibility to Lipopolysaccharide-Induced Neurotoxicity in the Rat Brain: Role of Microglia. J. Neurosci. 20, 6309–6316.

Kim Y. and Joh T (2006) Microglia, major player in the brain inflammation: their roles in the pathogenesis of Parkinson's disease. Experimental and Molecular Medicine 38(4): 333–347.

Kortekaas R, Leenders KL, van Oostrom JC, Vaalburg W, Bart J, Willemsen AT, Hendrikse NH (2005) Blood-brain barrier dysfunction in parkinsonian midbrain in vivo. Ann Neurol 57: 176–179.

Kostic V, Przedborski S, Flaster E, Sternic N (1991) Early development of levodopa-induced dyskinesias and response fluctuations in young-onset Parkinson's disease. Neurology 41:202–205.

Kotake Y, Ohta S (2003) MPP analogs acting on mitochondria and inducing neurodegeneration. Curr Med Chem 10:2507–2516.

Kotenko SV, Izotova LS, Pollack BP, Mariano TM, Donnelly RJ, Muthukumaran G, Cook JR, Garotta G, Silvennoinen O, Ihle JN (1995) Interaction between the components of the interferon gamma receptor complex. J. Biol. Chem. 270 (36): 20915–21.

Kreutzberg GW (1995) Microglia, the first line of defence in brain pathologies. Arzneimittelforschung. 45(3A):357-60.

Kunas RC, McRae A, Kesselring J, Villiger PM (1995) Antidopaminergic antibodies in a patient with a comples autoimmune disorder and rapidly progressin Parkinson's disease. J Allergy Clin Immunol.; 96 (5 pt1):688-90.

Kurkowska-Jastrzebska I, Wrońska A, Kohutnicka M, Członkowski A, Członkowska A (1999a) MHC class II positive microglia and lymphocytic infiltration are present in the

substantia nigra and striatum in mouse model of Parkinson's disease. Acta Neurobiol Exp (Wars) 59(1):1-8.

Kurkowska-Jastrzebska I, Wrońska A, Kohutnicka M, Członkowski A, Członkowska A (1999b) The inflammatory reaction following 1-methyl-4-phenyl-1,2,3, 6-tetrahydropyridine intoxication in mouse. Exp neurol. 156: 50-61.

Langston JW, Forno LS, Tetrud J, Reeves AG, Kaplan JA, Karluk D (1999) Evidence of active nerve cell degeneration in the substantia nigra of humans years after 1-methyl-4-phenyl-1,2,3,6-tetrahydropyridine exposure. Ann Neurol;46:598-605.

Langston JW, Quik M, Petzinger G, Jakowec M, Di Monte DA (2000) Investigating levodopa-induced dyskinesias in the parkinsonian primate.
Ann Neurol 47:S79–89.

Lawson L J, Perry V H, Gordon S (1992) Turnover of resident microglia in the normal adult mouse brain. Neuroscience 48: 405–415.

Le W, Rowe D, Jankovic J, Xie W, Appel S (2009) Effects of cerebrospinal fluid from patients with Parkinson disease on dopaminerg Lancet. 13; 373(9680):2055-66.

Lee B, Dawson V, Dawson T (2012) Leucine rich repeat kinase 2 (LRRK2) as a potential therapeutic target for Parkinson’s disease. Trends Pharmacol Sci. 33(7): 365–373.

Lee HJ, Kim NY, Jang MK, Son HJ, Kim KM, Sohn DH, Lee SH, Ryu JH (1999)A sesquiterpene, dehydrocostus lactone, inhibits the expression of inducible nitric oxide synthase and TNF-alpha in LPS-activated macrophages. Planta Med. 65(2):104-8.

Lee AK, Sung SH, Kim YC, Kim SG (2003) Inhibition of lipopolysaccharide-inducible nitric oxide synthase, TNF-alpha and COX-2 expression by sauchinone effects on I-kappaBalpha phosphorylation, C/EBP and AP-1 activation. Br J Pharmacol. 139(1):11-20.

Lees AJ, Hardy J, Revesz T (1999) Parkinson's disease. Arch Neurol.; 56:194–200

Lehnardt S, Massillon L, Follett P, Jensen FE, Ratan R, Rosenberg PA, Volpe JJ, Vartanian T (2003) Activation of innate immunity in the CNS triggers neurodegeneration through a Toll-like receptor 4-dependent pathway. Proc Natl Acad Sci USA 100:8514–8519.

Lesage S, Brice A (2009) Parkinson's disease: from monogenic forms to genetic susceptibility factors. Hum. Mol. Genet. 18 (R1): R48–59.

Lev N, Ickowicz D, Melamed E, Offen D (2008) Oxidative insults induce DJ-1 upregulation and redistribution: implications for neuroprotection. Neurotoxicology. 29(3):397-405

Levesque S, Wilson B, Gregoria V, Thorpe L, Dallas S, Polikov V, Hong JS, Block M (2010) Reactive microgliosis: extracellular μ-calpain and microglia-mediated dopaminergic neurotoxicity. Brain; 133(3): 808–821.

Levi G, Minghetti L, Aloisi F (1998) Regulation of prostanoid synthesis in microglial cells and effects of prostaglandin E2 on microglial functions. Biochimie 80(11):899-904.

Li FQ, Wang T, Pei Z, Liu B, Hong JS (2005) Inhibition of microglial activation by the herbal flavonoid baicalein attenuates inflammation-mediated degeneration of dopaminergic neurons. J Neural Transm 112:331–347.

Li J, Uversky VN, Fink AL (2001) Effect of familial Parkinson's disease point mutations A30P and A53T on the structural properties, aggregation, and fibrillation of human alpha-synuclein. Biochemistry 40 (38): 11604–13.

Liberatore GT, Jackson-Lewis V, Vukosavic S, Mandir AS, Vila M, McAuliffe WG, Dawson VL, Dawson TM, Przedborski S (1999) Inducible nitric oxide synthase stimulates dopaminergic neurodegeneration in the MPTP model of Parkinson disease. Nat Med 5:1403–1409.

Lida M, Miyazaki I, Tanaka K, Kabuto H, Iwata-Ichikawa E, Ogawa N (1999) Dopamine D2 receptor-mediated antioxidant and neuroprotective effects of ropinirole, a dopamine agonist. Brain Research 838:51–59.

Lin NY, Beyer C, Gießl A (2012) Autophagy regulates TNFα-mediated joint destruction in experimental arthritis. Ann. Rheum. Dis.

Lin SK, Kok SH, Lin LD, Wang CC, Kuo MY, Lin CT, Hsiao M, Hong CY (2007) Nitric oxide promotes the progression of periapical lesion via inducing macrophage and osteoblast apoptosis. Oral Microbiol Immunol.22(1):24-9.

Ling Z, Zhu Y, Tong Cw, Snyder JA, Lipton JW, Carvey PM (2006) Progressive dopamine neuron loss following supra-nigral lipopolysaccharide (LPS) infusion into rats exposed to LPS prenatally. Exp Neurol.199(2):499-512.

Liu B, Du L, Hong JS (2000) Naloxone protects rat dopaminergic neurons against inflammatory damage through inhibition of microglia activation and superoxide generation. J Pharmacol Exp Ther 293:607–617.

Liu B, Gao HM, Hong JS. (2003) Parkinson's disease and exposure to infectious agents and pesticides and the occurrence of brain injuries: role of neuroinflammation. Environ Health Perspect;111(8):1065-73.

Liu B, Gao HM, Wang JY, Jeohn GH, Cooper CL, Hong JS (2002) Role of Nitric Oxide in Inflammation-Mediated Neurodegeneration. Ann N Y Acad Sci. ;962:318-31.

Liu M and Bing G (2011) Lipopolysaccharide Animal Models for Parkinson's Disease. Parkinson's Disease Article ID 327089.

Lodish H, Berk A, Matsudaira P, Kaiser CA, Krieger M, Scott MP, Zipursky SL, Darnell J (2004) "3". Molecular cell biology (5th ed.). New York: W.H. Freeman and CO. pp. 66–72.

Lyons A, Downer EJ, Crotty S, Nolan YM, Mills KH, Lynch MA (2007) CD200 ligand receptor interaction modulates microglial activation in vivo and in vitro: a role for IL-4. J Neurosci. 1;27(31): 8309-13.

MacLeod D., Rhinn H., Kuwahara T., Zolin A., Paolo G., McCabe B., Marder K., Honig L, Clark L., Small S., Abeliovich A (2013) RAB7L1 Interacts with LRRK2 to Modify Intraneuronal Protein Sorting and Parkinson's Disease Risk. Neuron, 77 (3), 425-439.

Mamane Y, Heylbroeck C, Genin P,Algarte M, Servant MJ, LePage C, De Luca C, Kwon H, Lin R, Hiscott J (1999) Interferon regulatory factors: the
next generation. Gene 237:1–14.

Mandel S, Grunblatt E, Youdim M (2000) cDNA microarray to study gene expression of dopaminergic neurodegeneration and neuroprotection in MPTP and 6-hydroxydopamine models: implications for idiopathic Parkinson's disease. J Neural Transm Suppl 60:117–124.

Manzanillo PS, Ayres JS, Watson RO, Collins AC, Souza G, Rae CS, Schneider DS, Nakamura K, Shiloh MU, Cox JS (2013) The ubiquitin ligase parkin mediates resistance to intracellular pathogens. Nature. 26; 501(7468):512-6.

Marsden C. D. (1994) Problems with long-term levodopa therapy for Parkinson's disease. Clin. Neuropharmacol.17, Suppl. 2,S32-44.

Matthews W (2006) Ali's Fighting Spirit". Neurology Now (American Academy of Neurology) 2 (2): 10–23.

Matsubayashi H, Inoue A, Amano T, Seki T, Nakata Y, Sasa M, Sakai N (2004) Involvement of alpha7- and alpha4beta2-type postsynaptic nicotinic acetylcholine receptors in nicotine-induced excitation of dopaminergic neurons in the substantia nigra: a patch clamp and single-cell PCR study using acutely dissociated nigral neurons. Brain Res Mol Brain Res; 129:1-7.

McCormack AL, Mak SK, Shenasa M, Langston WJ, Forno LS, Di Monte DA (2008) Pathologic modifications of apha-synuclein in 1-methyl-4-phenyl-1,2,3,6-tetrahydropyridine (MPTP)-treated squirrel monkeys. J Neuropathol Exp Neurol Aug; 67 (8):793-802.

McCoy MK, Martinez TN, Ruhn KA, Szymkowski DE, Smith CG, Botterman BR, Tansey KE, Tansey MG (2006)Blocking soluble tumor necrosis factor signaling with

dominant-negative tumor necrosis factor inhibitor attenuates loss of dopaminergic neurons in models of Parkinson's disease. J Neurosci.13;26(37):9365-75.

McGeer PL, Itagaki S, Boyes BE, McGeer EG (1988) Reactive microglia are positive for HLA-DR in the substantia nigra of Parkinson's and Alzheimer's disease brains. Neurology;38:1285-9.

McGeer PL, McGeer EG (2002) Inflammatory processes in amyotrophic lateral sclerosis. Muscle Nerve 26:459–470.McGeer PL, Schwab C, Parent A, Doudet D (2003) Presence of reactive microglia in monkey substantia nigra years after 1-methyl-4-phenyl-1,2,3,6-tetrahydropyridine administration. Ann Neurol; 54:599-604.

Meissner W, Prunier C, Guilloteau D, Chalon S, Gross CE, Bezard E (2003)Time-course of nigrostriatal degeneration in a progressive MPTP-lesioned macaque model of Parkinson's disease. Mol Neurobiol 28:209–218.

Mevorach, D; Zhou, JL; Song, X; Elkon, KB (1998) Systemic exposure to irradiated apoptotic cells induces autoantibody production. J Exp Med.188:387–392.

Michel PP, Alvarez-Fischer D, Guerreiro S, Hild A, Hartmann A, Hirsch EC (2007) Role of activity-dependent mechanisms in the control of dopaminergic neuron survival. J Neurochem 101:289-97

Mira MT, Alcaïs A, Nguyen VT, Moraes MO, Di Flumeri C, Vu HT, Mai CP, Nguyen TH, Nguyen NB, Pham XK, Sarno EN, Alter A, Montpetit A, Moraes ME,Moraes JR, Doré C, Gallant CJ, Lepage P, Verner A, Van De Vosse E, Hudson TJ, Abel L, Schurr E (2004) Susceptibility to leprosy is associated with PARK2 and PACRG Nature 12;427(6975):636-40.

Mizuta I, Nishimura M, Mizuta E, Yamasaki S, Ohta M, Kuno S, Ota M (2001) Relation between the high production related allele of the interferon-gamma (IFN-gamma) gene and age at onset of idiopathic Parkinson's disease in Japan. J Neurol Neurosurg Psychiatry 71:818–819.

Monahan AJ, Warren M, Carvey PM (2008) Neuroinflammation and peripheral immune infiltration in Parksinon's disease: an autoimmune hypothesis. Cell Transplant 17 (4):363-72.

Mogi M, Harada M, Kondo T, Mizuno Y, Narabayashi H, Riederer P, Nagatsu T (1996) The soluble form of Fas molecule is elevated in parkinsonian brain tissues. Neurosci Lett;220:195-8.

Moore DJ, West AB, Dawson VL, Dawson TM (2005) Molecular pathophysiology of Parkinson's disease. Annu Rev Neurosci; 28:57-87.

Moran LB, Graeber MB (2008) Towards a pathway definition of Parkinson's disease: a complex disorder with links to cancer, diabetes and inflammation. Neurogenetics; 9:1-13.

Mosley RL, Hutter-Saunders JA, Stone DK, Gendelman HE (2012) Inflammation and adaptive immunity in Parkinson's disease. Cold Spring Harb Perspect Med. 2(1):a009381.

Moss DW, Bates TE (2001) Activation of murine microglial cell lines by lipopolysaccharide and interferon-gamma causes NO mediated decreases in mitochondrial and cellular function. Eur J Neurosci13:529–538.

Mount MP, Lira A, Grimes D, Smith PD, Faucher S, Slack R, Anisman H, Hayley S, Park DS (2007) Involvement of interferon-gamma in microglial-mediated loss of dopaminergic neurons. J Neurosci. 21;27(12):3328-37.

Muhammad A, Flores I, Zhang H, Yu R, Staniszewski A, Planel E, Herman M, Ho L, Kreber R, Honig LS, Ganetzky B, Duff K, Arancio O, Small SA (2008) Retromer deficiency observed in Alzheimer's disease causes hippocampal dysfunction, neurodegeneration, and Aβ accumulation. Proc. Natl. Acad. Sci. U.S.A. 105 (20): 7327–32.

Murphy KM, Reiner SL (2002) The lineage decisions of helper T cells. Nat Rev Immunol 2:933–944.

Nagatsu T, Mogi M, Ichinose H, Togari A (2000) Changes in cytokine and neurotrophins in Parkinson ’s disease. J neural transm Suppl 60:277-290.

Nagatsu T, Mogi M, Ichinose H, Togari A (2000) Cytokines in Parkinson’s disease. J Neural Transm Suppl 58:143–151.

Nakamura S, Nagano I, Yoshioka M, Onodera J, Kogure K (1992) Detection of interferon-gamma and IL-6 producing cells in cerebrospinal fluid
cells in the central nervous system infectious diseases using immunocytochemistry. Rinsho Shinkeigaku 32:143–147.

Narendra DP, Jin SM, Tanaka A, Suen DF, Gautier CA, Shen J, Cookson MR, Youle RJ (2010) PINK1 is selectively stabilized on impaired mitochondria to activate Parkin. PLoS Biol. 26;8(1):e1000298.

Navarro A (2007) Pesticides and impairment of mitochondrial function in relation with the parkinsonian syndrome. Front Biosci; 12:1079-93.

Neff, F., Wei, X., No¨lker, C., Bacher, M., Du, Y., and Dodel, R. (2008) Immunotherapy and naturally occurring autoantibodies in neurodegenerative disorders. Autoimmun. Rev.7, 501–507

Nimmerjahn F, Ravetch J (2006) Fcgamma receptors: old friends and new family members. Immunity 24 (1): 19–28.

Nixon R (2013) The role of autophagy in neurodegenerative disease. Nature Medicine 19,983–997.

Noguchi Y, Yoshikawa T, Matsumoto A, Svaninger G, Gelin J (1996) Are cytokines possible mediators of cancer cachexia? Surg Today 26:467–475.

Nussbaum, R.L. and Ellis, C.E. (2003) Alzheimer's Disease and Parkinson's Disease. N Engl J Med 2003;348(14):1356-1364.

Ohmori, H; Kanayama, N (2005) Immunogenicity of an inflammation-associated product, tyrosine nitrated self-proteins. Autoimmun Rev 4:224–229.

Okun E, Mattson MP, Arumugam TV (2010) Involvement of Fc receptors in disorders of the central nervous system. Neuromolecular Med. 12:164–178.

Okuno T, Nakatsuji Y, Kumanogoh A, Moriya M, Ichinose H, Sumi H, Fujimura H, Kikutani H, Sakoda S (2005) Loss of dopaminergic neurons by the induction of inducible nitric oxide synthase and cyclooxygenase-2 via CD40: relevance to Parkinson’s disease. J Neurosci Res 81:874–882.

Olanow CW (2007) The pathogenesis of cell death in Parkinson's disease–2007. Mov Disord;22 Suppl 17:S335-42.

Olanow CW, McNaught KS (2006) Ubiquitin-proteasome system and Parkinson's disease.Mov Disord;21:1806-23.

Olanow C., Tatton W (1999) Etiology and Pathogenesis of Parkinson's Disease. Annual Review of Neuroscience 22: 123-144.

Orr CF, Rowe DB, Mizuno Y, Mori H, Halliday GM (2005) A possible role for humoral immunity in the pathogenesis of Parkinson's disease. Brain 128 (pt11): 2665-74.

Otten M, van Egmond M (2004). The Fc receptor for IgA (FcalphaRI, CD89). *Immunol Lett* **92** (1–2): 23–31

Ouchi Y, Yoshikawa E, Sekine Y, Futatsubashi M, Kanno T, Ogusu T, Torizuka T (2005) Microglial activation and dopamine terminal loss in early Parkinson's disease. Ann Neurol 57:168–175.

Palucka K & Banchereau J. Linking innate and adaptive immunity (1999) Nat Med 5: 868−870.

Pan L, Pei P (2003) Signaling transduction by IgG receptors. Chin Med J (Engl) 116 (4): 487–94.

Papachroni KK, Ninkina N, Papapanagiotou A, Hadjigeorgiou GM, Xiromerisiou G, Papadimitriou A, Kalofoutis A, Buchman VL (2007) Autoantibodies to alpha-synuclein in inherited Parkinson's disease. J Neurochem 101, 749-756.

Patel AS, Lin L, Geyer A (2012) Autophagy in idiopathic pulmonary fibrosis". PLoS ONE 7 (7): e41394.

Pawankar R (2001) Mast cells as orchestrators of the allergic reaction: the IgE-IgE receptor mast cell network. Curr Opin Allergy Clin Immunol 1 (1): 3–6.

Paxinos G, Franklin KBJ (2001) The mouse brain in stereotaxic coordinates. San Diego: Academic.

Peracchio C, Alabiso O, Valente G, Isidoro C (2012) Involvement of autophagy in ovarian cancer: a working hypothesis". J Ovarian Res 5 (1): 22.

Perry VH (2004) The influence of systemic inflammation on inflammation in the brain: implications for chronic neurodegenerative disease. Brain Behav Immun 18:407–413.

Petiniot, L. K., Weaver, Z., Barlow, C., Shen, R., Eckhaus, M., Steinberg, S.M., Ried, T., Wynshaw-Boris, A., and Hodes, R. J. (2000) Recombinase-activating gene (RAG) 2-mediated V(D)J recombination is not essential for tumorigenesis in Atm-deficient mice. Proc. Natl. Acad. Sci. U.S.A. 97, 6664–6669.

Platten M, Wick W, Wischhusen J, Weller M (2001) N-[3,4-dimethoxycinnamoyl]-anthranilic acid (tranilast) suppresses microglial inducible nitric oxide synthase (iNOS) expression and activity induced by interferon-gamma (IFN-gamma). Br J Pharmacol 134:1279–1284.

Przedborski S, Jackson-Lewis V, Naini AB, Jakowec M, Petzinger G, Miller R, Akram M (2001) The parkinsonian toxin 1-methyl-4-phenyl-1,2,3,6-tetrahydropyridine (MPTP): a technical review of its utility and safety. J Neurochem 76:1265–1274.

Qin L, Liu Y, Wang T, Wei SJ, Block ML, Wilson B, Liu B, Hong JS (2004) NADPH oxidase mediates lipopolysaccharide-induced neurotoxicity and proinflammatory gene expression in activated microglia. J Biol Chem. 9; 279(2):1415-21.

Quik M, Bordia T, O'Leary K (2007) Nicotinic receptors as CNS targets for Parkinson's disease. Biochem Pharmacol; 74:1224-34.

Raivich G, Bohatschek M, Werner A, Jones LL, Galiano M, Kloss CU, Zhu XZ, Pfeffer K, Liu ZQ (2003) Lymphocyte infiltration in the injured brain:

role of proinflammatory cytokines. J Neurosci Res 72:726–733.

Ramirez A, Heimbach A, Grundemann J, Stiller B, Hampshire D, Cid LP, Goebel I, Mubaidin AF, Wriekat AL, Roeper J, Al-Din A, Hillmer AM, Karsak M, Liss B, Woods CG, Behrens MI, Kubisch C (2006) Hereditary parkinsonism with dementia is caused by mutations in ATP13A2, encoding a lysosomal type 5 P-type ATPase. Nat Genet 38 (10): 1184–91.

Ramesh G, MacLean AG, Philipp MT (2013) Cytokines and chemokines at the crossroads of neuroinflammation, neurodegeneration, and neuropathic pain. Mediators Inflamm. 2013:480739.

Ramonet D., Podhajska A., Stafa K., Sonnay S., Trancikova A., Tsika E., Pletnikova O., Troncoso J.C., Glauser L., Moore D.J. (2012) PARK9-associated ATP13A2 localizes to intracellular acidic vesicles and regulates cation homeostasis and neuronal integrity. Hum. Mol. Genet. 21:1725-1743.

Ray PW, Goeddel DV (1982) Structure of the human immune interferon gene. Nature 298 (5877): 859–63

Rhodes SL, Fitzmaurice AG, Cockburn M, Bronstein JM, Sinsheimer JS, Ritz B (2013) Pesticides that inhibit the ubiquitin-proteasome system: Effect measure modification by genetic variation in SKP1 in Parkinson′s disease. Environ Res.126:1-8.

Ritter MR, Banin E, Moreno SK, Aguilar E, Dorrel MI, Friedlander M (2006) Myeloid progenitors differentiate into microglia and promote vascular repair in a model of ischemic retinopathy. Journal of Clinical Investigation 116 (12): 3266–3276

Rissi DR, Oliveira FN, Rech RR, Pierezen F, Lemos RAA, Barros CSL (2006) Epidemiology, clinical signs and contribution of the encephalic lesions in cattle affected by meningoencephalitis caused by bovine herpesvirus-5. *Pesquisa Vetreinaria Brasileira* **26** (2): 123–132.

Rock RB, Gekker G, Hu S, Sheng WS, Cheeran M, Lokensgard JR, Peterson PK (2004) Role of microglia in central nervous system infections. Clin Microbiol Rev.17(4):942-64.

Rowe DB, Le W, Smith RG, Appel SH (1998) Antibodies from patients with Parkinson's disease react with protein modified by dopamine oxidation. J Neurosci Res. 1998 ;53(5):551-8.

Rymar VV, Sasseville R, Luk KC, Sadikot AF (2004) Neurogenesis and stereological morphometry of calretinin-immuno reactive GABAergic inter-
neurons of the neostriatum. J Comp Neurol 469:325–339.

Sadir R, Forest E, Lortat-Jacob H. (1998) The heparan sulfate binding sequence of interferon-gamma increased the on rate of the interferon-gamma-interferon-gamma receptor complex formation. J. Biol. Chem. 273 (18): 10919–10925.

Samii A, Nutt JG, Ransom BR (2004). Parkinson's disease. Lancet 363 (9423): 1783–93

Schapira A. (2004) Disease modification in Parkinson's disease. Lancet Neurology 3:362–368.

Schapira A, Olanow CW (2003) Rationale for the use of dopamine agonists as neuroprotective agents in Parkinson's disease. Annals of Neurology 53: S149–S157.

Schatz, D. G., and Baltimore, D. (2004) Uncovering the V(D)J recombinase. Cell 116, S103-S106.

Schiesling C, Kieper N, Seidel K, Kruger R (2008) Review: familial Parkinson's disease–genetics, clinical phenotype and neuropathology in relation to the common sporadic form of the disease. Neuropathol Appl Neurobiol; 34:255-71.

Schoenborn JR, Wilson CB (2007) Regulation of interferon-gamma during innate and adaptive immune responses. Adv. Immunol. 96: 41–101.

Schroder K, Hertzog PJ, Ravasi T, Hume DA (2004) Interferon-gamma: an overview of signals, mechanisms and functions. J. Leukoc. Biol. 75 (2): 163–89.

Schultheis PJ, Hagen TT, O'Toole KK, Tachibana A, Burke CR, McGill DL, Okunade GW, Shull GE (2004) Characterization of the P5 subfamily of P-type transport ATPases in mice. Biochem Biophys Res Commun 323 (3): 731–8.

Seegal RF, Brosch KO, Bush B (1986) High-performance liquid chromatography of biogenic amines and metabolites in brain, cerebrospinal fluid, urine and plasma. J Chromatogr 377:131–144.

Serra, P. A., Pluchino, S., Marchetti, B., Desole, M. S., and Miele, E. (2008) The MPTP mouse model: cues on DA release and neural stem cell restorative role. Parkinsonism Relat. Disord.14, S189-S193.

Sharma S, Moon C, Khogali A, Haidous A, Chabenne A, Ojo C, Jelebinkov M, Kurdi Y, Ebadi M (2013) Biomarkers in Parkinson's disease. Neurochemistry International 63 (3): 201-229

Sherer TB, Betarbet R, Kim JH, Greenamyre JT (2003a) Selective microglial activation in the rat rotenone model of Parkinson's disease. Neurosci Lett 341: 87-90.

Sherer TB, Kim JH, Betarbet R, Greenamyre JT (2003b) Subcutaneous rotenone exposure causes highly selective dopaminergic degeneration and alpha-synuclein aggregation. Exp Neurol. 179(1): 9-16.

Simunovic F,Ming Y, Wang Y, Macey L, Brown L, Krichevsky A, Andersen S,Stephens R, Benes F, Sonntag K (2009) Gene expression profiling of substantia nigra dopamine neurons: further insights into Parkinson's disease pathology Brain; 132(7): 1795–1809.

Singleton AB, Farrer M, Johnson J, Singleton A, Hague S, Kachergus J, Hulihan M, Peuralinna T, Dutra A, Nussbaum R, Lincoln S, Crawley A, Hanson M, Maraganore D, Adler C, Cookson MR, Muenter M, Baptista M, Miller D, Blancato J, Hardy J, Gwinn-Hardy K (2003) Alpha-Synuclein locus triplication causes Parkinson's disease. Science 302 (5646): 841.

Smeyne RJ, Jackson-Lewis V (2005) The MPTP model of Parkinson’s disease. Brain Res Mol Brain Res 134:57–66.

Smith PD, Crocker SJ, Jackson-Lewis V, Jordan-Sciutto KL, Hayley S, Mount MP, O’Hare MJ, Callaghan S, Slack RS, Przedborski S, Anisman H, Park DS (2003) Cyclin-dependent kinase 5 is a mediator of dopaminergic neuron loss in a mouse model of Parkinson’s disease. Proc Natl Acad Sci USA 100:13650–13655.

Snyder H, Wolozin B. (2004) Pathological proteins in Parkinson's disease: focus on the proteasome. J Mol Neurosci. 24(3):425-42.

Soltys Z, Ziaja M, Pawlinski R, Setkowicz Z, Janeczko K (2001) Morphology of reactive microglia in the injured cerebral cortex. Fractal analysis and complementary quantitative methods. J Neurosci Res 63:90–97.

Stein MP, Mold C, Du Clos TW. (2000) C-reactive protein binding to murine leukocytes requires Fc gamma receptors. J Immunol.164:1514–1520.

Stocco, Andrea; Lebiere, Christian; Anderson, John R. (2010) Conditional Routing of Information to the Cortex: A Model of the Basal Ganglia's Role in Cognitive Coordination". Psychological Review 117 (2): 541–74.

Stone, D. K., Reynolds, A. D., Mosley, R. L., and Gendelman, H. E. (2009) Innate and adaptive immunity for the pathobiology of Parkinson's disease. Antioxid. Redox Signal. 11, 2151–2166.

Storch, A., Ludolph, A. C., and Schwarz, J. (2004) Dopamine transporter: involvement in selective dopaminergic neurotoxicity and degeneration. J. Neural Transm.111, 1267–1286.

Streit WJ, Walter SA, Pennell NA (1999) Reactive microgliosis. Prog Neurobiol;57: 563-81.

Surmeier DJ (2007) Calcium, ageing, and neuronal vulnerability in Parkinson's disease. Lancet Neurol; 6:933-8.

Suzumura A, Takeuchi H, Zhang G, Kuno R, Mizuno T (2006) Roles of glia-derived cytokines on neuronal degeneration and regeneration. Ann NY Acad Sci 1088:219–229.

Szalai AJ, Hu X, Raman C, Barnum SR (2005) Requirement of the Fc receptor common gamma-chain for gamma delta T cell-mediated promotion of murine experimental autoimmune encephalomyelitis. Eur J Immunol. 35:3487–3492.

Tanaka M, Kim YM, Lee G, Junn E, Iwatsubo T, Mouradian MM (2004) Aggresomes formed by alpha-synuclein and synphilin-1 are cytoprotective. J. Biol. Chem. 279 (6): 4625–31.

Takai, T., Li, M., Sylvestre, D., Clynes, R., and Ravetch, J. V. (1994) FcR gamma chain deletion results in pleiotrophic effector cell defects. Cell 76, 519–529.

Takai T, Ono M, Hikida M, Ohmori H, Ravetch JV (1996) Augmented humoral and anaphylactic responses in Fc gamma RII-deficient mice. Nature 25 (379): 346–9.

Tarassishin L, Suh HS, Lee SC (2011) Interferon regulatory factor 3 plays an anti-inflammatory role in microglia by activating the PI3K/Akt pathway. J Neuroinflammation. 30;8:187.

Teismann P, Tieu K, Cohen O, Choi DK, Wu DC, Marks D, Vila M, Jackson-Lewis V, Przedborski S (2003) Pathogenic role of glial cells in Parkinson's disease. Mov Disord; 18(2):121-9.

Theodore S, Cao S, McLean PJ, Standaert DG (2008) Targeted overexpression of human alpha-synuclein triggers microglial activation and an adaptive immune response in a mouse model of Parkinson disease. J Neuropathol Exp Neurol.67(12):1149-58.

Thiel DJ, le Du MH, Walter RL, D'Arcy A, Chène C, Fountoulakis M, Garotta G, Winkler FK, Ealick SE (2000) Observation of an unexpected third receptor molecule in the crystal structure of human interferon-gamma receptor complex. Structure 8 (9): 927–36.

Tsujimoto Y, Shimizu S (2005) Another way to die: autophagic programmed cell death". Cell Death Differ. 12 (Suppl 2): 1528–34.

Ulvestad, E., Williams, K., Matre, R., Nyland, H., Olivier, A., and Antel, J. (1994) Fc receptors for IgG on cultured human microglia mediate cytotoxicity and phagocytosis of antibody-coated targets. J. Neuropathol. Exp. Neurol. 53, 27–36.

Ulvestad, E., Williams, K., Vedeler, C., Antel, J., Nyland, H., Mørk, S., and Matre, R. (1994) Reactive microglia in multiple sclerosis lesions have an increased expression of receptors for the Fc part of IgG. J. Neurol. Sci. 121, 125–131.

Utz, PJ; Anderson P (1998) Posttranslational protein modifications, apo ptosis, and the bypass of tolerance to autoantigens. Arthritis Rheum;41:1152–1160.

Van Den Eeden SK, Tanner CM, Bernstein AL, Fross RD, Leimpeter A, Bloch DA, Nelson LM (2003) Incidence of Parkinson's disease: variation by age, gender, and race/ethnicity. Am J Epidemiol. 1;157(11):1015-22.

Van den Herik-Oudijk IE, Ter Bekke MW, Tempelman MJ, Capel PJ, Van de Winkel JG (1995) Functional differences between two Fc receptor ITAM signaling motifs. Blood 1;86(9):3302-7.

Vanhaverbeke C, Simorre JP, Sadir R, Gans P, Lortat-Jacob H (2004) NMR characterization of the interaction between the C-terminal domain of interferon-gamma and heparin-derived oligosaccharides. Biochem. J. 384 (Pt 1): 93–9.

Verhoeven K, De Jonghe P, Coen K, Verpoorten N, Auer-Grumbach M, Kwon JM, FitzPatrick D, Schmedding E, De Vriendt E, Jacobs A, Van Gerwen V, Wagner K, Hartung HP, Timmerman V (2003) Mutations in the small GTP-ase late endosomal protein RAB7 cause Charcot-Marie-Tooth type 2B neuropathy. Am J Hum Genet. 72(3):722-7.

Vilariño-Güell C, Wider C, Lynch T, Melamed E, Rajput A, Rajput AH, Solida A, Wu RM, Uitti RJ, Wszolek ZK, Vingerhoets F, Farrer MJ. (2011) VPS35 mutations in Parkinson disease. Am J Hum Genet. 15;89(1):162-7.

Wahner AD, Bronstein JM, Bordelon YM, Ritz B (2007) Nonsteroidal antiinflammtory drugs may protect against Parkinson's disease. Neurology 69:1836-1842.

Waldmann TA (2006) The biology of interleukin-2 and interleukin-15: implications for cancer therapy and vaccine design. Nat. Rev. Immunol 6 (8): 595–601.

Wang XJ, Yan ZQ, Lu GQ, Stuart S, Chen SD (2007) Parkinson's disease IgG and C5a-induced synergistioc dopaminergic neurotoxicity: role of microglia. Neurochem Int.; 50 (1):39-50.

Watanabe Y, Himeda T, Araki T (2005) Mechanisms of MPTP toxicity and their implications for therapy of Parkinson's disease. Med Sci Monit.; 11(1):RA17-23.

Weerkamp NJ, Tissingh G, Poels PJ, Zuidema SU, Munneke M, Koopmans RT, Bloem BR. (2013) Nonmotor symptoms in nursing home residents with Parkinson's disease: prevalence and effect on quality of life. Am Geriatr Soc.61(10):1714-21.

Wei X, Zhao L, Liu J, Dodel RC, Farlow MR, Du Y (2005) Minocycline prevents gentamicin-induced ototoxicity by inhibiting p38 MAP kinase phosphorylation and caspase 3 activation. Neuroscience 131:513–521.

Whitton PS (2007) Inflammation as a causative factor in the aetiology of Parkinson's disease. Br. J. Pharmacol. 150:963-976.

Wichmann T, DeLong MR (2003) Pathophysiology of Parkinson's Disease: The MPTP Primate Model of the Human Disorder. Ann. N.Y. Acad. Sci. 991: 199-213.

Widner B, Leblhuber F, Fuchs D (2002) Increased neopterin production and tryptophan degradation in advanced Parkinson's disease. J Neural Transm 109:181–189.

Wood, Paul (2003). *Neuroinflammation: Mechanisms and Management*. Humana Press.

Wu DC, Jackson-Lewis V, Vila M, Tieu K, Teismann P, Vadseth C, Choi DK, Ischiropoulos H, Przedborski S (2002) Blockade of microglial activation is neuroprotective in the 1-methyl-4-phenyl-1,2,3,6-tetrahydropyridine mouse model of Parkinson disease. J Neurosci;22:1763-71.

Wu DC, Teismann P, Tieu K, Vila M, Jackson-Lewis V, Ischiropoulos H, Przedborski S (2003) NADPH oxidase mediates oxidative stress in the 1-methyl-4-phenyl-1,2,3,6-tetrahydropyridine model of Parkinson's disease. Proc Natl Acad Sci USA 100:6145–6150.

Wu G, Pang S, Feng X, Zhang A, Li J, Gu K, Huang J, Dong H, Yan B (2011) Genetic analysis of lysosomal alpha-galactosidase A gene in sporadic Parkinson's disease. Neurosci Lett. 2011 Aug 1; 500(1):31-5.

Xia Y, Saitoh T, Uéda K, Tanaka S, Chen X, Hashimoto M, Hsu L, Conrad C, Sundsmo M, Yoshimoto M, Thal L, Katzman R, Masliah E (2001) Characterization of the human alpha-synuclein gene: Genomic structure, transcription start site, promoter region and polymorphisms". J. Alzheimers Dis. 3 (5): 485–494.

Xia Y, Saitoh T, Uéda K, Tanaka S, Chen X, Hashimoto M, Hsu L, Conrad C, Sundsmo M, Yoshimoto M, Thal L, Katzman R, Masliah E (2002) Characterization of the human alpha-synuclein gene: Genomic structure, transcription start site, promoter region and polymorphisms: Erratum p489 Fig 3. J. Alzheimers Dis. 4 (4): 337.

XieZ, Morgan TE, Rozovsky I,Finch CE (2003) Aging and glial responses to lipopolysaccharide in vitro: greater induction of IL-1 and IL-6, but smaller induction of neurotoxicity. Exp Neurol 182:135–141.

Xilouri M, Kyratzi E, Pitychoutis PM, Papadopoulou-Daifoti Z, Perier C, Vila M, Maniati M, Ulusoy A, Kirik D, Park DS, Wada K, Stefanis L (2012) Selective neuroprotective effects of the S18Y polymorphic variant of UCH-L1 in the dopaminergic system. Hum Mol Genet. 15;21(4):874-89.

Yang L, Sugama S, Chirichigno JW, Gregorio J, Lorenzl S, Shin DH, Browne SE, Shimizu Y, Joh TH, Beal MF, Albers DS (2003) Minocycline enhances MPTP toxicity to dopaminergic neurons. J Neurosci Res 74:278–285.

Yang W, Chen L, Ding Y, Zhuang X, Kang UJ (2007) Paraquat induces dopaminergic dysfunction and proteasome impairment in DJ-1-deficient mice. Hum Mol Genet.16(23):2900-10.

Yasuda T, Nihira T, Ren YR, Cao XQ, Wada K, Setsuie R, Kabuta T, Wada K, Hattori N, Mizuno Y, Mochizuki H (2009) Effects of UCH-L1 on alpha-synuclein over-expression mouse model of Parkinson's disease. J Neurochem.108(4):932-44.

Yokota O, Terada S, Ishizu H, Ujike H, Ishihara T, Nakashima H, Yasuda M, Kitamura Y, Uéda K, Checler F, Kuroda S (2002) NACP/alpha-synuclein, NAC, and beta-amyloid pathology of familial Alzheimer's disease with the E184D presenilin-1 mutation: a clinicopathological study of two autopsy cases. Acta Neuropathol. 104 (6): 637–48.

Yokoyama, H., Kuroiwa, H., Yano, R., and Araki, T. (2008) Targeting reactive oxygen species, reactive nitrogen species and inflammation in MPTP neurotoxicity and Parkinson's disease. Neurol. Sci.29, 293–301.

Youle RJ, Narendra DP (2011) Mechanisms of mitophagy. Nat Rev Mol Cell Biol. 2011 Jan;12(1):9-14. Zeng HY, Zhu XA, Zhang C, Yang LP, Wu LM, Tso MO (2005)

Identification of sequential events and factors associated with microglial activation, migration, and cytotoxicity in retinal degeneration in rd mice. Invest Ophthalmol Vis Sci 46:2992–2999.

Zhang P, Yu L, Gao J, Fu Q, Dai F, Zhao Y, Zheng L, Zhao S (2001) Cloning and characterization of human VPS35 and mouse Vps35 and mapping of VPS35 to human chromosome 16q13-q21. Genomics 70 (2): 253–7.

Zhao X, Nothwehr S, Lara-Lemus R, Zhang BY, Peter H, Arvan P (2007) Dominant-negative behavior of mammalian Vps35 in yeast requires a conserved PRLYL motif involved in retromer assembly". Traffic 8 (12): 1829–40.

Zimprich A, Benet-Pagès A, Struhal W, Graf E, Eck S, Offman M, Haubenberger D, Strom T (2011) A Mutation in VPS35, Encoding a Subunit of the Retromer Complex, Causes Late-Onset Parkinson Disease. Am J Hum Genet. 15; 89(1): 168–175.

Ziv Y, Ron N, Butovsky O, Landa G, Sudai E, Greenberg N, Cohen H, Kipnis J, Schwartz M (2006) Immune cells contribute to the maintenance of neurogenesis and spatial learning abilities in adulthood. Nat Neurosci.9(2):268-75

# Appendix 1: Additional Publications

# Role of Cdk5-Mediated Phosphorylation of Prx2 in MPTP Toxicity and Parkinson's Disease

Neuron

(2007) Volume 55, Issue 1, Pages 37–52

Dianbo Qu[1], Juliet Rashidian[1, 3], Matthew P. Mount[1, 3],Hossein Aleyasin[1, 3], Mohammad Parsanejad[1], **Arman Lira[1]**, Emdadul Haque[1], Yi Zhang[1], Steve Callaghan[1], Mireille Daigle[1], Maxime W.C. Rousseaux[1], Ruth S. Slack[1], Paul R. Albert[1], Inez Vincent[2], John M. Woulfe[1], David S. Park[1,]

[1] Ottawa Health Research Institute, Neuroscience Group, University of Ottawa, Ottawa, K1H 8M5 ON, Canada

[2] Centre for Molecular Medicine and Therapeutics, University of British Columbia, 950 West 28th Avenue, Vancouver, V5A 4H4 BC, Canada

## Author statement of contribution

Arman Lira performed the experiments and data analysis for 2 figures (supplemental figures 4 and 5). Arman Lira added rotenone or MPP+ to midbrain cell cultures and quantified the expression of phospho-PRDX in DA neurons using immunocytochemical analysis.

## Summary

We reported previously that calpain-mediated Cdk5 activation is critical for mitochondrial toxin-induced dopaminergic death. Here, we report a target that mediates this loss. Prx2, an antioxidant enzyme, binds Cdk5/p35. Prx2 is phosphorylated at T89 in neurons treated with $MPP^+$ and/or MPTP in animals in a calpain/Cdk5/p35-dependent manner. This phosphorylation reduces Prx2 peroxidase activity. Consistent with this, $p35^{-/-}$ neurons show reduced oxidative stress upon $MPP^+$ treatment. Expression of Prx2 and Prx2T89A, but not the phosphorylation mimic Prx2T89E, protects cultured and adult neurons following mitochondrial insult. Finally, downregulation of Prx2 increases oxidative stress and sensitivity to $MPP^+$. We propose a mechanistic model by which mitochondrial toxin leads to calpain-mediated Cdk5 activation, reduced Prx2 activity, and decreased capacity to eliminate ROS. Importantly, increased Prx2 phosphorylation also occurs in nigral neurons from postmortem tissue from Parkinson's disease patients when compared to control, suggesting the relevance of this pathway in the human condition.

# Introduction

Parkinson's disease (PD) is a neurodegenerative disorder characterized by motor symptoms including tremor, muscle rigidity, paucity of voluntary movements, and postural instability (Hoehn and Yahr, 1967 and Lang and Lozano, 1998). The pathological hallmarks of PD are the loss of dopaminergic (DAergic) neurons in the substantia nigra pars compacta (SNc) and formation of Lewy bodies (Braak et al., 2003). The pathogenic process in PD is not clearly understood. A small portion (less than 10%) of PD patients have familial forms of the disease, and several PD genes have been identified (Abou-Sleiman et al., 2006). However, the vast majority of patients have idiopathic forms of PD. Parkinsonism can be induced in humans by exposure to the mitochondrial complex 1 toxin, 1-methyl-4-phenyl-1,2,3,6-tetrahydropyridine (MPTP). This DAergic toxin results in parkinsonism symptoms indistinguishable from those of Parkinson's disease (Burns et al., 1985 and Langston et al., 1983). Experimentally, it induces specific loss of DAergic neurons in the SNc (Burns et al., 1983) and produces a profound reduction of striatal dopamine levels with little alteration in other catecholamine neurotransmitter systems (Jonsson et al., 1986). Degeneration is a consequence of conversion of MPTP by glia to its toxic metabolite $MPP^+$ followed by specific uptake by DAergic neurons and presumed targeting of the mitochondria (Lang and Lozano, 1998).

The cellular consequences of mitochondrial dysfunction as induced by agents such as MPTP are numerous and include poor calcium homeostasis and oxidative stress (Wang and Yuen, 1994). How this dysregulation occurs and the consequence/management of

these stresses are not fully understood. Recently, and consistent with improper calcium management, we reported that calpains are activated and required for MPTP-induced death in adult mice in vivo (Crocker et al., 2003). Calpains are conserved cysteine proteases regulated by calcium and possessing diverse biological function (Sorimachi et al., 1997). This was consistent with earlier reports of elevated calpain levels in postmortem PD patients (Mouatt-Prigent et al., 1996). We also showed that calpains were more activated in PD patients than in control individuals (Crocker et al., 2003). Importantly, calpain inhibition not only limited DAergic loss but also improved animal behavior following toxin treatment (Crocker et al., 2003).

What are the possible downstream targets of calpain activation? We recently provided evidence that the activator of Cdk5, p35, may be critical (Smith et al., 2003 and Smith et al., 2006). Cdk5, not thought to be central to the core cell-cycle machinery, has been implicated in brain function including neuronal development, neuritic outgrowth, and neurotransmitter (dopamine) signaling (Dhavan and Tsai, 2001). Cdk5 activity is regulated by its activating partners, p35 and p39 (Dhavan and Tsai, 2001). While important for brain development, recent evidence has shown that inappropriate activation of the Cdk5/p35 signal may lead to neuronal death through pathogenic activation of calpains, which proteolytically cleave p35 to a more active p25 form (Dhavan and Tsai, 2001) at least in cultured systems. However, its functional role in adult degeneration in vivo as well as in PD was unknown. To this end, we found that Cdk5 plays an essential role in DAergic loss in vivo (Smith et al., 2003 and Smith et al., 2006). For example, we observed that MPTP induced Cdk5 activation and that inhibition of such activity with DN Cdk5 expression, Cdk inhibitors, or p35 deficiency attenuated DAergic death and

behavioral deficits associated with MPTP treatment (Smith et al., 2003 and Smith et al., 2006). This observation is made more significant by observations of increased p35 in postmortem PD brains (Nakamura et al., 1997). It is also entirely consistent with our observations that calpains are activated, are required for death, and mediate p35 to p25 cleavage in the MPTP model of PD (Smith et al., 2003). In support of this, we showed that inhibition of calpain led to reduced p35 to p25 conversion and Cdk5 activation (Smith et al., 2006). This suggested to us a model by which deregulated calcium leads to calpain activation, inappropriate Cdk5 activity, and DAergic cell death (Smith et al., 2006). However, the mechanism(s) by which Cdk5 promotes DAergic loss is still unknown. To address this, we presently performed mass spectrometry-based interactomics to identify Cdk5-interacting proteins. We identified an intriguing target that has direct implications for the way in which cells handle oxidative stress, linking Cdk5 activity with oxidative stress, a common theme in PD.

Oxidative stress is thought to be a critical mediator of damage in PD (Przedborski, 2005). Reactive oxygen species (ROS) has been observed in the SNc of PD patients and animal models of PD (Przedborski, 2005). Importantly, neurons in general have high levels of ROS. Therefore, systems to handle such stress are of paramount importance. Peroxidases are a key in this management system. Three types of peroxidases, peroxiredoxins (Prxs), catalase, and glutathione peroxide (GPx), function to eliminate $H_2O_2$ in mammalian cells (Rhee et al., 2005). In mammalian cells, six isoforms of Prx were identified. Although Prxs as a family are relatively ubiquitous, there is some specificity in regards to cell type and subcellular localization. For instance, Prx1 is distributed in the cytoplasm of oligodendrocytes and microglia, while Prx2 is located in the cytoplasm of neurons, and

Prx3 is localized in the mitochondria of neurons (Jin et al., 2005). Whether and how Prxs participate in neuronal damage as well as how they are regulated have yet to be examined.

Presently, we report that Prx2 directly associates with the Cdk5 kinase complex through p35. In addition, Cdk5 phosphorylates Prx2 at T89 resulting in reduction of Prx2 peroxidase activity and neuronal death in $MPP^+$-treated cells in vitro and the MPTP mouse model of PD in vivo. Prx2 activity is functionally relevant since modulation of Prx2 activity is protective. Importantly, $p35^{-/-}$ neurons have reduced ROS and improved survival consistent with the above findings. These findings provide a mechanistic link of how a mitochondrial damaging agent, through calpain-mediated Cdk5 activation and downregulation of an important antioxidant enzyme, can increase oxidative load leading ultimately to death.

# Results

### Identification of Prx2 as a Cdk5-Interacting Protein

We have shown that Cdk5 plays an essential role in loss of DAergic neurons in the MPTP mouse model of PD (Smith et al., 2003 and Smith et al., 2006). It has also been demonstrated that Cdk5/p35 exists as macromolecular complexes in brain extracts, implying that Cdk5 associates with different proteins and functions in different signaling pathways (Lee et al., 1996). To identify these complexes, we initially utilized bacterially expressed GST-p10, a C-terminal truncated form of p35 containing a 98 amino acid residue N terminus fused with GST, as a bait to isolate p35-interacting proteins from mouse brain extracts. The interacting proteins were eluted with 1 M NaCl from GST-immobilized GSH beads. The eluted proteins were visualized by Coomassie blue staining after separation by SDS-PAGE (Figure 1A). The visualized specific bands were subjected to protein identification by tandem mass spectrometry. One of three specifically isolated proteins was found to be Prx2 for which three identified peptides matches were found (Figure 1B).

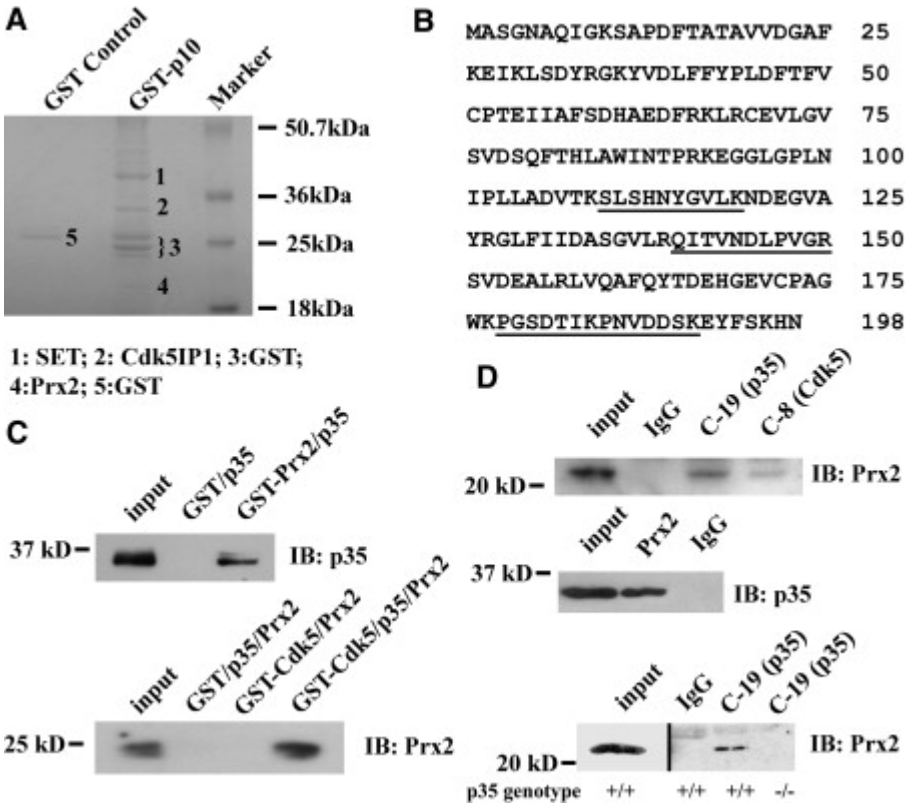


**Figure 1.** Identification of Prx2 as Cdk5/p35 Interactor(A) Isolation of Cdk5-interacting proteins by affinity purification. Fifty micrograms of bacterially expressed GST and GST-p10 as bait was immobilized on GSH beads and coincubated with 1 mg of mouse brain homogenate at 4°C for 3 hr. The eluted proteins were precipitated by TCA after elution by 1 M NaCl. The precipitates were separated by 10% of SDS-PAGE then visualized by colloidal Coomassie Blue staining.(B) Identification of Prx2 by a tandem mass spectrometry. The specific bands from GST-p10 were excised from the stained SDS-PAGE for mass spectrometric sequencing. Three underlined peptides were sequenced by the mass spectrometry and matched to mouse Prx2.(C) Confirmation of the interaction between Prx2 and Cdk5/p35. Two micrograms of bacterially expressed GST and

GST-Prx2 was incubated with 10 μg of His-p35 at 4°C for 2 hr. The GST-tagged proteins were retrieved with GSH beads. The proteins were subjected to SDS-PAGE and detected using C-19 for p35 by western blots (top panel). Similar to the above description, GST was incubated with His-p35 and His-Prx2 or GST-Cdk5 was incubated with His-Prx2 alone or with both His-p35 and His-Prx2 at 4°C for 2 hr. The bound proteins were separated by SDS-PAGE and detected by western blot using anti-Prx2 antibody after retrieval of GST-fused proteins by GSH-Sepharose (bottom panel).(D) Association of Prx2 with Cdk5/p35 in vivo. (Top panel) Control IgG, C-19 for p35, and C-8 for Cdk5 were incubated with 500 μg of mouse brain lysate. Antibodies were isolated by IP beads and the coupled proteins were subjected to SDS-PAGE followed by anti-Prx2 western blot. (Middle panel) Control IgG or anti-Prx2 (Abcam) as indicated was incubated with mouse brain lysate. Following immunoprecipitation, samples were subjected to western blot analyses using anti-p35 antibody. (Bottom panel) Control IgG or anti-p35 were incubated with WT (+/+) or p35-deficient (−/−) mouse brain lysate as indicated. Following immunoprecipitation, samples were subjected to western blot analyses using anti-Prx2 antibody. Note that all lanes are from the same gel. However, because of the high intensity of the input-positive control signal, exposure time was reduced for this lane.

Figure options

Prx2 is an antioxidative enzyme with peroxidase activity. Importantly, it also contains a conserved motif optimal for Cdks. Because of these reasons and the potential importance of ROS in PD, we chose this target for our study. To confirm the interaction between p35

and Prx2, an in vitro binding assay was carried out utilizing bacterially expressed proteins. GST-Prx2 or GST alone was incubated with His-tagged p35 and subjected to SDS-PAGE and western blot analyses using p35 antibody. A specific interaction was observed only with GST-Prx2 (Figure 1C). Similarly, a reverse binding experiment was performed where GST control or GST-Cdk5 was incubated with His-Prx2 alone or with both His-p35 and His-Prx2. Specific interaction was only observed with GST-Cdk5, His-p35, and His-Prx2 coincubation (Figure 1C). Finally, we also examined whether we could detect interaction through a means independent of bacterially expressed proteins by utilizing the yeast two-hybrid interaction assay. Consistent with our previous results, we could also detect interaction between p10 and Prx2 (Figure S1 available with this article online). These results indicate that Prx2 specifically interacted with the Cdk5/p35 complex through its association with p35.

To test whether endogenous Prx2 may exist in a complex with Cdk5/p35 in vivo, immunoprecipitation was performed using control IgG, p35 (C-19), and Cdk5 (C-8) antibodies on brain extracts (Figure 1D). The complexes were then analyzed by SDS-PAGE and Western blot analyses using a Prx2 antibody. Both immunoprecipitates using either Cdk5 or p35 antibody showed an associated Prx2 signal by western blot while the control IgG did not. The reverse interaction assay where immunoprecipitation with Prx2 preceded western blot analyses for p35 was also performed using brain extracts. Consistent with the previous pulldown, a specific interaction between Prx2 and p35 was also observed (Figure 1D). Finally, to further confirm the specificity of the interaction assay, we also performed a p35 immunoprecipitation using p35 wild-type (WT) or knockout brain extracts followed by western blot analyses utilizing Prx2 antibody. A

positive interaction was only observed with WT brain extract and not with p35-deficient brains. Taken together, this indicates that endogenous Prx2 associates with Cdk5/p35 in vivo.

## Prx2 Is a Substrate of Cdk5 and Its Peroxidase Activity Is Regulated through Phosphorylation by Cdk5

The consensus sequence of Cdk5 phosphorylation is Pro (P)-directed Ser (S) or Thr (T) surrounded in the +3 position by basic amino acids, Arg (R), Lys (K), or His (H) (Songyang et al., 1996). There is a potential motif in Prx2 containing Pro-directed Thr, $T^{89}$PRK, optimal for Cdk5 phosphorylation. To investigate whether Prx2 is a substrate of Cdk5, Prx2 and Prx2T89A, a Prx2 mutant in which nonphosphorylatable Ala (A) replaced Thr (T), were subjected to in vitro kinase assay with Cdk5 alone, Cdk5/p35, or Cdk5/p25 active complexes. Incubation of bacterially expressed Prx2 or Prx2T89A with Cdk5 alone did not result in any radiolabel signal, indicating that the activating binding partner of Cdk5 was required for phosphorylation. The recombinant Prx2 was phosphorylated when either p35 or p25 was present along with Cdk5. In contrast, the recombinant Prx2T89A showed almost no detectable phosphorylation (Figure 2A). This indicates that both Cdk5/p35 and Cdk5/p25 can phosphorylate Prx2 and that almost all the phosphorylation occurs on the T89 residue.

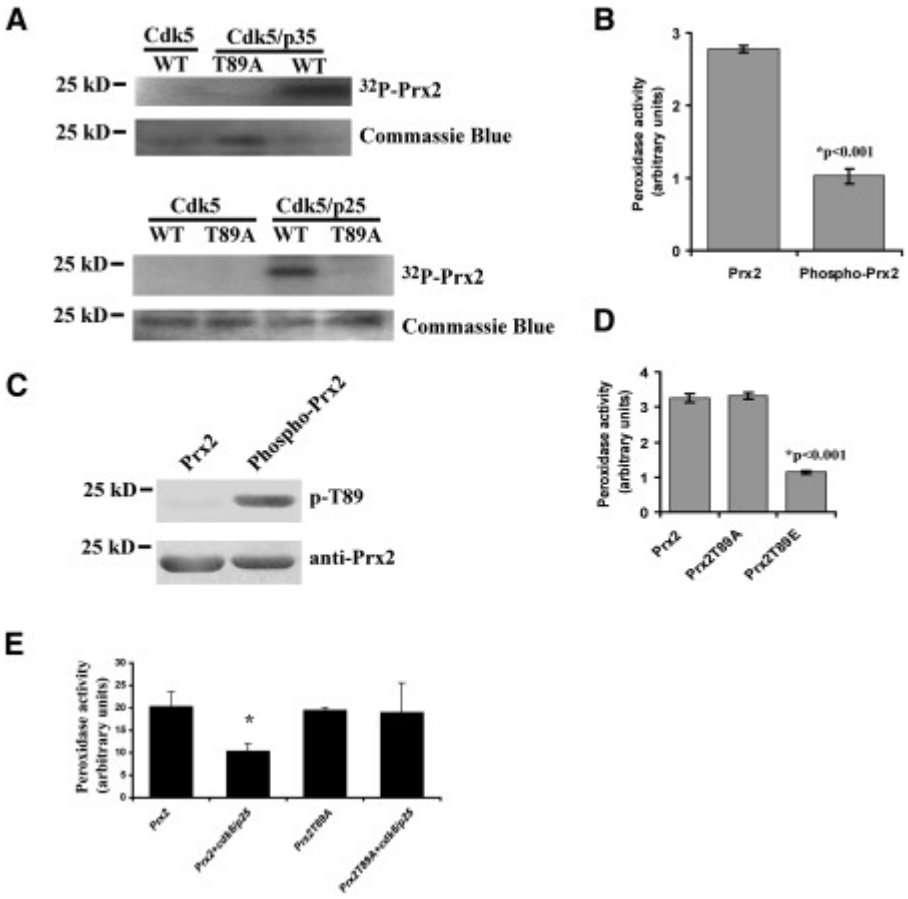


Figure 2. Prx2 Is an In Vitro Substrate of Cdk5, and Peroxidase Activity of Prx2 Is Modulated through Phosphorylation(A) Prx2 is a substrate of Cdk5/p35 and Cdk5/p25. One microgram of purified His-Prx2 or His-PrxT89A was incubated with 50 ng of purified GST-Cdk5, GST-Cdk5/GST-p35, or GST-Cdk5/GST-p25 and 1 μCi of [γ-$^{32}$P]ATP at 30°C for 30 min. The proteins were separated by SDS-PAGE for autoradiography.(B) Peroxidase activity of Prx2 is reduced by phosphorylation. Two hundred micrograms of His-Prx2 was incubated with 10 μg of GST-Cdk5/GST-p25 and 10 μM ATP at 30°C for 6 hr. The reaction mixture was separated by Q-column to isolate phospho-Prx2 from Prx2 after clearing GST-tagged Cdk5 and p25 by GSH-Sepharose. 0.5 μg of Prx2 or phospho-Prx2

was used for the peroxidase assay at 30°C for 10 min. The consumption of NADPH was measured at 340 nm wavelength by spectrophotometer. The data are the mean ± SEM (n = 3).(C) Determination of purity of phospho-Prx2 and confirmation of specificity of p-T89 for phospho-Prx2. One microgram of Prx2 or purified phospho-Prx2 as isolated in (B) was probed by western blot analyses using the p-T89 antibody or a pan-Prx2 antibody.(D) Peroxidase activity of Prx2T89E is lower than Prx2. 0.5 μg of purified His-Prx2, His-Prx2T89A, or His-PrxT89E was assayed for peroxidase activity as described above in (B). The data is the mean ± SEM (n = 4).( E) Peroxidase activity of Prx2T89A is not affected by Cdk5 phosphorylation. Ten micrograms of purified His-Prx2 or His-Prx2T89A was incubated with or without GST-Cdk5/GST-p25 (3 μg each) overnight at 30°C in the presence of 2 mM DTT. Following dialyses, peroxidase activity was measured as described in (B). The data are the mean ± SEM (n=3).

To assess the effects of Cdk5-mediated Prx2 phosphorylation on peroxidase activity, WT Prx2 was purified from bacteria. It was then incubated with GST-Cdk5 and GST-p25 purified from bacteria. Afterwards, phospho-Prx2 was separated from nonphosphorylated Prx2 by Q-column. Equal amounts of phosphorylated and nonphosphorylated Prx2 were then assessed for peroxidase activity by monitoring the $H_2O_2$-dependent oxidation of NADPH in the presence of thioredoxin (Trx) and Trx reductase. The peroxidase activity of phospho-Prx2 was 37% of that of nonphosphorylated Prx2 (Figure 2B). To confirm isolation and phosphorylation of Prx2 as just described, we generated a phospho-antibody specific for phosphorylated T89 of Prx2. The phospho-T89 (p-T89) antibody recognized phosphorylated Prx2 but not the nonphosphorylated form isolated by Q-column upon

western blot analyses (Figure 2C). A pan-Prx2 antibody was also isolated and shows that total Prx2 levels were approximately equal between nonphosphorylated and phosphorylated forms (Figure 2C).

The above results indicate that Cdk5 phosphorylation of Prx2 results in downregulation of peroxidase activity. To confirm this and ascertain that this is due to phosphorylation at T89, we isolated bacterially expressed Prx2, the Prx2T89A mutant, and a Prx2T89E mutant designed to mimic phosphorylation. Equal amounts of proteins were assayed for peroxidase activity. Importantly, the mutant Prx2T89E resulted in a 66% reduction in peroxidase activity compared to Prx2. The mutant Prx2T89A on the other hand was not significantly different from WT (Figure 2D). Importantly, we would predict that if Cdk5-mediated phosphorylation of Prx2 at T89 leads to downregulation of peroxidase activity, the Prx2T89A mutant should not be responsive to Cdk5 phosphorylation. Consistent with this notion, phosphorylation of recombinant WT Prx2 but not the Prx2T89A mutant by Cdk5 in vitro led to reduced peroxidase activity (Figure 2E). Finally, we also observed that phosphatase treatment of WT Prx2 previously phosphorylated by Cdk5 reversed the decrease in peroxidase (see Figure S2). Taken together, our data, at least in vitro, indicate that Cdk5 phosphorylates Prx2 at T89, which results in reduced Prx2 activity.

Prx2 Plays a Protective Role in Cortical Neurons Insulted by Neurotoxin $MPP^+$

We next determined whether Prx2 and its phosphorylation may play a role in neuronal death induced via mitochondrial stress by evaluating the effects of $MPP^+$, the active metabolite of MPTP, on death of cultured cortical neurons. It is important to note that these cultures are completely neuronal as evaluated by MAP2 staining (see Figure S3).

We first evaluated the effect of $MPP^+$ on T89 phosphorylation utilizing the phospho-specific antibody p-T89 for phosphorylated Prx2 at T89. Analysis of an $MPP^+$ time course by western blot indicated a maximal increase in phospho-Prx2 signal at 24 hr (Figure 3A). This coincided with the peak in Cdk5 kinase activity measured under the same conditions (Figure 3B). In the latter assay, immunoprecipitated Cdk5 from neurons treated by $MPP^+$ at different time points was subjected to a kinase assay using histone H1 as a substrate. The increase in Prx2 phosphorylation at T89 was also observed in cortical neurons analyzed by immunofluorescence using the same phospho-T89 antibody after $MPP^+$ treatment (Figures 3C, 3D, and 3E). There was a notable increase in phospho-labeling upon $MPP^+$ stress in the soma and neurites. This increase of fluorescence was quantified over a number of neurons by image analyses, showing a 90% increase in neurites and 62% increase in the soma. Blocking peptide treatment was used as a control for specificity and shows the required loss of fluorescent signal. Importantly, levels of Prx2 did not dramatically change upon $MPP^+$ treatment. This was observed both with western blot (Figure 3A) and upon immunofluorescent analyses (Figure 3C). Similar observations of increased phosphorylation of Prx2 were also observed in midbrain cultures containing dopamine neurons exposed to $MPP^+$ (see Figure S4). In addition, we also observed Prx2 phosphorylation when midbrain neurons were treated with another mitochondrial toxin, rotenone (Greenamyre et al., 2003) (see Figure S5).

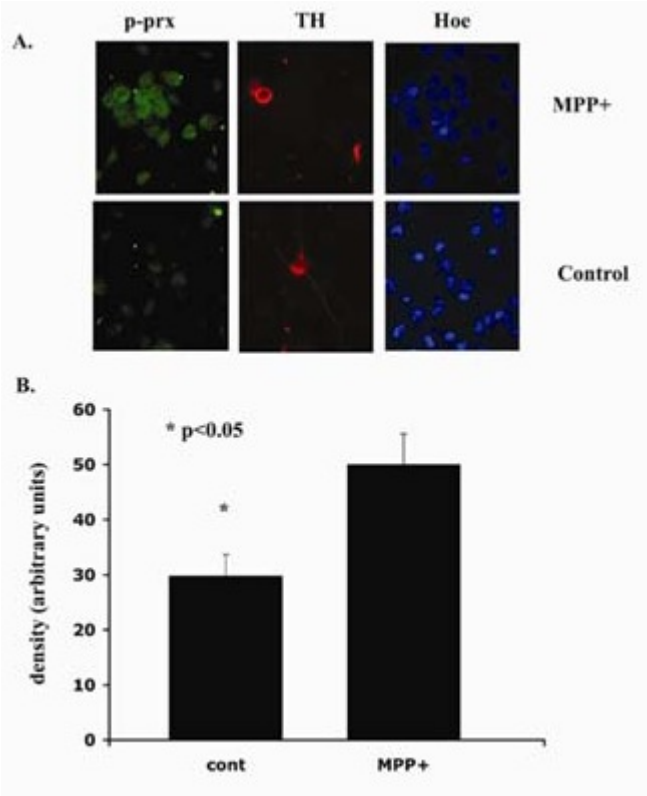


**Figure S4.** Midbrain mesencephalic cultures show increased phospho-Prx2 staining upon MPP+ treatment. Midbrain cultures were treated with 20μM MPP+ for 24 hours and then fixed and analyzed by immunofluorescence using p-T89 antibody (green), TH antibody (red) or Hoechst staining (blue). (A) Representative immunofluorescence staining as indicated. Note that midbrain cultures have only a small percentage of neurons that are dopaminergic. In addition, increase in phospho-Prx2 staining is not specific to dopamine neurons. (B) Quantitation of phospho-Prx2fluorescence intensity of dopaminergic TH positive neurons.

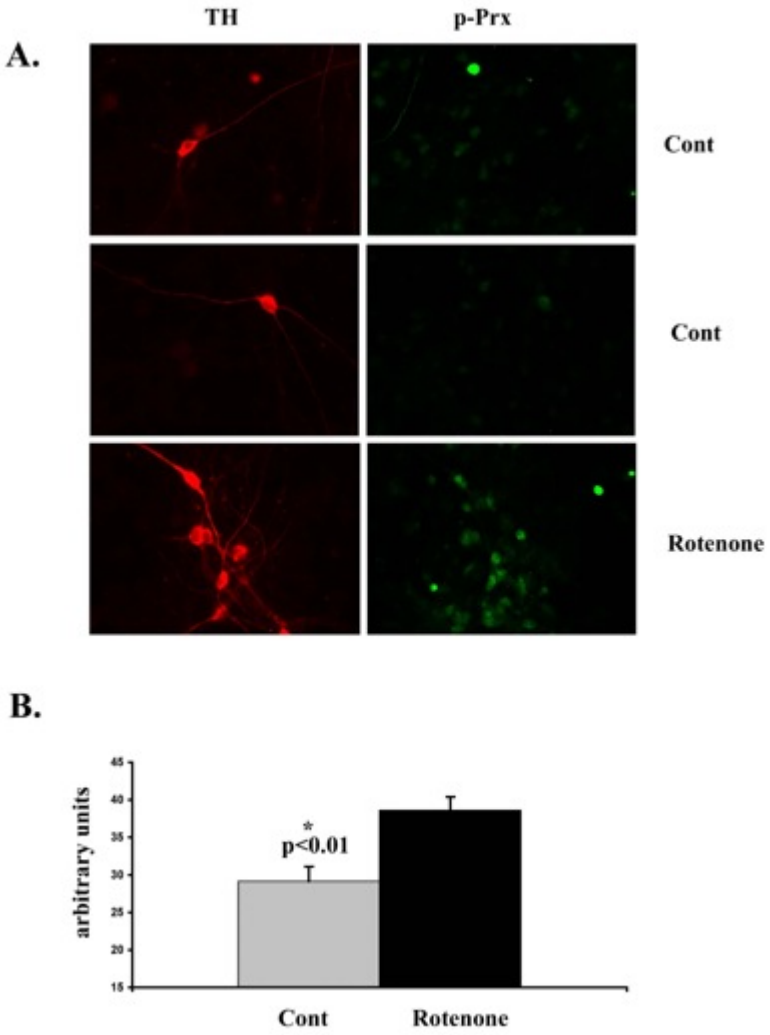


**Figure S5.** Midbrain mesencephalic cultures show increased phospho-Prx2 staining upon rotenone treatment. Midbrain cultures were treated with 25 μM rotenone for 72 hours and then fixed and analyzed by immunofluorescence using p-T89 antibody (green) and TH antibody (red). (A) Representative immunofluorescence staining as indicated. Note that midbrain cultures have only a small percentage of neurons that are dopaminergic. Two representative control nonrotenone treated fields are provided. (B) Quantitation of phospho-Prx2 fluorescence intensity of dopaminergic TH positive neurons.

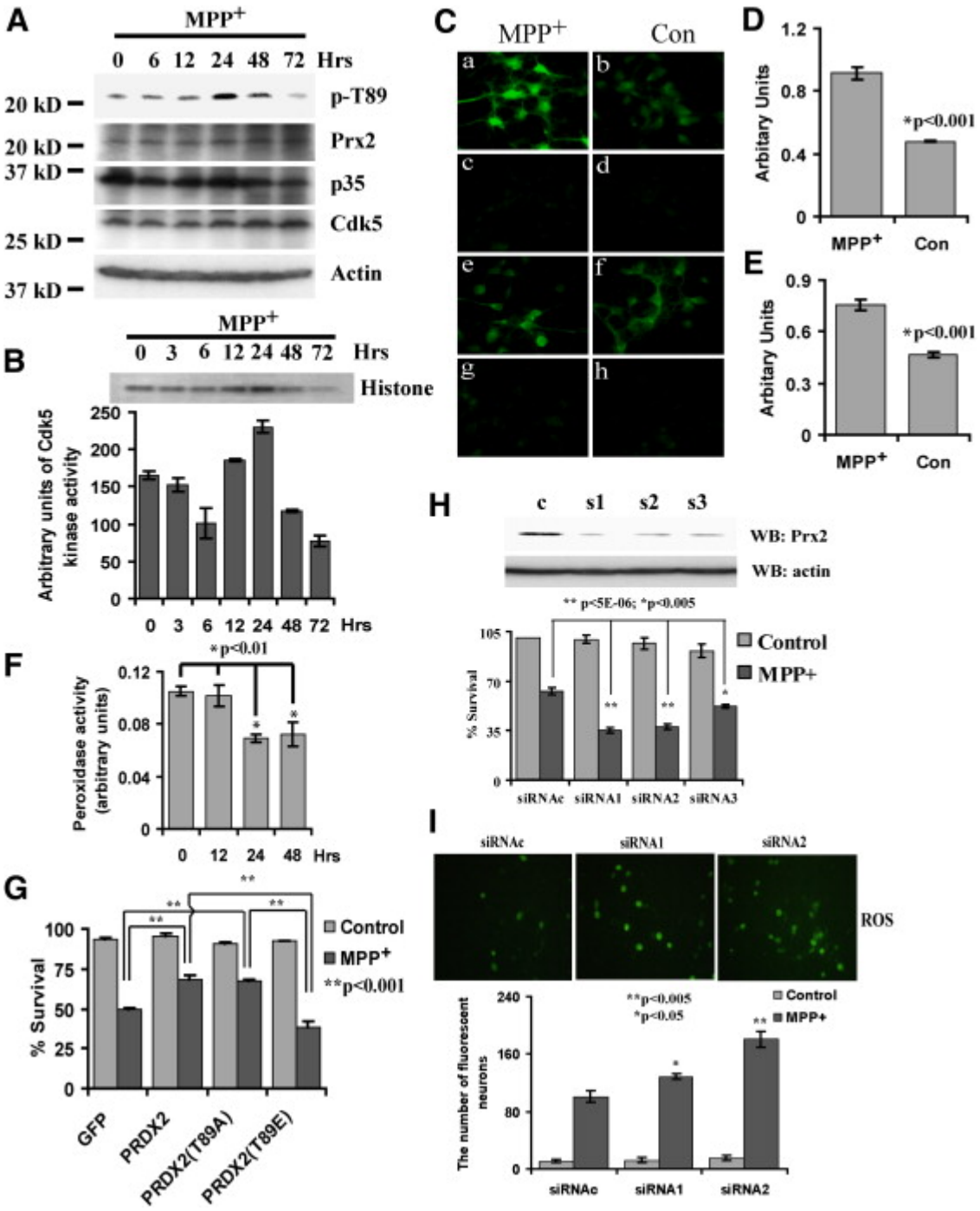


**Figure 3.** Reduction of Prx2 Peroxidase Activity and Associated Phosphorylation at T89 in Neurons after $MPP^+$ Treatment(A) Increase of phospho-Prx2 after $MPP^+$ insult. Cultured cortical neurons were treated with 20 μM $MPP^+$. The treated neurons were harvested at different time points, 6, 12, 24, 48, or 72 hr after $MPP^+$

treatment. Forty micrograms of cell lysate was analyzed by western blot analyses utilizing p-T89, anti-Prx2, C-19 for p35, C-8 for Cdk5, or anti-β-actin antibodies. Similar results were observed in three independent experiments.(B) Increase of Cdk5 kinase activity in neurons after $MPP^+$ treatment. Neurons were treated as above described. Cdk5 was isolated from 50 μg of cell lysate by immunoprecipitation using the C-8 antibody and was incubated with 0.5 μCi of [$\gamma$-$^{32}$P]ATP at 30°C for 30 min using histone H1 as a substrate. The proteins were separated by SDS-PAGE for autoradiography. The density of autoradiographic bands was normalized from three experiments and is presented as mean ± SEM.(C) Increase of phospho-Prx2 in neurons by immunofluorescent staining. After 24 hr treatment by $MPP^+$, neurons were fixed by 4% paraformaldehyde. (a–d) Neurons were incubated with p-T89 antibody and coincubated with the appropriate phosphorylated peptide sequence used to produce the antibody (c and d) or the control nonphosphorylated peptide sequence (a and b). (e–h) Neurons were fixed as above and stained with our pan-Prx2 antibody without (e and f) or with (g and h) a quenching peptide used to produce the antibody as control. The images were captured by fluorescent microscopy.(D and E) Distribution of phospho-Prx2 in neurons treated by $MPP^+$. The fluorescent signal in soma (D) or dendrites (E) was measured from 200 neurons through image analysis. The data are the mean ± SEM.(F) Downregulation of Prx2 peroxidase activity after $MPP^+$ treatment. Prx2 was isolated from cultured neurons treated with $MPP^+$ for the indicated times using a monoclonal anti-Prx2 antibody obtained from Abcam. Peroxidase activity was measured as described above. The data are the mean ±

SEM (n = 3).(G) Prx2 protects neuron form death after $MPP^+$ treatment. Cortical neurons were infected with virus expressing GFP alone or along with Prx2, Prx2T89A, or Prx2T89E and cultured for 3 days. The cells were exposed to $MPP^+$ for 48 hr and neuronal survival was evaluated by assessing nuclear integrity of GFP-positive neurons. The data are the mean ± SEM (n = 3). Similar results were obtained when equivalent constructs were transfected (data not shown).(H) Downregulation of Prx2 by siRNA oligonucleotide treatment sensitizes cortical neurons to $MPP^+$ treatment. Three independent siRNA sequences (s1/siRNA1, s2/siRNA2, s3/siRNA3) and a control sequence (c/siRNAc) were evaluated for their ability to downregulate endogenous Prx2 levels in cortical neurons as described in Experimental Procedures (top panel). (Bottom graph) Transfected cultures were then assayed for survival following 48 hr $MPP^+$ treatment by MTT assay. The data are the mean ± SEM (n = 3).(I) Downregulation of Prx2 by siRNA oligonucleotide treatment increases ROS levels following $MPP^+$ treatment. (Top panel) Representative DCF fluorescence in control (siRNAc) or siRNA1 or siRNA2 oligonucleotide-treated cultures after treatment with 20 μM $MPP^+$ for 24 hr under a fluorescent microscope. (Bottom graph) Quantification of the number of DCF fluorescence-positive cells in cells treated as above. Random fields were analyzed for the number of DCF-positive neurons. The data are the mean ± SEM (n = 4).

We next determined whether a reduction in Prx2 activity accompanied the increase in T89 phosphorylation by analyzing a time course following $MPP^+$ treatment of cortical neurons. Importantly, Prx2 activity decreased at 24 hr, opposite to that of T89 Prx2

phosphorylation and Cdk5 activation (Figure 3F). These results suggest that Prx2 peroxidase activity is regulated by T89 phosphorylation in cultured neurons following mitochondrial insult.

To evaluate whether T89 phosphorylation of Prx2 plays a role in neuronal death induced by $MPP^+$, cortical neurons were infected with virus expressing Prx2, Prx2T89A, and Prx2T89E. The viability of the infected neurons was assessed by evaluating nuclear integrity after exposing cultures to $MPP^+$ for 48 hr. Expression of Prx2 and Prx2T89A significantly protected neurons from death in comparison to that of GFP and Prx2T89E (Figure 3G). Conversely, we also evaluated whether downregulation of Prx2 might sensitize neuronal cultures to $MPP^+$ treatment. We designed three different siRNA sequences to Prx2. The siRNA sequences 1 and 2 showed the most significant reduction in Prx2 levels (Figure 3H). These siRNA sequences sensitized the neuronal cultures to the toxic effects of $MPP^+$ treatment (Figure 3H). Finally, we also examined for ROS under these conditions by 2′, 7'-Dicholororescein diacetate (DCF) staining. As shown in Figure 3I, both siRNA sequences 1 and 2 significantly increased the number of DCF-positive neurons. Taken together, our results suggest a model by which a decrease of Prx2 peroxidase activity mediated through T89 phosphorylation after $MPP^+$ insult enhances oxidative stress, resulting in neuronal death.

T89 Phosphorylation of Prx2 Is Mediated by Cdk5 in Neurons after $MPP^+$ Treatment

To investigate whether T89 of Prx2 is phosphorylated in neurons by Cdk5, lysates from WT and $p35^{-/-}$ neurons treated with $MPP^+$ were analyzed by western blot. Absence of p35 led to a significant decrease of phosphorylation of Prx2 at T89 (Figure 4A). It is

important to note, however, that this reduction was not absolute, suggesting that, at least in the present in vitro paradigm, other activators of Cdk5 such as p39 might also be present. It might also be due to the actions of other kinases. Prx2 levels were not observed to vary between WT and $p35^{-/-}$ neurons with or without $MPP^+$ treatment. To further confirm this reduction in phospho-Prx2 signal with p35 deficiency, we carried out immunofluorescent analyses. In $p35^{-/-}$ neurons, the increase in phospho-T89 signal observed upon $MPP^+$ treatment in WT neurons was significantly reduced (Figure 4B). Consistent with this observation, similar inhibition of Prx2 phosphorylation was observed with treatment of the Cdk inhibitor Roscovitine, but not with the GSK3 inhibitor lithium (see Figure S6). These data indicate that the phosphorylation of Prx2 at T89 in neurons following $MPP^+$ insult is significantly dependent upon Cdk5 activity. Next, we examined peroxidase activity of Prx2 in WT and $p35^{-/-}$ neurons following $MPP^+$ treatment. The data clearly showed that Prx2 peroxidase activity was decreased following $MPP^+$ treatment in WT neurons. However, this reduction did not occur in $p35^{-/-}$ neurons (Figure 4C). This indicates that peroxidase activity of Prx2 is regulated via phosphorylation by Cdk5. These data also suggested that $p35^{-/-}$ neurons should show reduced oxidative stress and resistance to $MPP^+$-induced neuronal death. To test this, ROS levels were measured utilizing DCF. ROS was significantly increased in WT neurons upon $MPP^+$ exposure as measured by both average intensity (54% increase) (Figures 4E and 4F) and number of DCF-positive neurons (34% increase) (data not shown). In contrast, $p35^{-/-}$ neurons showed reduced ROS levels upon $MPP^+$ treatment (35% decrease average density, Figure 4F; 25% decrease total number of cells, data not shown) when compared to WT littermate controls. $p35^{-/-}$ neurons were also substantially

protected from $MPP^+$-induced death when compared to WT littermate control neurons (Figure 4D). Finally, based upon our previous observations that calpain-mediated activation of Cdk5 is important for neuronal death (Smith et al., 2006), we would predict that calpain inhibition should also block Prx2 phosphorylation. Consistent with this, cotreatment of $MPP^+$-exposed neuronal cultures with the calpain inhibitor PD150606 (Sedarous et al., 2003 and Wang et al., 1996) led to decreased Prx2 signal as measured by immunofluorescence analyses (Figures 4G and S7). Taken together, our data indicate that Cdk5 kinase activity has a critical role in the reduction of Prx2 peroxidase activity through phosphorylation of Prx2 at T89 following $MPP^+$ insult and that this is a contributing factor to ROS increase and the ensuing neuronal death.

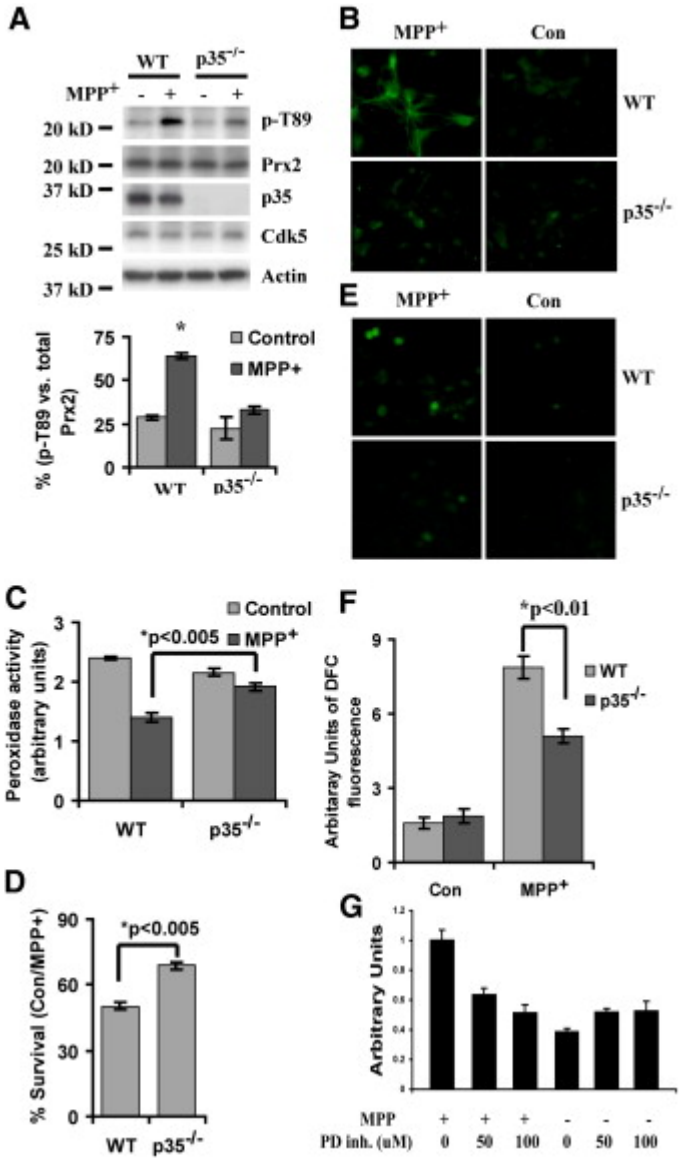


**Figure 4.** Prx2 Is a Substrate of Cdk5 in Neurons Treated with $MPP^+$(A and B) Cdk5 phosphorylates Prx2 in neurons treated by $MPP^+$. (A) Neurons from WT or $p35^{-/-}$ embryos were treated with $MPP^+$ insult for 24 hr. The cell lysates were subjected to SDS-PAGE and p-T89 western blot analyses. The membranes were then stripped and reprobed with anti-Prx2, C-19 for p35, C-8 for Cdk5, or anti-β-actin. The bottom panel shows densitometric values of phospho-Prx2 relative to

Prx (p-T89/total Prx2*100). Each value is the mean ± SEM (n = 3). (B) Likewise, cultures as indicated were subjected to immunofluorescent staining utilizing the p-T89 antibody. Similar results were obtained in three independent experiments.(C) Phosphorylation of Prx2 at T89 by Cdk5 reduces peroxidase activity. Cortical cultures from WT or $p35^{-/-}$ embryos were treated with $MPP^+$ for 24 hr as described above. Peroxidase activity assay was carried out also as described above. The data are the mean ± SEM (n = 3).(D) $p35^{-/-}$ neurons are resistant to $MPP^+$-induced death. Neurons from WT or $p35^{-/-}$ embryos were exposed to $MPP^+$ for 48 hr. The viability of neurons was measured by MTT assay. The survival percentage was obtained by comparing value from the $MPP^+$-treated neurons to that of the nontreated neurons in either $p35^{-/-}$ or WT neuronal cultures. The data are presented as mean ± SEM (n = 3).(E and F) The role of Cdk5/p35 in $MPP^+$-induced ROS. (E) Representative DCF fluorescence in WT and $p35^{-/-}$ neurons after treatment with 20 μM $MPP^+$ for 24 hr under a fluorescent microscope. (F) Quantification of DCF fluorescence signal in WT and $p35^{-/-}$ neurons either treated or untreated with $MPP^+$. Random fields were analyzed for average fluorescence intensity. The data are the mean ± SEM (n = 4).(G) Calpain inhibitors block increase in $MPP^+$-induced phospho-Prx2 signal. Cortical neuronal cultures were untreated or treated with 20 μM $MPP^+$ and/or the calpain inhibitor PD150606, as indicated. Cultures were fixed and stained for phospho-Prx2 and Hoechst. For representative pictures, please see Figure S7. The fluorescent signal in soma was measured by image analyses from 45 neurons in 3 random fields. The data are presented as mean ± SEM.

Prx2 Prevents the Loss of DAergic Neurons in the SNc in MPTP Mouse Model of PD

The phosphorylation of Prx2 at T89 by Cdk5 has a functional role in neuronal death in the $MPP^+$-induced cell death model. These data led us to further investigate the effects of Prx2 on neuronal death in an in vivo mouse model of PD. We employed the MPTP mouse model of PD to assess roles of Prx2 in the loss of DAergic neurons. We first determined the effects of expression of WT Prx2 and its mutants, Prx2T89A and Prx2T89E, on survival of DAergic neurons following MPTP administration. These constructs were targeted unilaterally to the SNc DAergic neurons using an adenoviral-mediated gene delivery approach as we have previously performed (Crocker et al., 2001, Crocker et al., 2003, Kalia et al., 2004, Kim et al., 2005 and Smith et al., 2003). Protein expression of adenoviral Prx2 and its mutant was verified by western blot analysis (Figure 5B). We found that expression of Prx2 and Prx2T89A resulted in significant DAergic neuroprotection following MPTP treatment when compared with the contralateral untreated side or with GFP-injected control animals as analyzed by counting the number of tyrosine hydroxylase (TH) positive neurons (Figures 5A and 5B). In contrast, expression of Prx2T89E showed similar effects to GFP controls (Figures 5A and 5B). As an independent assessment of survival, we also examined for the number of neurons in the SNc region by cresyl violet staining. This also ensures that loss of neurons by MPTP treatment is not simply due to loss of TH expression. Our cresyl violet analysis was similar to that of TH assessment (Figure 5C). These data indicate that Prx2 can

modulate DAergic neuron survival in the SNc following MPTP administration and suggest that the T89 regulatory site may be important in this DAergic cell death process.

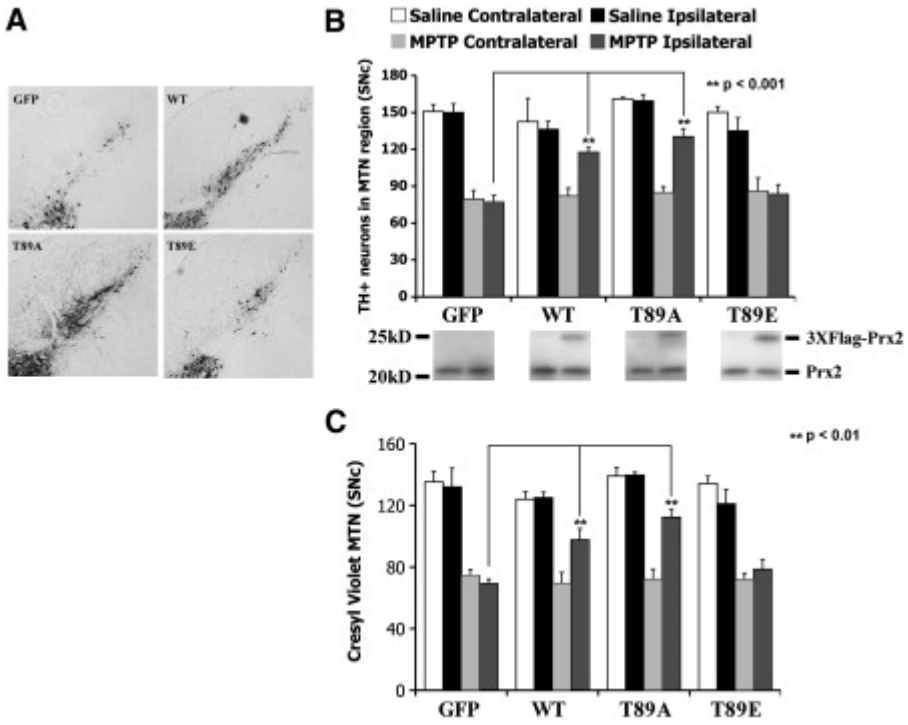


**Figure 5.** Prx2 Protects DAergic Loss following MPTP Administration(A) The adenoviruses (2 μl, 1 × $10^7$ particles per μl) expressing Prx2, Prx2T89A, and Prx2T89E were injected directly into the striatum of animals 7 days before initiation of MPTP treatment. A GFP-expressing virus was used as a control. Brains were sectioned into 14 μm slices for TH DAB staining. Representative pictures of the ipsilateral side of animals injected with the indicated virus and treated with MPTP were shown.(B) Quantification of the number of DAergic neurons from ipsilateral or controlateral for the indicated treatment groups are shown. The data are presented as mean ± SEM (n = 4–5/group). Expression of

Prx2, Prx2T89A, and Prx2T89E in the SNc extracts was confirmed by western blot analyses using a pan-antibody for Prx2.(C) Quantitation of neurons in the SNc region by cresyl violet staining. The data are presented as mean ± SEM (n = 4/group).

Cdk5-Mediated Phosphorylation of Prx2 at T89 Plays a Pivotal Role in DAergic Neuron Damage by Regulation of Prx2 Peroxidase Activity in an MPTP Mouse Model of PD

The above in vivo evidence only demonstrates that Prx2 could potentially be important in the MPTP model. To further support this, we examined whether endogenous Prx2 may be modulated at T89 following MPTP treatment. Accordingly, the SNc extracts obtained from mice treated with MPTP for various times were subject to western blot analyses. As shown in Figure 6A, Prx2 phosphorylation increased following MPTP treatment, reaching the highest level of phosphorylation at 3 days following injected MPTP. To determine whether the phosphorylation of Prx2 at T89 is mediated by Cdk5, the SNc lysates from $p35^{-/-}$ mice or WT littermate controls were treated with MPTP and analyzed 3 days post-treatment. The level of phosphorylated Prx2 in $p35^{-/-}$ mice was significantly less than that in WT mice after MPTP treatment (Figure 6B). To further confirm the increase in the level of phosphorylated Prx2 in DAergic neurons in SNc of MPTP-treated mice, we assessed Cdk5-phosphorylated Prx2 by immunofluorescence analyses. Phosphorylated Prx2 was clearly observed in DAergic neurons in the SNc of WT mice treated with MPTP but not substantially observed in that of $p35^{-/-}$ mice (Figure 6C). We quantified the average fluorescent signal from TH-positive neurons by image analyses. As shown in Figure 6D, the fluorescent signal of phospho-Prx2 in WT SNc increased

approximately 30%–50% in comparison to untreated WT controls or treated and untreated p35$^{-/-}$ mice.

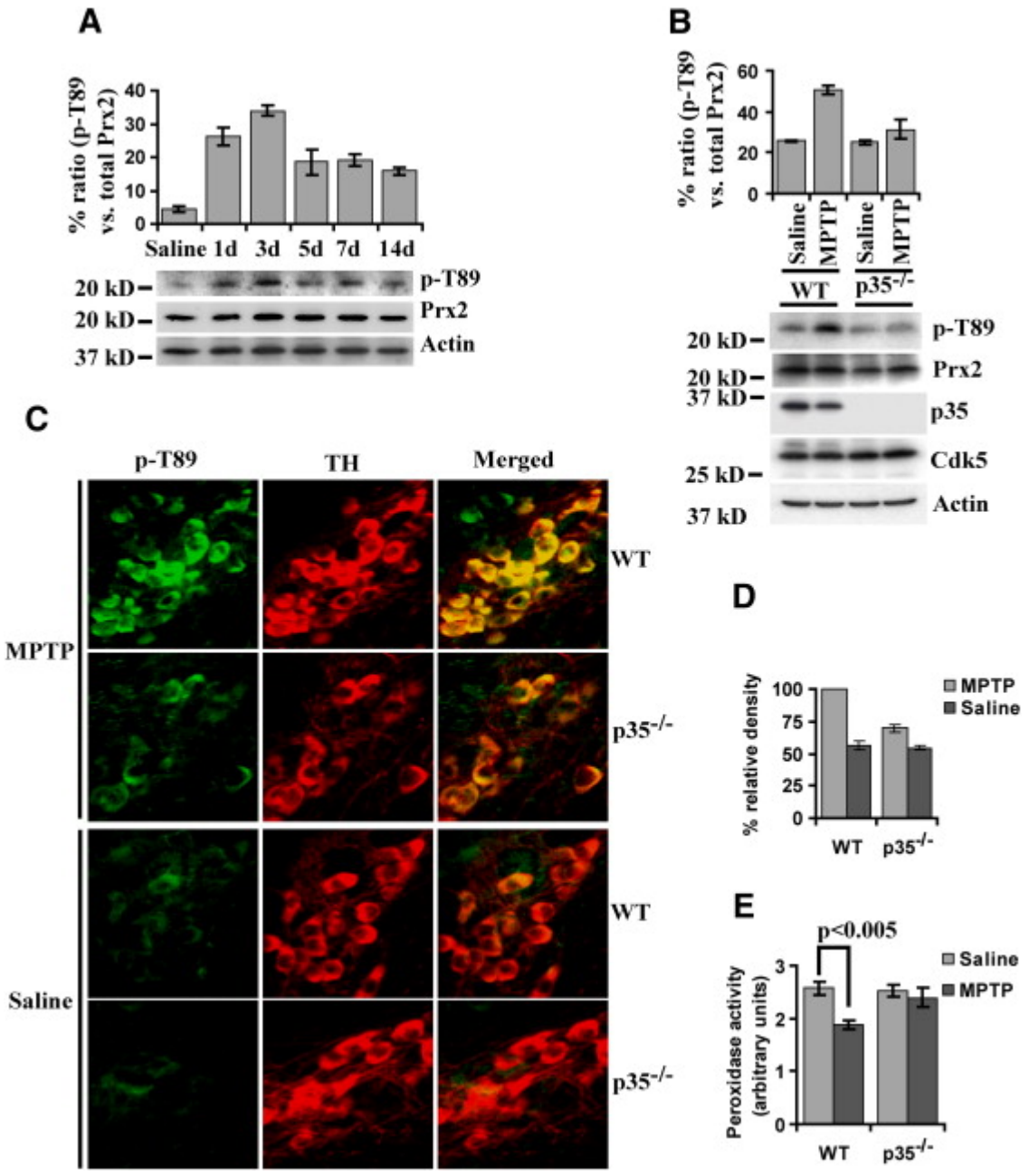


**Figure 6.** Peroxidase Activity of Prx2 Is Regulated in an In Vivo MPTP Mouse Model of PD(A) Phosphorylation of Prx2 at T89 is increased after MPTP

administration. The SNc extracts were obtained from animals treated with MPTP for the indicated times. (Bottom panel) The SNc lysates were subjected to SDS-PAGE and western blot probed as indicated using p-T89, anti-Prx2, and anti-β-actin antibodies. The top panel shows densitometric values of phospho-Prx2 relative to Prx (p-T89/total Prx2*100). Each value is the mean ± SEM (n = 3).(B) Prx2 is a substrate of Cdk5 complexes in DAergic neurons from MPTP-administrated mice. (Bottom panel) The SNc lysates from WT or $p35^{-/-}$ mice 3 days following MPTP or saline administration were analyzed by western blot analyses using p-T89, anti-Prx2, anti-p35 (C-19), anti-Cdk5 (C-8), and anti-β-actin antibodies. The top panel shows densitometric values of phospho-Prx2 relative to Prx (p-T89/total Prx2*100). Each value is the mean ± SEM (n = 3).(C) Increased phospho-Prx2 is colocalized with TH-positive neurons. The sections from WT or $p35^{-/-}$ mice were analyzed 3 days following MPTP or saline treatment. Sections were double-stained using p-T89 antibody (green) and anti-TH monoclonal (red) antibody for 24 hr at 4°C. The sections were incubated with Alex-488-conjugated antibody specific for rabbit IgG and Alex-594-conjugated antibody for mouse IgG for 3 hr at room temperature. The sections were visualized by fluorescent microscopy.(D) The fluorescent signals from the p-T89 labeling (C) were quantified densitometrically by imaging analysis. Three sets of animals (n = 1 animal/treatment group/set) were individually stained and analyzed by densitometric analyses. 40–50 TH-positive neurons for each animal (over 3–6 slides/animal) were measured for p-T89 signal. This value was then averaged. Within each set of animals, the average value for each treatment group was

normalized to the WT MPTP value. The values were then averaged for all three sets of animals for an n = 3 (mean ± SEM).(E) Downregulation of peroxidase activity of Prx2 is mediated by Cdk5 in mice administrated by MPTP. Prx2 was isolated from 50 μg of SNc lysates from WT or $p35^{-/-}$ mice obtained 3 days following treatment with saline, or MPTP was analyzed for peroxidase activity. The data are presented as mean ± SEM (n = 3).

To examine whether the peroxidase activity of Prx2 is affected in the MPTP mouse model of PD, Prx2 was isolated from $p35^{-/-}$ SNc or WT littermate controls with and without MPTP treatment and assayed for activity. Prx2 isolated from WT mice treated by MPTP showed a significant decrease in peroxidase activity in comparison to untreated WT controls. In contrast, $p35^{-/-}$ animals did not show this reduction following MPTP treatment (Figure 6E). Finally, we have previously shown that calpains are central for Cdk5 activation (Smith et al., 2006). Consistent with this, adenoviral-mediated expression of the calpain inhibitor calpastatin blocks increase in phospho-Prx2 following MPTP treatment in vivo (Figure S8). Taken together, these data indicate that calpain-mediated Cdk5 activation mediates phosphorylation and reduction of Prx2 activity in an in vivo model of PD and that this activity plays an important role in the death of DAergic neurons.

**Relevance to Human PD**

While the above evidence strongly implicates the importance of Prx2 in the MPTP model of PD, we directly examined its potential relevance to human PD. Accordingly, we first examined the phospho-Prx2 signal in human PD postmortem samples and controls. The

equivalent T89 site is also present in human Prx2. As shown in Figure 7, nigral DAergic neurons from human midbrain PD and control samples were clearly detected by the presence of neuromelanin, granular brown pigmented regions detectable even without staining (see arrowheads in Figures 7A and 7B). When stained using phospho-Prx2 antibody and DAB visualization, little or no signal was detected in the perikarya of dopamine neurons from control midbrain samples. However, significant staining (black color) was observed in soma of dopamine neurons from PD patients (see arrow, Figure 7A). Staining in the region of neurons that resemble dopamine neurons in size and location but that did not contain neuromelanin was also observed in PD samples. Staining of neuritic processes was observed in both control and PD samples. The number of phospho-Prx2-positive dopamine neurons was then quantified from five PD and six control samples. As shown in Figure 7C, a significant increase in phospho-Prx2-positive neurons was observed in PD patient samples when compared to controls.

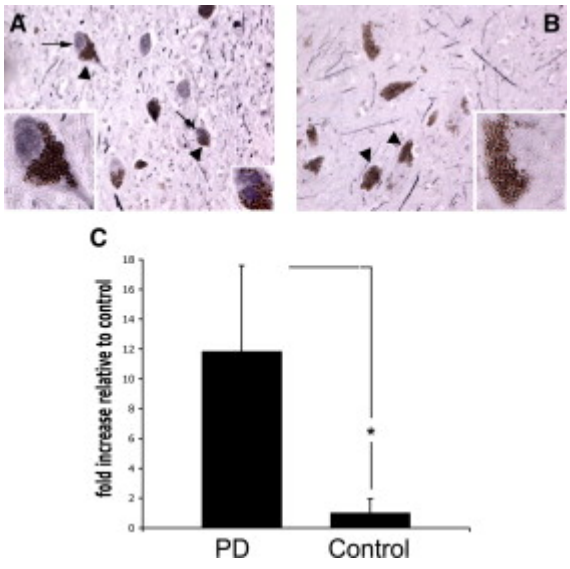

**Figure 7.** Prx2 Phosphorylation in Human PDPhosphorylation of Prx2 is increased in human PD. Human substantia nigra obtained from (A) PD and (B) control individuals. Sections were immunostained using p-T89 Prx2 antibody and visualized by DAB staining. Neuromelanin pigment indicative of dopamine nigral neurons is present as punctate brown staining (arrowheads) while the phospho-Prx2 signal shows as black staining in the soma (arrows). Two examples of phospho-Prx2 positive (A) and negative (B) neurons are labeled with arrows/arrowheads. (C) Quantitation of phospho-Prx2-positive neurons in PD (n = 5) and control (n = 6) individuals are shown (mean ± SEM). $^{*}p < 0.05$ (Student's t test).

Finally, we examined whether familial PD genes may impact Prx2 phosphorylation. The PD gene, *dj-1*, has also been linked to management of ROS ( Bonifati et al., 2003 and Kim et al., 2005). Interestingly, DJ-1 expression blocked Prx2 phosphorylation in neurons treated with $MPP^{+}$ (Figure S6C). Modulation of another PD gene, *pink1* (Valente et al., 2004), however, did not affect Prx2 phosphorylation, suggesting some specificity in the way PD genes impact Prx2 phosphorylation (Figure S6D). Taken together, our human patient data as well as that with DJ-1 further support the importance of Prx2 in PD.

# Discussion

ROS are generated as a result of normal metabolism (Adam-Vizi, 2005). However, generation of excessive oxidative load beyond a cell's homeostatic capacity can be deleterious. Mitochondrial dysfunction and excess ROS have been strongly implicated in the pathogenesis of PD (Jenner, 1998 and Przedborski, 2005). However, how these events are initiated, are regulated, and interact to promote neuronal death is not completely clear. Recently, we demonstrated that calpain-mediated Cdk5 activation plays an essential role in DAergic loss in the MPTP model of PD (Crocker et al., 2003, Smith et al., 2003 and Smith et al., 2006). These findings were important since they provided a plausible link between the actions of a mitochondrial damaging agent (MPTP) and activation of a pathogenic calcium-dependent process (calpain activation) consistent with known deregulation of calcium homeostasis in PD. However, the manner by which Cdk5 regulates downstream pathogenic events was not completely known. Presently, we identified a novel Cdk5 target, Prx2, an antioxidant enzyme with peroxidase activity (Rhee et al., 2005). We provide evidence that Prx2 is a physiological substrate of Cdk5. Cdk5 activation downregulates Prx2 peroxidase activity in PD models of death both in culture and in animals. Modulation of Prx2 activity also regulates neuronal loss. These data provide a mechanistic link of how the mitochondrial damaging agent MPTP leads to nigral loss by Cdk5 activation, phosphorylation/inactivation of an important antioxidant enzyme, and consequent increase in oxidative load (see Figure 8). The observation of increased Prx2 phosphorylation in human PD tissue as well as modulation by DJ-1 also indicates the potential importance of this pathway in human PD.

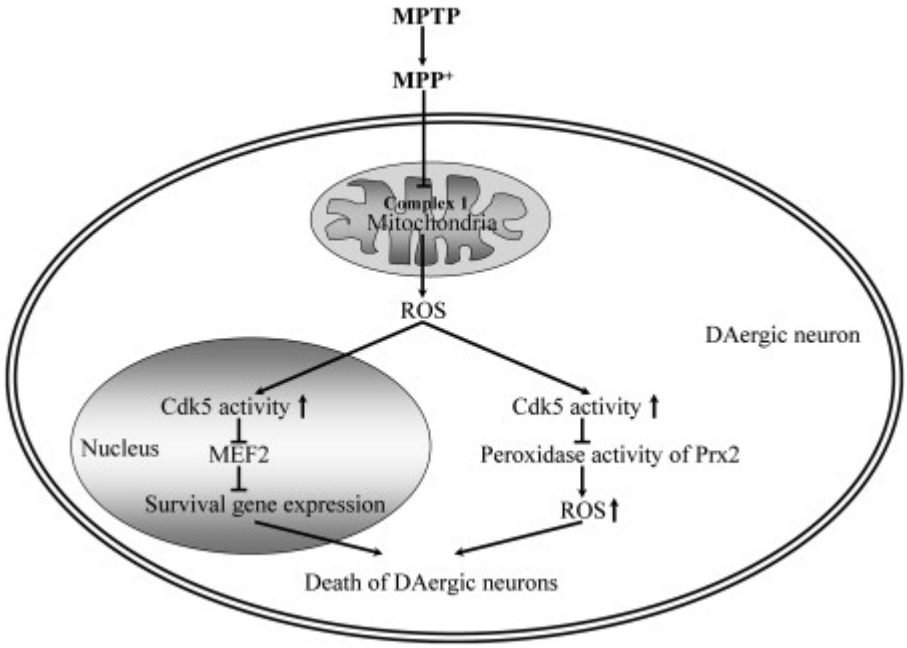


**Figure 8.** Model of Cdk5-Mediated DAergic Loss in MPTP Mouse Model of PDCdk5 kinase activity is activated by mitochondrial stress induced by $MPP^+$, a metabolite of MPTP. Activated Cdk5 regulates DAergic loss through phosphorylation of cytoplasmic substrate Prx2 to inhibit its antioxidative ability and phosphorylation of nuclear target Mef2 to inhibit Mef2 prosurvival function.

Prx2 Interacts with Cdk5/p35 Complexes and Is a Substrate of Cdk5

Our results demonstrate that Cdk5/p35 interacts with Prx2. Prx2 is a member of the Prx family that contains at least six members. The identification of the Prx2 form as an interacting partner is particularly relevant since Prx2 is localized to neurons, including the DAergic neurons of the SNc (Jin et al., 2005 and Sarafian et al., 1998). This is, in turn, consistent with known DAergic functions of Cdk5, particularly in models of PD as reported previously (Smith et al., 2003 and Smith et al., 2006). In contrast, Prx1, also

localized to the cytoplasm, is distributed in oligodendrocytes and microglia (Jin et al., 2005). These results, particularly in vivo, point to a neuron-specific Cdk5-Prx pathway of ROS management rather than a non-cell-autonomous mode of action regulated by other brain cell types such as glia. It is important to point out that this does not exclude the potential importance of other Prx members in neuronal loss. For example, Prx3, a mitochondrially localized enzyme (Watabe et al., 1994), also has potential Cdk5 sites. It will be interesting to determine whether this member might also play a Cdk5-dependent role in mitochondrial stress-induced death.

Our initial results indicated that the N-terminal portion of p35 was sufficient to bind to Prx2. However, it is important to note that both p35 and p25 can efficiently phosphorylate Prx2, at least in vitro. This suggests that stable binding to a Cdk5/p35 complex per se mediated by the p10 fragment is not required for efficient phosphorylation. We speculate that the p10 portion may be an important regulatory domain that regulates how efficiently p35 or Cdk5/p25 complexes may phosphorylate Prx2. Careful analyses will have to be performed to further study this interesting observation. Nonetheless, our results indicate not only that both Cdk5 complexes phosphorylate Prx2 on T89, but also that this modification significantly downregulates its activity.

Under basal conditions, p35 is abundantly localized to the inner cellular membrane, through a myristoylation anchor (Patrick et al., 1999). Appropriate activation of this form of Cdk5/p35 is the presumptive “normal” activity of this complex. However, p35 can be converted to a pathogenic p25 form by calpain-mediated cleavage (Lee et al., 2000,

Smith et al., 2003 and Smith et al., 2006). This results in a more stable active Cdk5 activator as well as the potential to be mislocalized to the nucleus (Gong et al., 2003 and O'Hare et al., 2005). One suggested nuclear target of the Cdk5/p25 complex is Mef2, which we and others have shown is important in models of oxidative stress in vitro (Gong et al., 2003) and following MPTP in vivo (Smith et al., 2006).

Cytoplasmic Cdk5 activity might also be pathogenic. For example, a portion of p25 could also be localized to the cytoplasm, and cytoplasmic targets such as tau have been previously proposed for Cdk5 particularly in models of Alzheimer's disease (Patrick et al., 1999). In this regard, we have identified an important cytoplasmic target of Cdk5 that could be regulated by either Cdk5/p35 or Cdk5/p25 complexes. The observation that Cdk5/p25 complexes efficiently phosphorylate Prx2 on T89, however, is consistent with a pathogenic role of this complex.

Cdk5-Mediated Prx2 Downregulation in PD and Oxidative Stress

The identification of Prx2 as a target of Cdk5 is particularly relevant since DAergic neurons are thought to be particularly susceptible to oxidative stress (Smythies and Galzigna, 1998). There are several lines of evidence that support a link between ROS and PD. For example, ROS levels are very high in PD patients (Jenner, 1998 and Przedborski, 2005). Numerous enzymes that produce ROS have been implicated as critical in in vivo models of PD (Przedborski, 2005). Damaging ROS has also been shown to occur in animals following exposure to mitochondrial poisons (Ara et al., 1998 and Schapira, 2001). Importantly, the mitochondria, a major source of oxidative stress, participates in PD pathogenesis (Przedborski, 2005). Consistent with this notion, familial forms of PD

have been associated with mitochondrial dysfunction. Indeed, the familial PD gene *dj-1* is thought to possess direct antioxidant functions ( Bonifati et al., 2003, Canet-Aviles et al., 2004, Dawson and Dawson, 2003, Kim et al., 2005, Martinat et al., 2004 and Shendelman et al., 2004).

Our evidence suggests that regulation of Prx2 is important in a toxin model of PD. For example, alteration of Prx2 levels modulates death both in vitro and in vivo following $MPP^+$/MPTP. It must be noted, however, that there are limitations to relating the in vivo MPTP model to PD and caution must be observed in making any direct comparisons to the human condition. For example, the relatively acute toxic nature of the MPTP model might not reflect accurately what occurs in the idiopathic PD. Accordingly, to support our MPTP data, we also report that phosphorylation of Prx2 also occurs in the nigral region of PD patients. This is consistent with the relevance of our findings to the human condition. However, standard and important caveats to interpreting any postmortem data apply here as well.

Using the MPTP model as an important first step in understanding the nigral degenerative process, we have identified how Prx2 is modulated to promote death following exposure to this mitochondrial toxin. We have shown previously that Cdk5 is hyperactivated and plays a major functional role in dopamine loss in the MPTP model (Smith et al., 2003). It is likely that Cdk5 acts to modify several downstream targets. For example, we had also previously shown that Cdk5 targets the nuclear transcription factor and survival factor Mef2 on a site known to suppress its activity (Smith et al., 2006). However, cytoplasmic targets may also be critical. We believe that Prx2 is one such important cytoplasmic

factor. This is supported by our data showing that Prx2 is phosphorylated at T89 both in vitro and in vivo following $MPP^+$/MPTP and that this is associated with a decrease in peroxidase activity. In support of this, a mutant mimicking constitutively phosphorylated Prx2T89E does not protect neurons from mitochondrial insult, whereas WT or a mutant lacking the T89 phosphorylation site effectively promotes survival. Most importantly, Prx2 phosphorylation is dependent on the Cdk5 complex since p35-deficient animals, which are resistant to death induced by $MPP^+$ or MPTP, have reduced Prx2 phosphorylation and Prx2 peroxidase activity. It is important to highlight that, in addition to peroxidase activity, Prx2 is also thought to possess some chaperone activity at least in cell lines (Moon et al., 2005). The relevance of this in the present context is not completely known. However, we have determined that the higher molecular weight complexes of Prx2 indicative of its chaperone activity do not change following $MPP^+$ insult, suggesting that its chaperone activity may not be relevant in this model (D.Q. and D.S.P., unpublished results). Finally, as mentioned previously, whether other members of Prx may be important in nigral degeneration is unknown. Intriguingly, Prx1 has been shown to be phosphorylated by cell-cycle Cdk members (Yang et al., 2002). The latter has been also implicated in neuronal death (Bu et al., 2002, Busser et al., 1998, McShea et al., 1997, Nguyen et al., 2003, Osuga et al., 2000, Rashidian et al., 2005, Rideout et al., 2003, Wang et al., 2002 and Zhang et al., 2004). Therefore, whether/how other Prx members are regulated by Cdk members will be of further interest.

In summary, we have uncovered an important mechanism by which calpain-mediated Cdk5 activation regulates DAergic neurodegeneration in an MPTP model of PD via downregulation of Prx2 peroxidase activity. We propose that this loss significantly

enhances the ROS environment and leads to DAergic neuron loss (Figure 8). This central pathway in addition to other pathways mediated by additional calpain or Cdk5 targets ultimately lead to nigral degeneration in response to MPTP (Figure 8). These findings are particularly relevant to human PD since both deregulated Cdk5 and increased ROS have been shown in the human PD condition (Jenner, 1998, Nakamura et al., 1997 and Przedborski, 2005). Furthermore, we presently, show that phosphorylated Prx2 is increased in human PD patients and that Prx2 phosphorylation is also modified by *dj-1*, a known PD gene (Bonifati et al., 2003). How the latter links to Prx2 phosphorylation will be of great interest in future studies. Taken together, our findings suggest that strategies to modulate Prx2 activity serve as beneficial targets for treatment of PD. This is of particular importance since Cdk5 is thought to have normal beneficial roles in neurons (Li et al., 2002) and modulating a relevant downstream target rather than Cdk5 directly may be a better therapeutic strategy with regard to this pathway.

# Experimental Procedures

## Animals

Eight-week-old male C57BL/6 mice (22–28 g; Charles River Laboratories, USA) were used for MPTP experiments. All animal experiments conformed to the guidelines set forth by the Canadian Council for the Use and Care of Animals in Research (CCAC) and the Canadian Institutes for Health Research (CIHR) and had approval from the University of Ottawa Animal Care Committee.

## Antibodies

The following antibodies were utilized: Tyrosine hydroxylase (TH) (Immunostar, USA), C-8 for Cdk5 (Santa Cruz, USA), C-19 for p35 (Santa Cruz, USA), β-Actin (monoclonal, Sigma, Canada), Prx2 (monoclonal, Abcam, UK), and Alex-labeled secondary antibodies (Invitrogen, Canada). Prx2 and phospho-Prx2T89 polyclonal antibodies were generated and initially purified from rabbit using standard protocols from Biogenes (Berlin, Germany) by immunization with carrier protein-conjugated phosphopeptide, LAWINpTPRKEGGLG. The phospho-Prx2 antibody p-T89 was obtained by first purifying the serum using the phosphorylated peptide. The pan-Prx2 antibody was obtained using the nonphosphorylated peptide. The phospho-specific antibody was further purified by adsorbing onto bacterially expressed and purified GST-Prx2 to remove any remaining crossreactivity to nonphosphorylated Prx2. MAP2 was obtained from Santa Cruz (H-300; 1:300).

## Isolation of p35-Binding Proteins

The assay was carried out as previously described (Qu et al., 2002).

**Mass Spectrometry**

The specific bands on GST-p10 lane were subjected for protein identification by a tandem mass spectrometry as previously described (Shevchenko et al., 1996 and Wilm et al., 1996).

**Fusion Proteins**

All GST and His fusion proteins were expressed in *E. coli* and affinity purified using GSH-beads and Ni-NTA Agarose (QIAGEN Inc, Canada) as per manufacturer's instruction.

**In Vitro Binding Assay**

The binding assay was performed as previously described (Qu et al., 2002).

**Yeast Two-Hybrid**

Plasmid construction: Plasmids were constructed using standard subcloning procedures. Briefly, an NcoI/SalI digest of p10 and an NcoI/BamHI digest of Prx2 were subcloned into NcoI/XhoI-digested pAS2-1 (Clontech, Canada) and Nco/BamHI-digested pACT2 (Clontech), respectively. Yeast two-hybrid screening (Clontech) pAS2-p10 and pACT2-Prx were transformed into Y187 and AH109 strains by the LiAc method (Ito et al., 1993) and plated onto SD-Trp$^-$ and SD-Leu$^-$ plates, respectively, as previously described (Mao

et al., 2004). Plates were incubated for 5 days at 30°C. Resultant colonies were mated and selected on SD-Leu$^-$Trp$^-$His$^-$ for 3–7 days at 30°C.

**Immunoprecipitation**

Samples were harvested in lysis buffer (50 mM Tris-HCl [pH 7.4], 100 mM NaCl, 1 mM EDTA, 1 mM DTT, and 0.2% Triton X-100) supplemented with protease inhibitors. Immunoprecipitations (IPs) were performed through incubation of antibodies with lysates overnight followed by incubation with anti-rabbit or anti-mouse Ig IP beads (eBiosciences, USA) at 4°C for 1 hr. The beads were washed three times by lysis buffer without protease inhibitors.

**Neuronal Cultures**

The primary culture of mouse cortical neurons was carried out as described previously (Fortin et al., 2001 and Xiang et al., 1996). Alternatively, for midbrain neuronal cultures, the whole midbrain, without meninges and blood vessels, was collected from embryos aged 13.5 days gestation and processed as above and as similarly described (Liu et al., 2000). Cultures were subject to 20 μM $MPP^+$ or rotenone (as indicated in text). In select experiments, neurons were also pretreated with the calpain inhibitor PD150606 (Calbiochem, Canada), the Cdk inhibitor, roscovitine (Sigma, Canada), or lithium (BDH, Canada) for 3 hr and then cotreated with 20 μM $MPP^+$. For survival using $p35^{-/-}$ neurons, littermate controls, or siRNA knockdowns, the MTT assay was utilized as per manufacturer's instruction (Sigma, Canada). For transfection or infection cultures, the

alternative strategy described below was utilized since only a small percentage of the neurons in culture were targeted.

**ROS Imaging**

Cortical neurons were incubated with 10 μM DCF for 20 min at 37°C and washed three times with NB medium. The fluorescence signal of oxidized DCF was observed by an inverted fluorescent microscope equipped with a 100 W xenon lamp and filter (for oxidized DCF, excitation = 488 nm and emission = 510 nm). At least four random fields were quantified for DCF-positive cells and/or average intensity by image analyses.

**Infection and Calcium Phosphate Transfection of Cultured Neurons**

Cortical neurons were mixed with adenovirus at MOI of 50 prior to plating and were then immediately seeded to 24-well plates and cultured for three days as previously described (Aleyasin et al., 2004, O'Hare et al., 2005 and Zhang et al., 2006). The cultures were exposed to $MPP^+$ for 48 hr. Cultures were then fixed and stained with Hoechst 33258 (0.5 ng/ml) and neuronal survival was evaluated by assessing nuclear integrity of GFP-positive neurons as previously described (Aleyasin et al., 2004). For transfection, 3 days after plating cortical neurons were transiently transfected using a modified calcium phosphate precipitation protocol (Xia et al., 1996 and Zhang et al., 2006). In brief, neurons were transfected with 1 μg of total plasmid DNA (0.75 μg of plasmid DNA and 0.25 μg of pEGFP as a reporter) purified using an EndoFree Plasmid Maxi kit (QIAGEN, Inc, Canada). Twenty-four hours post-transfection, neurons were treated with 20 μM $MPP^+$ (48 hr) and were fixed in 4% paraformaldehyde (containing 0.2% picric acid in

0.1M phosphate buffer [pH 6.9]) and evaluated as described above. Alternatively, neurons were transfected with double-stranded short-interfering RNA (siRNA) to Prx2 or CY3-labeled control duplex (60 pmol siRNA/24- well) as previously described (Zhang et al., 2006). We have observed that targeting of duplexes to neurons is much more efficient than that of plasmids and have used this procedure previously (Aleyasin et al., 2004 and Zhang et al., 2006). The Prx2 duplexes (s1: GCUUUCGGACUACAGAGGG, s2: GGGAUUCUUUAAGAGCUCU, s3: CCAAAUAAUUACUAGGCCU) along with a Cy3-labeled control duplex were obtained from Ambion (Austin, TX, USA). Forty-eight hours post-transfection, neurons were treated with $MPP^+$ (20 μM). At appropriate times, the cells were assayed for survival by MTT method (48 hr) or ROS as described above. Alternatively, cultures were analyzed by Western blot analyses for Prx2 levels (24 hr).

**Peroxidase Activity Assay**

Peroxidase activity was carried out by measurement of the consumption of NADPH (Fisher) which was mediated by Trx (Sigma, Canada) and Trx reductase (Sigma, Canada) at 30°C for 10 min for bacterially expressed proteins and 1 hr for precipitated proteins from cultured neurons or the SNc. In brief, 0.5 μg of bacterially expressed proteins or the precipitated proteins was incubated with 5 μM Trx, 1 μM Trx reductase, and 100 μM NADPH in HEPES (pH 7.5). The reaction was initiated by the addition of $H_2O_2$ at a final concentration of 0.2 mM. The consumption of NADPH was measured at 340 nm by spectrophotometer.

**MPTP Administration**

Mice received one intraperitoneal (i.p.) injection of MPTP·HCl per day (25 mg of free base per kg of body weight per injection; Sigma) for 3 or 5 consecutive days (Crocker et al., 2001, Kalia et al., 2004, Kim et al., 2005 and Smith et al., 2003); control mice received an equivalent volume of 0.9% saline. Brains were extracted at indicated times and either perfused for immunohistochemical analyses or quickly removed and dissected for biochemical analyses.

**Intrastriatal Administration of Adenoviruses**

The adenoviruses expressing Prx2, Prx2T89A, and Prx2T89E were engineered using pAdEasy system as previously described (Sedarous et al., 2003). We and others have previously shown that adenoviruses can target the SNc from the striatum by retrograde transport (Crocker et al., 2001, Crocker et al., 2003, Kalia et al., 2004, Kim et al., 2005 and Smith et al., 2003). Each adenovirus was injected directly into the striatum of animals 7 days before initiation of MPTP treatment (as described above). A GFP-containing construct was used as a control. A single unilateral injection of each virus (2 μl, $1 \times 10^7$ particles per μl) was delivered to the right striatum (0.5 mm rostral, 2.2 mm right of bregma, and 3.4 mm below the skull surface). Each adenovirus injection was given at a constant rate (0.5 μl/min) by using a syringe pump system. Brains were extracted for immunohistochemistry and western blot analysis 14 days after the first MPTP treatment. Double-labeling experiments with GFP (present in all viral vectors) and TH indicated that the majority of SNc TH-positive neurons at the level of the medial terminal nucleus were also GFP positive for all viruses injected (GFP control, Prx2, Prx2T89A, and Prx2T89E).

**Immunocytochemistry**

Mice were perfused transcardially and brains were fixed in paraformaldehyde and cryoprotected as previously described (Crocker et al., 2003). Serial coronal sections (14 μm thickness) of the ventral midbrain were collected as free-floating sections in 0.01 M PBS/0.02% sodium azide or collected on slides. Sections were then incubated in primary antibody (to TH, 1:10,000; p-T89, 1:100, in 0.3% Triton X-100/0.01 M PBS) for 24 hr at 4°C. For TH staining on floating sections, slices were then incubated with biotinylated secondary antibody and streptavidin horseradish peroxidase-conjugated tertiary antibody and visualized by using a 3,3′-diaminobenzidine/glucose oxidase reaction as previously described (Crocker et al., 2003). To examine the distribution of phosphorylated Prx2 in DAergic neurons, a double-labeling immunofluorescence approach was used. After incubation with the specific primary antibody at 4°C, immunolabeling was visualized by using either Alex-488-conjugated anti-rabbit IgG (1:2000) or Alex-594-conjugated anti-mouse IgG (1:2000).

**Quantification of DAergic Neuron Loss**

The number of DAergic (TH-positive) neurons was only counted from the sections in the region containing the medial terminal nucleus (MTN) because this region has been previously shown to be expressed at the highest level of virus-mediated gene expression after intrastriatal infection (Crocker et al., 2001). We also used the MTN as a landmark to evaluate consistent levels of the SNc. Neurons ipsilateral and contralateral to the viral injection were assessed as described above in at least three sections per animal. The number of neurons from ipsilateral or contralateral was then counted as previously

described. Alternatively, cresyl violet staining was performed to validate determination of nigral counts as previously described (Crocker et al., 2003).

**Western Blot Analysis for the SNc**

The western blot assay was performed as previously described (Smith et al., 2003). In brief, 50 μg of protein was analyzed by SDS-PAGE using antibodies to phospho-Prx2T89, Prx2, and β-actin.

**Human Brain Samples**

Paraffin-embedded blocks of postmortem human midbrain were collected from the Ottawa Hospital Department of Pathology. Autopsies were performed according to the policies and procedures of The Ottawa Hospital with consent from the next-of-kin. The tissue was deparaffinized in xylene and subjected to citrate antigen retrieval (Martins et al., 1999) prior to DAB staining. Diagnoses of PD were made based on medical histories and postmortem confirmation (J.M.W.). The mean average age for PD ($n = 5$; 4 males and 1 female) and control patients ($n = 6$; 6 males) was $72.6 \pm 3.7$ and $72.5 \pm 3.6$, respectively, and showed no significance ($p < 0.986$). Postmortem intervals for PD and control samples did not differ significantly ($p < 0.3$).

# Acknowledgments

This work was partially supported by the Parkinson's Disease Foundation and the Parkinson's Society of Canada (D.Q.) and the Heart and Stroke Foundation (J.R., H.A.)

and by funds from the Canadian Institutes of Health Research, the Parkinson's Society Canada, the Parkinson's Disease Foundation, the Parkinson's Research Consortium, the US army, and the Heart and Stroke Foundation of Ontario (D.S.P.).

# C-reactive protein expression in a rodent model of chronic cerebral hypoperfusion

**Brain Research**

Volume 1414, 26 September 2011, Pages 85–93

Wafa M. Juma[a], **Arman Lira[b]**, Ali Marzuka, Zaynab Marzuk[a], Antoine M. Hakima, [c], [d], Charlie S. Thompson[d]

aNeuroscience Graduate Program, University of Ottawa, ON, Canada K1H 8M5
bDepartment of Cellular and Molecular Medicine, University of Ottawa, Ont., Canada K1H 8M5
cFaculty of Medicine, University of Ottawa, 451 Smyth Road, Ottawa, Ont., Canada K1H 8M5
dOttawa Health Research Institute, Ottawa, Ont., Canada K1H 8M5

## Author statement of contribution

For over two years, Arman Lira taught and supervised the cell culture work for all *in vitro* experiments in this manuscript, including neuronal cells, mixed glia and microglia harvesting. Arman Lira also assisted in the immunocytochemical studies of microglia and data analysis from various figures.

## Abstract

White matter lesions (WML) are a clinically significant, common feature of the aging brain and have been associated with cognitive decline and depression. They are a manifestation of cerebral small vessel disease, which is associated with the progression of vascular dementia. Recent research has been focused on identifying biomarkers which may have a correlation with WML. Previous population based studies have indicated a relation between the serum level of the acute phase protein, C-reactive protein (CRP), and WML. However no previous studies have demonstrated its expression and relation to WML in brain tissue itself. Here we use the rodent model of permanent bilateral common carotid artery ligation (BCCAL) to assess CRP expression during chronic cerebral hypoperfusion (CCH). Our results show that CRP is up-regulated at the mRNA and protein levels in brain tissue from BCCAL animals. The expression of CRP mRNA was upregulated on day 3 following surgery. Because previous studies, as well as the present study, have shown that microglial activity is prominent after the third day of CCH, we sought to determine the role of microglia in CRP expression. Results indicate that cultured microglia express mRNA and protein for CRP and this expression is increased when cells are treated with interleukin-1β (IL-1β), interleukin-6 (IL-6) or a combination of the two.. This finding could indicate a possible role for CRP in the progression of small vessel disease in the brain and provide a therapeutic target.


---

## Highlights

► Chronic cerebral hypoperfusion causes white matter damage in Long Evans rats. ► C-reactive protein (CRP) was detected at the protein and mRNA level in the brain of rats subjected to chronic cerebral hypoperfusion. ► CRP mRNA and protein was detected in cultured rat brain microglia.

# 1. Introduction

White matter lesions (WML) are a manifestation of cerebral small vessel disease, which is one of the common causes of vascular dementia (Black, 2005). They appear as hyper intense signals on T2-weighted magnetic resonance images (MRI) and occur in 94% of the elderly population aged 64 and over (Simpson, JE et al., 2007). With the widespread use of this imaging technique it has become apparent that many individuals can have a significant amount of white matter change without having had a clinically recognized transient ischemic attack (TIA) or complete stroke (Pohjasvaara et al., 2000). In addition, the presence of more severe white matter lesions increases stroke risk (Bokura et al., 2006).

Recent research has been focused on identifying parameters which may have a correlation with WML. To this effect C-reactive protein (CRP) has been proposed as a candidate, however, its definite relation has yet to be elucidated. C-reactive protein (CRP), named for its capacity to precipitate the somatic C-polysaccharide of *Streptococcus pneumonia* (Tillett and Francis, 1930), was the first acute-phase protein to be described (Hirschfield and Pepys, 2003). Plasma CRP is produced only by hepatocytes (Pepys and Hirschfield, 2003). Extra hepatic synthesis of CRP has also been reported in neurons in Alzheimer patients (Yasojima et al., 2000), atherosclerotic plaques (Jialal et al., 2004), lymphocytes (Kuta and Baum, 1986), alveolar macrophages (Dong and Wright, 1996), aortic endothelial cells (Venugopal et al., 2005), coronary artery smooth muscle cells (Calabro et al., 2003), and adipocytes (Calabro et al., 2005). Induction of CRP in hepatocytes is principally regulated at the transcriptional level by the cytokine

interleukin-6 (IL-6), an effect which can be enhanced by interleukin-1β (IL-1β) (Kushner et al., 1995). More recently some population based studies have explored the relation between serum CRP and WML and, while some reported an association between the two ( [Fornage et al., 2008] and [van Dijk et al., 2005]), others did not find an apparent correlation ( [Schmidt et al., 2005] and [Wada et al., 2008]). Reasons for these controversial results were attributed to differences in the participant's health status (Schmidt et al., 2005) and to the ethnic status (Wada et al., 2008). It is clear that the findings from the population-based studies need to be explored further. To the best of our knowledge the study of CRP in an animal model of chronic cerebral hypoperfusion manifesting WML has not been previously documented.

Microglia, the surveillance cells of the brain, have been shown to attain an activated state in association with WML in rat brain (Farkas et al., 2004) and Simpson et al. (2007) have reported the presence of activated microglia in both periventricular and deep subcortical WML in human brain. The direct relation between microglial activity and WML suggests an important role for the known and "unknown" effectors of microglia in these processes. White matter injury and microglial activation have been reported to occur in a rodent of chronic cerebral hypoperfusion ( [Farkas et al., 2004] and [Wakita et al., 1994]). Previous studies using this model, where both common carotid arteries are permanently ligated, have reported WM rarefaction (vacuolation), axonal disruption, gliosis and microglial activation in lesional areas ( [Simpson et al., 2007], [Wakita et al., 1994] and [Wakita et al., 2002]). In the present study we have used this model to study the association between microglial activation, WML and CRP expression.

# 2. Results

### 2.1. Characteristics of WM injury following BCCAL

H&E staining of paraffin embedded sections showed an increase in WM vacuolation in the optic tract as early as 3 days after BCCAL (Fig. 1C). Vacuolation increased throughout the time period of the study and at 30 days vacuoles occupied 9.62 ± 0.70% of the total area of the optic tract seen in paraffin sections, while the area occupied by vacuoles in sham operated rats was 0.83 ± 0.13% (Fig. 1C). In the corpus callosum vacuolation was not as severe as that found in the optic tract but was evident from days 7–30 after BCCAL when compared to the sham operated animals (Figs. 1D, E). Vacuolation was not found in the internal capsule at any time point in the study. These observations are consistent with previously reported studies ( [Farkas et al., 2004], [Farkas et al., 2007], [Suenaga et al., 1994], [Wakita et al., 1994] and [Wakita et al., 2002]) which indicate that the first and most affected area to show vacuolation is the optic tract and consequently the corpus callosum while the internal capsule is well preserved.

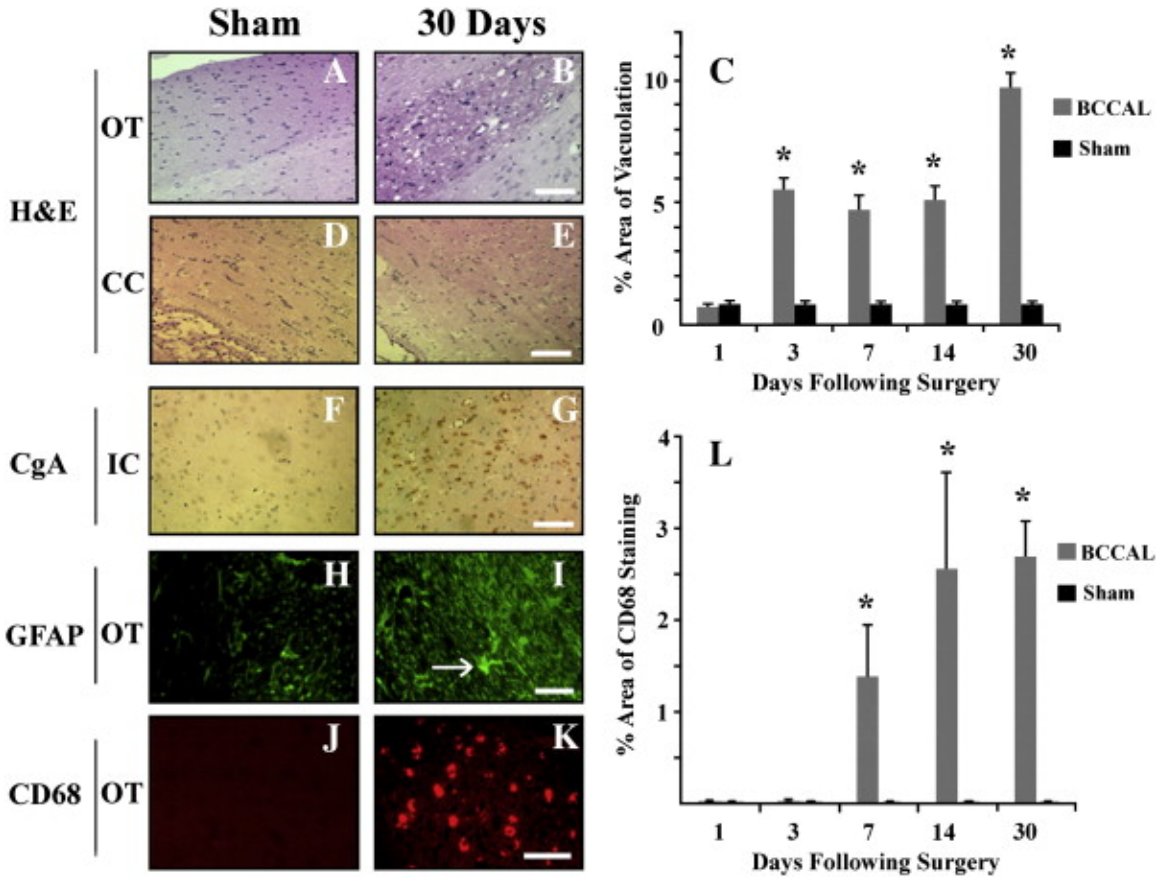


**Fig. 1.** Characteristic features of WM injury induced by BCCAL. Increased vacuolation of white matter was observed in the optic tract (A, B) and corpus callosum (D, E) of rats exposed to CCH for 30 days compared to sham operated rats. Scale bar = 100 μm. C. Quantification of vacuole area in the optic tract indicates a significant increase in total area by day 3 following surgery (n = 3). F, G. Chromogranin A immunoreactivity was increased in the internal capsule of rats exposed to CCH for 30 days. (Scale bar = 100 μm.) Reactive gliosis, as indicated by increased GFAP immunoreactivity, was present in the optic tract of rats exposed to CCH for 30 days (I) but not sham operated rats (H). Large GFAP positive cells were present in the optic tract of rats exposed to CCH (white arrow in I). Scale bar = 50 μm. Elevated CD68 immunoreactivity revealed significant activation of microglia in the optic tract of rats exposed to CCH (K) compared to sham operated rats (J). Scale bar = 50 μm. L. Quantification of the total area occupied by CD68 immunoreactivity in optic tracts indicated a significant

increase by day 7 following surgery. Data are presented as mean ± SEM (n = 3). *Indicates a statistically significant increase ($p < .05$) over sham operated rats.

A few fibers in the internal capsule of 30 day sham-operated animals were immunoreactive for CgA, a marker of axonal injury. Much more intense immunoreactivity was observed in the internal capsule of animals 30 days following BCCAL surgery (Figs. 1F, G). Compared to the optic tract, which had the most severe vacuolation (rarefaction), the CgA-immunopositive fibers were most numerous in the internal capsule. This is consistent with previously reported studies ( [Suenaga et al., 1994] and [Wakita et al., 2002]) which demonstrate that CgA-immunopositive fibers were most numerous in the internal capsule following BCCAL.

As previously reported ( [Farkas et al., 2004], [Farkas et al., 2007] and [Wakita et al., 1994]), regions of the brain showing the greatest degree of white matter damage showed the most intense glial activation (Figs. 1H–L). Thus, immunostaining for GFAP and CD68 was most intense in the optic tract and less so in the corpus callosum and internal capsule. An interesting observation was the appearance of large, GFAP positive cells in the optic tract (Fig. 1I, arrow). Large astrocytes known as clasmatodendritic astrocytes have been previously reported in association with WML ( [Kawamoto et al., 2006], [Simpson et al., 2007] and [Tomimoto et al., 1997]).

CD68 immunoreactivity was markedly increased in the optic tracts, demonstrating an association between active microglia and WM injury, as previously reported ( [Farkas et al., 2004], [Farkas et al., 2007], [Simpson et al., 2007] and [Wakita et al., 1994]). CD68 expression showed a significant increase by day 7 following BCCAL surgery and by day 30 the total area occupied by CD68 immunoreactivity was 2.69 ± 0.39% vs. 0.02 ± 0.01% for sham animals (Fig. 1L). The increase in CD68 immunoreactivity in the optic tracts occurred after a substantial amount of vacuolation had already taken place, suggesting that activated microglia might not be involved in the initial stages of the process of vacuolation. The corpus callosum and internal capsule both showed similar, low levels of CD68 immunoreactivity and there was no apparent difference between BCCAL rats and sham operated rats (data not shown).

### 2.2. WML and CRP expression

Western blotting was used to assess levels of CRP protein in brain tissue from BCCAL rats and sham operated rats. Protein extracted from liver was used as positive controls, as the liver is the main source of CRP in the plasma ( [Black et al., 2004] and [Pepys and Hirschfield, 2003]). Mean CRP protein levels were greater in brain tissue from BCCAL rats than in tissue from sham operated rats on every day tested and reached statistical significance on day 3 (Figs. 2A, B, C). Although brain tissue was perfused with saline at the time of sacrifice it is possible that some plasma remained in the tissue and this could be a source of the CRP protein detected in brain tissue. Therefore, PCR analysis was used to detect the presence of CRP mRNA in brain tissue and RNA extracted from liver was used as a positive control. Levels of CRP mRNA in brain tissue extracted from BCCAL rats exceeded those from sham operated rats on every day tested and were significantly greater on days 3 and 7 (Figs. 2D, E, F). The observation that CRP mRNA and protein can be detected in brain tissue from sham operated rats 30 days following surgery suggests that there is a constitutive level of CRP expression in the brain. Elisa assay of serum CRP levels from BCCAL animals and Sham operated animals did not show a significant difference (data not shown).

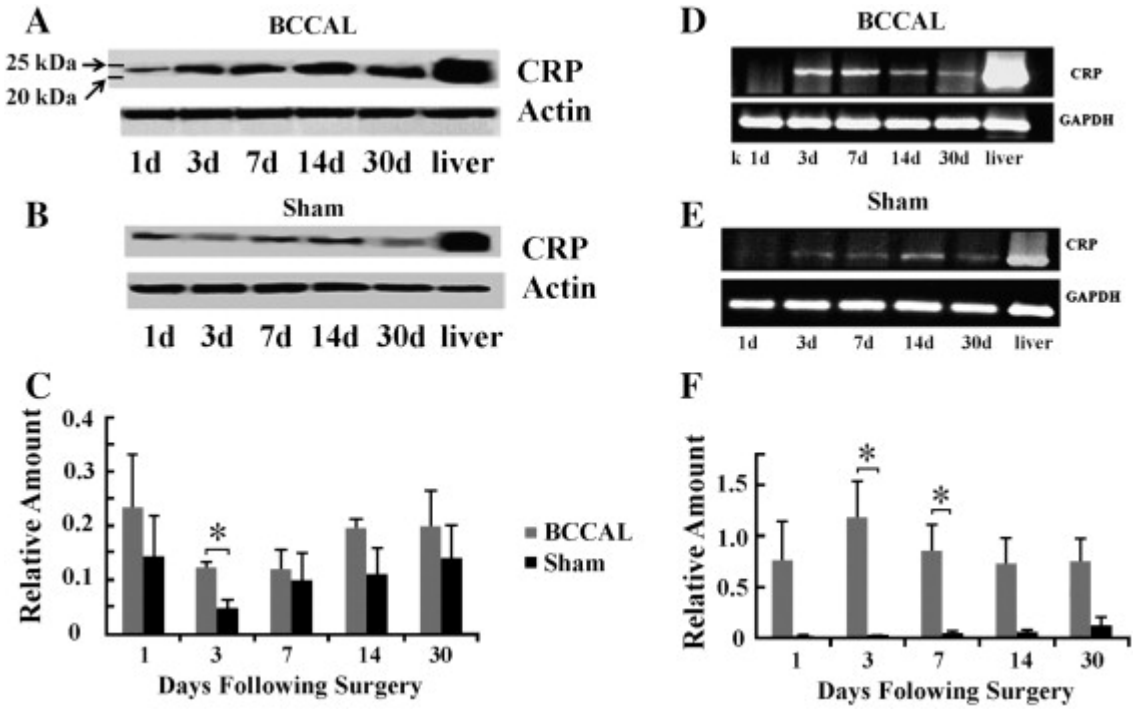


**Fig. 2.** CRP expression in rat brain tissue from BCCAL and sham operated animals. (A) and (B) show Western blots for BCCAL and SHAM, respectively. Upper bands show

protein expression for CRP at 1, 3, 7, 14 and 30 days after surgery while lane 6 shows CRP in liver tissue as a positive control. β-Actin was used as a loading control. (C) Quantification of the relative amount of CRP protein expression in BCCAL rats compared to sham operated rats. A significant increase in CRP expression occurred on day 3. (D) and (E) CRP mRNA levels in BCCAL rats and sham operated rats, respectively. Upper lanes show mRNA expression at days 1, 3, 7, 14 and 30 days following surgery. GAPDH was used as a loading control. (F) Quantification of relative the amount of CRP mRNA expression in BCCAL rats and sham operated rats. Data are presented as mean ± SEM in C and F (n = 3). *Indicates a statistically significant increase ($p < .05$) over sham operated rats.

**2.3. CRP and microglia**

Previous studies using both rat and mouse models of chronic cerebral hypoperfusion have reported the activation of microglia within days of surgery ( [Watanabe et al., 2006], [Shibata et al., 2004] and [Wakita et al., 1994]). In the present study the expression of both CRP mRNA and CRP protein was significantly elevated within 3 days following surgery and the expression of the macrophage marker CD68 was increased by day 7. We therefore used cultured rat brain microglia to test the hypothesis that microglia could mediate the increase in CRP expression. IL-6 and IL-1β were added to the culture medium to determine whether these cytokines could induce CRP expression. Microglia possess receptors for IL-1β and IL-6 ( [Hanisch, 2002], [Kim and de Vellis, 2005] and [Kim and de Vellis, 2005]) and these cytokines would be present in the in vivo environment associated with WML ( [Baumann and Gauldie, 1994] and [Ramadori and

Christ, 1999]). Concentrations of IL-6 (30 ng/ml or 50 ng/ml), IL-1β (30 ng/ml or 50 ng/ml) or a combination of IL-6 + IL-1β (30 ng/ml or 50 ng/ml) were selected for use based on a previous report in the literature (Venugopal et al., 2005). RNA extracted from control cultures of rat microglia showed detectable levels of CRP mRNA (Fig. 3A). The addition of either IL-6 or IL-1β at concentrations of either 30 ng/ml or 50 ng/ml resulted in an upregulation of CRP mRNA (Figs. 3A–C). Western blotting revealed the presence of CRP in protein extracted from microglial cultures but treatment with either IL-6 or IL-1β or a combination of the two did not significantly increase the amount of CRP protein in the extracts (Figs. 3D, E). However, it is possible that CRP protein was secreted into the culture medium and not recovered in the protein extraction process.

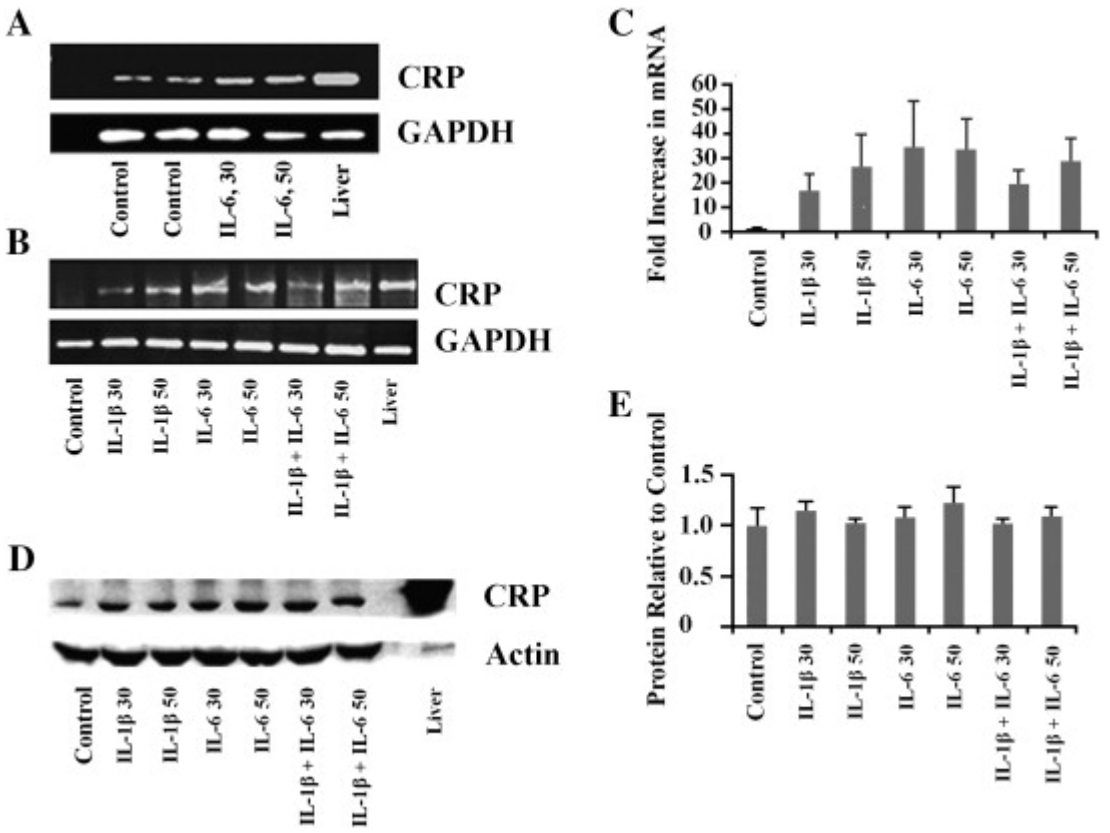

**Fig. 3.** CRP expression in cultured rat microglia. (A) and (B) mRNA expression in control cultures and cultures treated with IL-6, IL-1β or both. The cytokines were applied at a concentration of either 30 ng/ml or 50 ng/ml. RNA extracted from liver was used as a positive control and GAPDH as a loading control. (C) Quantification of relative amount of mRNA CRP expression in control and treated rat microglial cultures. (D) CRP protein expression in control cultures or cultures treated with IL-6, IL-1β or both, as in A and B. (E) Quantification of relative amount of CRP protein expression in control and treated rat microglial cultures. Values are shown as mean ± SEM for 3 independent experiments for each group.

Immunocytochemistry performed on microglial cultures revealed that more than 95% of the cells were positive for the microglial marker cd11b (data not shown). This antigen colocalized with CRP immunoreactivity, as shown in Fig. 4. Treatment of the cultures with IL-6 or IL-1β did not cause an apparent increase in CRP immunoreactivity, however, newly synthesized CRP may have been secreted into the culture medium. Following cytokine treatment the microglia did appear to adopt a more ramified appearance (Figs. 4B, C).

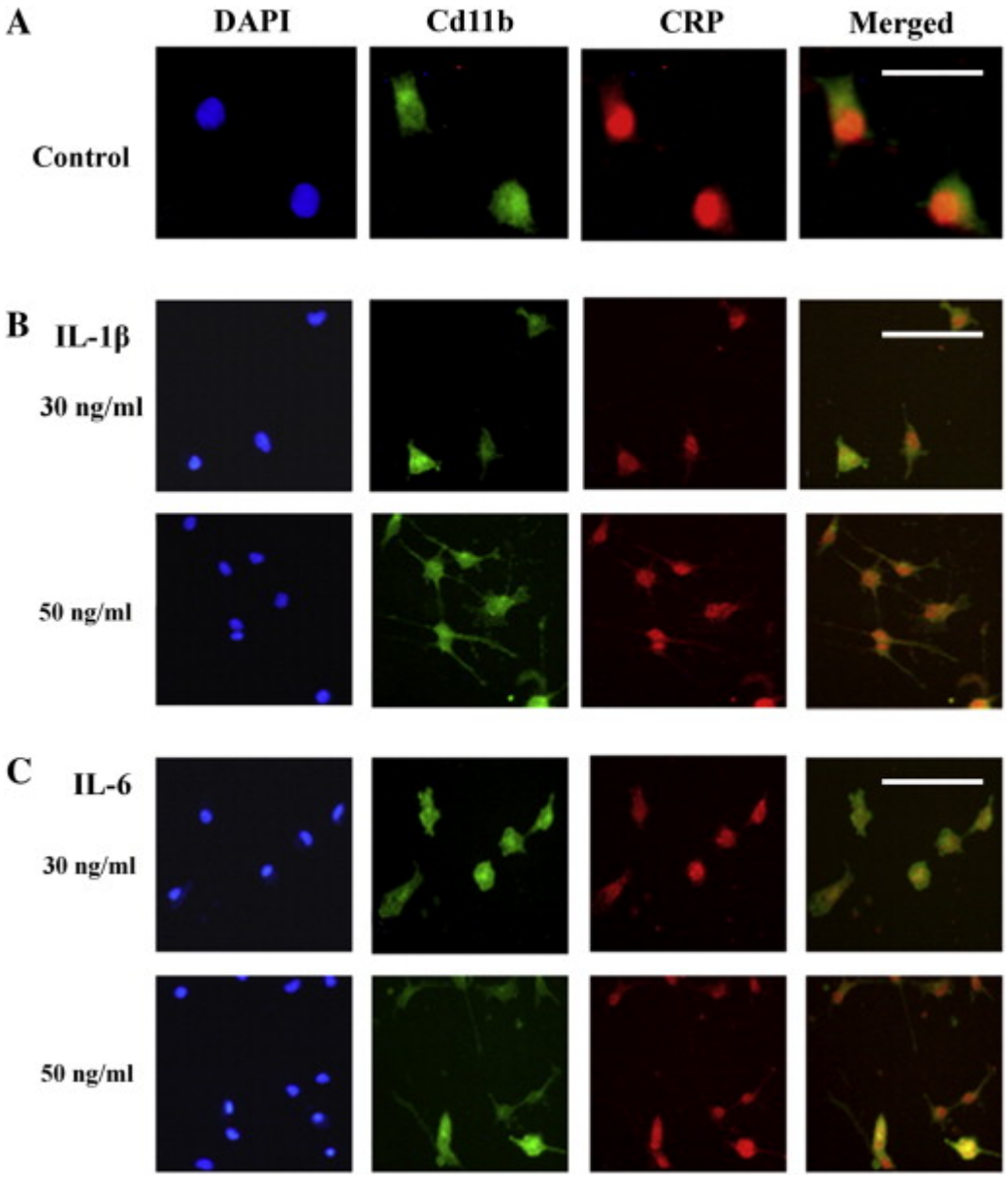


**Fig. 4.** Photomicrographs of cultured rat microglia stained for Cd11b and CRP and their co-localization. Nuclei were stained with DAPI. (A) Untreated microglial cultures. Scale bar, 20 μm. (B) and (C) show IL-1β/IL-6 treated microglial cultures at 30 ng/ml and 50 ng/ml, respectively, to indicate enhance microglial activity. Scale bar, 50 μm.

# 3. Discussion

The aim of the present study was to assess the expression of the acute phase protein CRP in brain tissue in a rodent model of chronic cerebral hypoperfusion. The vast majority of studies using the rodent model of BCCAO have used the Sprague Dawley or Wistar strains of rat. In the present study the Long Evans strain was used and the characteristic features of white matter rarefaction (vacuolation), astro- and microgliosis and axonal damage were evident, as previously reported in the literature for the other strains ( [Farkas et al., 2004], [Simpson et al., 2007], [Wakita et al., 1994] and [Wakita et al., 2002]). In general, white matter represents a distal end zone territory of blood supply from the choroidal arteries and hence reflects a greater vulnerability to blood flow reduction than gray matter (Schmahmann et al., 2008). White matter vacuolation and microglial activation were greatest in the optic tracts, as has been shown for Sprague Dawley and Wistar rats ( [Farkas et al., 2004], [Wakita et al., 1994], [Wakita et al., 2002] and [Watanabe et al., 2006]) and this is where the reduction in cerebral blood flow is the greatest in this model due to the anatomical arrangement of the vasculature ( [Farkas et al., 2007] and [Takamatsu et al., 1984]). Accordingly, a lesser degree of vacuolation was seen in the corpus callosum compared to the optic tracts. Interestingly there was no relation between the severity of WM damage and the occurrence of CgA immunolabeled fibers. Suenaga et al. (1994) have reported similar findings in human cerebrovascular WM lesions (Suenaga et al., 1994). One possible explanation for this discrepancy is that under severe ischemic conditions, CgA does not accumulate in spite of axonal injury, since the transport of these proteins is an energy-requiring process ( [Ferreira et al., 1993] and [Sherriff et al., 1994]). Thus, the number of CgA-immuno-positive fibers in the optic

nerve and optic tract may represent an underestimation of the real extent of axonal injury in these areas (Wakita et al., 2002).

Astrogliosis correlated with areas demonstrating greater WM injury. It is reported that reactive astrogliosis is commonly found adjacent to and extending far beyond the site of injury and is characterized by astrocyte proliferation and extensive hypertrophy of the cell body and cytoplasmic processes (Eng and Ghirnikar, 1994). Some astrocytes which appear to be clasmatodendritic astroglia were also noticed in the optic tract (Fig. 1). The role of clasmatodendritic astroglia in the pathogenesis of WM lesions is not entirely clear but they may clean the lesion sites by incorporating edema fluid and phagocytizing cell debris (Tomimoto et al., 1997). It has been suggested that clasmatodendritic astroglia eventually disappear, resulting in a numerical decrease in astroglia in the severe WM lesions as compared to the slight WM lesions (Tomimoto et al., 1996). Activated microglia, as demonstrated by CD68 immunostaining, showed an increase in the optic tract of BCCAL rats from day 7 of survival in comparison to the near null immunoreactivity demonstrated in SHAM animals. This increase was statistically significant from days 7–30 and was associated with the progressive appearance of vacuolation in the optic tracts from days 3–30 of survival. Chronic cerebral hypoperfusion has been suggested to contribute to WM pathology ( [Fernando et al., 2006] and [Irving et al., 2001]), and it has been shown to induce WM injury and microglial activation in the rat brain (Farkas et al., 2004). Microglial activation has been reported in the rat optic tract following the onset of ischemia (Ihara et al., 2001) and in the WM of patients with vascular dementia (Rosenberg et al., 2001) and AD (Lue et al., 2001). Our findings complement these previous observations and demonstrate significant

microglial activity immunostaining in the rat optic tract in an animal model exhibiting WML due to chronic hypoperfusion. Microglia may contribute to WM pathology by secreting an array of proinflammatory and neurotoxic molecules (Lue et al., 2001).

The similar levels of serum CRP detected by ELISA can be explained on the basis that the effects of surgery are similar in both groups and this results in an inflammatory state causing increased plasma levels of CRP. Chronic hypoperfusion is a long term, subtle event and animal trials for longer periods may provide a better way to assess serum levels of CRP once the effects of surgery and subsequent inflammation have subsided. CRP, a pentraxin, is an acute phase plasma protein produced predominantly by the liver and adipocytes. It can activate the classical complement pathway, stimulate phagocytosis, and bind to immunoglobulin receptors (FcγR) (Black et al., 2004). Its activity in humans, either pro- or anti-inflammatory, is dependent on the context in which it is acting (Black et al., 2004). The results presented here demonstrate an increased in CRP expression at the protein and mRNA levels in brain tissue of rats subjected to BCCAL compared to sham operated rats. The expression of CRP mRNA in the brain and the expression both CRP mRNA and protein by cultured microglia indicates that CRP protein is synthesized within the brain and does not need to cross the blood brain barrier in order to function within the brain parenchyma.

Previous studies have reported the activation of microglia in rats exposed to CCH from day 3 of survival onwards ( [Watanabe et al., 2006], [Shibata et al., 2004], [Wakita et al., 1994] and [Wakita et al., 2002]). In the present study the expression of CRP protein and mRNA was significantly elevated on day 3 of survival in BCCAL animals and coincided

with the appearance of WM vacuolation and a significant increase in microglial activity (CD68) in the optic tracts. CRP protein levels were greater in BCCAL rats than in sham operated rats on every day tested but reached statistical significance only on day 3 following surgery. Because CRP protein is secreted into the extracellular space it is possible that some was cleared prior to sacrifice and the measured levels underestimate the amount being synthesized. CRP mRNA expression was elevated on day 1 following surgery. This was not statistically significant because of the great variability in the levels form rat to rat but it does indicate that CRP expression may precede CD68 expression in this model. We therefore hypothesized that microglia could play a role in CRP expression and sought to assess this in-vitro.

Microglial cultures were found to express CRP at both the mRNA and protein levels. Double labeling of microglia with Cd11b (a microglia marker for active and ramified microglia) and anti-rat CRP demonstrated their co-localization in microglial cells. These results would therefore suggest that microglia are a source of CRP in the brain. It is important to note that the use of proteolytic and mechanical means to dissociate cells from CNS tissue during the isolation procedure causes microglia to become activated (Garden and Möller, 2006). Therefore, control microglial cultures might be expected to express genes found to be expressed by activated microglia. Activated microglia also secrete varying levels of IL-1β and IL-6 ( [Hanisch, 2002], [Kim and de Vellis, 2005] and [Kim and de Vellis, 2005]) and these cytokines are known to influence CRP expression. The aim of treating microglial cultures with IL-6 and IL-1β was to induce further CRP expression and determine whether increasing their concentrations, or their combination, could result in altered CRP expression. We found no relevant increase in CRP protein

expression but this might be expected, as CRP is a secreted protein. CRP mRNA was elevated in every case where cultures were exposed to IL-1β and IL-6 but this did not reach a level of statistical significance. One consideration regarding these results is that microglial activation generally increases cytokine expression and proinflammatory cytokines are the first to be released, including IL-6 and IL-1β ( [Garden and Möller, 2006] and [Kim and de Vellis, 2005]). Microglia also elaborate receptors for IL-6 and IL-1β and most other proinflammatory cytokines, resulting in autocrine feedback loops that are likely involved in the eventual down regulation of the inflammatory response (Garden and Möller, 2006). Thus, it is possible that exposure to increasing concentrations of IL-6 and IL-1β resulted in no increase in CRP expression because of auto regulatory feedback loops that terminate the expression of proinflammatory mediators by activated microglia.

In conclusion, the results presented here show a correlation between WML and CRP expression in rat brain tissue in a model of chronic hypoperfusion exhibiting characteristic features of WML. In addition we have demonstrated cultured rat microglia as a novel source for CRP expression. Further research could prove this to be a key finding in WML and all diseases associated with increased microglial activity e.g. Alzheimer's disease, Parkinson's disease and most other neuroinflammatory diseases of the brain.

# 4. Experimental procedures

## 4.1. Establishment of permanent bilateral common carotid artery ligation (BCCAL) model

All experiments conformed to the guidelines set forth by the Canadian Council for the Use and Care of Animals in Research (CCAC) with approval from the Ottawa Health Research Institute Animal Care Facility. An animal model of chronic hypoperfusion, which experimentally induces WML, was reproduced through BCCAL procedure (Wakita et al., 1994) conducted on Long Evans rats (weighing 350–450 g, Charles River, Saint-Constant, Quebec, Canada). Animals were anesthetized with isoflurane (5% induction, 2% maintenance) in a 70:30 mixture of oxygen and nitrous oxide. Rats were placed on heating pads and through a midline cervical incision; both common carotid arteries were exposed and double-ligated with silk sutures. The rectal temperature was maintained between 36.5 °C and 37.5 °C during the surgical procedure. After the operation, the rats were kept in cages with food and water ad libitum. Of the 36 BCCAL model animals six of them died within 5 days. Sham operated rats underwent the same surgical procedures except for ligation of the arteries. At 1, 3,7,14 and 30 days after ligation the animals were deeply anesthetized, blood samples for serum analysis of C-reactive protein obtained from the heart and then the animals were perfused transcardially with 0.9% normal saline. Brain samples intended for immunohistochemistry (n = 3 for BCCAL, n = 3 for sham) were further perfused with a fixative containing 4% paraformaldehyde in 0.1 M phosphate buffer (PB, pH 7.4), whereas those obtained for

PCR and Western blot (n = 3 for BCCAL, n = 3 for sham) were quick frozen in liquid nitrogen and kept at − 80 °C until used.

### 4.2. Hematoxylin and eosin staining (H&E)

Coronal brain blocks including the optic nerves and corpus callosum (Bregma 1.88 mm–2.8 mm) were embedded in paraffin for histological examination. Four micrometer-thick paraffin sections were cut on a microtome, and stained with a basic hematoxylin and eosin stain.

### 4.3. Immunohistochemistry

Paraffin embedded rat brain sections were deparaffinized and antigen retrieval step using citrate buffer (PH 6.0) was performed in a rapid microwave histoprocessor (model 5, Milestone). Following antigen retrieval, sections were rinsed with 1× PBS for 5 min. Non-specific binding sites were blocked with 10% Triton X-100 and donkey serum diluted in 1× PBS. Sections were then incubated with monoclonal anti-rat CD68 (Abcam, USA, 1:100), a marker for microglial activity, and glial fibrillary acidic protein (GFAP) (1:200), an astrocyte marker, diluted in 1× PBS with 10% Triton X-100 overnight at 4 °C in order to detect microglial cell activity and astrocytes respectively. Cy-3 conjugated donkey anti-mouse IgG antibody (1:200) and FITC (1:200) donkey anti-mouse IgG antibody were used for visualization of immunolabeling. DAPI was used to visualize nuclei.

Also following antigen retrieval other sections were incubated with rabbit polyclonal Chromogranin A antibody (Abcam, USA, 1:100), a marker for axonal injury, diluted in

TBS with 1% BSA. Subsequently sections were revealed using a highly sensitive biotin free polymer detection system (Cat#M4U534Biocare Medical); slides were incubated with anti-Rabbit MACH 4 Polymer HRP for 20 min at room. After each incubation the sections were rinsed for 5 min. with 0.01 M TBS pH 7.6. Finally the immunoreaction complex was visualized using a solution of Chromogen DAB (0.02% 3, 3′-diaminobenzidine tetrahydrochloride in 0.05 M Tris buffer, pH 7.6) with a substrate of hydrogen peroxide (0.001% $H_2O_2$) to catalyze the enzymatic reaction of the HRP.

### 4.4. Quantification of immunohistochemistry and H&E

To quantify immune cells in the optic tract and corpus callosum, digital images of CD68 stained sections (Bregma − 1.8 to − 2.8) were acquired using Axioskop 2 Mot microscope (Zeiss, Toronto, Canada) and Northern Eclipse software (Empix Imaging Inc., Mississauga, Canada) under 20× objective. Images were captured as gray scale (8 bit) with a fixed exposure, gain and offset and the intensity measured as % object area of immunoreactive cells of the total selected area. Two measures, one for each optic tract were made on each section by 3 independent investigators. The corpus callosum did not show significant immunoreactivity and measures were not done for it. For H&E basic stain, images were captured as gray scale (16 bit) and areas within the selected, demarcated optic tracts and corpus callosum which showed rarefaction(vacuolation) and did not take up the basic H&E stain were measured by threshold to the background and recorded as % object area of vacuoles of the total selected area. Two measures, one for each optic tract were made on each section by 3 independent investigators. The corpus callosum showed late vacuolations and data was not included.

### 4.5. Cell culture

Microglial cells were cultured from brain tissue of 2–3 day postnatal rat pups according to previous protocols (Mount et al., 2007). Postnatal 2–3 day old rat pups were used for microglial cultures. Brains were dissociated using a tissue grinder kit and plated in flasks with minimum essential medium supplemented with 5% heat-inactivated fetal bovine plasma, 5% heat-inactivated horse plasma, and 0.05 mg/ml gentamycin. Two days later, the medium was replenished, and the culture reached confluency 8 days later, these confluent mixed-glia cultures were shaken for 5 h at 180 rpm at 37 °C to separate microglia from astrocytes (Mount et al., 2007). This produced a yield of > 95% enriched microglia .After confluency the cells were plated in 12 well plates on cover slips or on 6 $cm^2$ dishes at a density of $2 \times 10^5/cm^2$ and treated with IL-1β, IL-6 or a combination of both. After 24 h cells were used for RNA or protein extraction.

### 4.6. Immunocytochemistry

Microglial cells cultured on cover slips in 12 well plates were used to demonstrate Cd11B (Serotec, USA, 1:200) and CRP (ICL [Immunology Consultants Laboratory Inc.], Newberg, USA, 1:200) immunostaining. Non-specific binding sites were blocked with 10% Triton X-100 and donkey serum diluted in 1× PBS. Sections were then incubated with mouse anti-rat Cd11b (a marker for microglia) and rabbit anti-rat C-reactive protein (for detection of C-reactive protein expression) diluted in 1× PBS with 10% Triton X-100 overnight at 4 °C. Cy-3 conjugated donkey anti-rabbit IgG antibody (Chemicon, 1:200) and FITC (Chemicon, 1:200) donkey anti-mouse IgG antibody were used for visualization of immunolabeling. DAPI was used to visualize nuclei.

### 4.7. CRP mRNA expression

RNA was extracted from the cells/tissue using TRIzol (Invitrogen, CAN.) reagent. The first strand of cDNA was synthesized using Superscript II Reverse Transcriptase (Invitrogen, CAN.) at a total RNA (3 μg/reaction for RNA extracted from brain tissue samples or 2 μg/reaction for RNA extracted from microglial cultures) and according to manufacturer's protocol. cDNA was amplified using primers (Invitrogen, CAN) specific for CRP (forward: 5′-CACGCTGATGTGAGCCGAAG-3′ and reverse: 5′-ACTTCAGTGCCCGCCAGTTC-3′). CRP was amplified for 35 cycles and yielded a band at 450 bp on 1% agarose gels. mRNA GAPDH was used as a loading control and samples normalized to it.

### 4.8. CRP protein expression

The cells were collected in lysis buffer containing 1M Tris 62.5 ml/L, 100 mM EDTA 25 ml/L, 100 mM EGTA 25 ml/L, 50% glycerol 200 ml/L, 20% SDS 100 ml/L and 1% Bromophenol Blue 10 ml/L. β-Mercaptoethanol 5% was added to the final solution at the time of use. The samples were sonicated briefly for 5 s and then boiled for 5 min. Tissue samples were grinded in a lysis buffer containing RIPA buffer and the protein loaded at a concentration of 30 μg/lane. All protein samples were loaded on ready prepared gels (Biorad) transferred to nitrocellulose membranes and blocked using 5% milk solution. Rabbit anti-rat CRP (ICL, USA) antibody was used as primary antibody, and after washing with 1× TBS-Tween 20 (3 times) the membranes were incubated with anti-rabbit HRP secondary antibody and developed using chemiluscent reagents. In all Western blot experiments, actin was used as an internal control and samples normalized to it.

### 4.9. CRP assay

CRP levels in the serum were measured using an enzyme-linked immunosorbent assay (ELISA) kit specific for rat CRP (ICL, USA) according to the manufacturer's instructions. Because of the limitation of availability of a highly sensitive rat CRP ELISA kit, CRP levels could not be measured in the media obtained from microglial cultures.

### 4.10. Statistical analysis

All results taken from 3 independent experiments for each group are presented as values ± SEM (standard error of mean). Probability based on Student *T*-Test is shown to be significant at $*p \leq 0.05$, $**p \leq 0.00005$ and $***p \leq 0.000005$ accordingly.

## Acknowledgments

Funds for this study were provided by the Heart and Stroke Foundation of Ontario Centre for Stroke Recovery and the Canadian Stroke Network. The authors would like to thank Kim Wong.

# Appendix 2: Permission to Reprint Published Manuscripts

## Journal of Biological Chemistry Manuscript:

Copyright Permission Policy
These guidelines apply to the reuse of articles, figures, charts and photos in the ***Journal of Biological Chemistry, Molecular & Cellular Proteomics*** and the ***Journal of Lipid Research***.
**For authors reusing their own material:**

Authors need **NOT** contact the journal to obtain rights to reuse their own material. They are automatically granted permission to do the following:

- Reuse the article in print collections of their own writing.
- Use an article in a thesis and/or dissertation.

## Journal of Neuroscience Manuscript:

**How to Obtain Permission to Reprint or Photocopy**
**Permission Requests**
Authors need NOT contact *The Journal* to obtain rights to reuse their own material.Requests for permission to reprint published material from a:
(1) Non-profit publisher should be emailed directly to jnpermissions@sfn.org or faxed to 202-962-4945
(2) For-profit publisher should be submitted online through the Copyright Clearance Center.
For more information, see *The Journal*'s Permissions Policy.

**Reprints**
Reprints of a single copy of an individual article are available from Infotrieve at http://www.infotrieve.com.

| | |
|---|---|
| **Subject:** | RE: Permission to Reprint |
| **From:** | "jn permissions" <jnpermissions@sfn.org> |
| **Date:** | Thu, 29 August, 2013 11:02 am |
| **To:** | |
| **Priority:** | Normal |
| **Options:** | View Full Header \| View Printable Version \| Download this as a file\| Add to Addressbook |

------Original Message------
From: jn permissions
To: arman at school
Cc: jn permissions
Subject: RE: Permission to Reprint
Sent: Aug 29, 2013 11:39 AM

Dear Arman Lira,

Thank you for your email. Permission is granted to reproduce the requested material listed below with NO fee in print and electronic format for use in your doctoral thesis/dissertation. Please contact me if you have any questions or if you need another form of permission.

Regards,
Chanelle Grannum
SfN Central Office
Journal of Neuroscience

SfN Article:
Matthew P. Mount, Arman Lira, David Grimes, Patrice D. Smith, Sylvie Faucher, Ruth Slack, Hymie Anisman, Shawn Hayley, and David S. Park Involvement of Interferon-γ in Microglial-Mediated Loss of Dopaminergic Neurons The Journal of Neuroscience, 21 March 2007, 27(12):3328-3337; doi:10.1523/JNEUROSCI.5321-06.2007

-----Original Message-----
From:
Sent: Wednesday, August 28, 2013 2:44 PM
To: jn permissions
Subject: Permission to Reprint

To whom this may concern,

In my PhD thesis, I would like to reprint a copy of our 2007 article entitle "Involvement of interferon-gamma in microglial-mediated loss of dopaminergic neurons". Can you please tell me what citation I should use?

Thank you,
Arman Lira

## Neuron Manuscript:

**Welcome**

**License Details**

Thank you very much for your order.

This is a License Agreement between Arman Lira ("You") and Elsevier ("Elsevier"). The license consists of your order details, the terms and conditions provided by Elsevier, and the payment terms and conditions.

Get the printable license.

| | |
|---|---|
| License Number | 3217780534386 |
| License date | Aug 28, 2013 |
| Licensed content publisher | Elsevier |
| Licensed content publication | Neuron |
| Licensed content title | Role of Cdk5-Mediated Phosphorylation of Prx2 in MPTP Toxicity and Parkinson's Disease |
| Licensed content author | Dianbo Qu,Juliet Rashidian,Matthew P. Mount,Hossein Aleyasin,Mohammad Parsanejad,Arman Lira,Emdadul Haque,Yi Zhang,Steve Callaghan,Mireille Daigle,Maxime W.C. Rousseaux,Ruth S. Slack,Paul R. Albert,Inez Vincent,John M. Woulfe,David S. Park |
| Licensed content date | 5 July 2007 |
| Licensed content volume number | 55 |
| Licensed content issue number | 1 |
| Number of pages | 16 |
| Type of Use | reuse in a thesis/dissertation |
| Portion | full article |
| Format | Electronic |
| Are you the author of this Elsevier article? | Yes |
| Will you be translating? | No |
| Title of your | The Immune Response in Parkinson's Disease |

| | |
|---|---|
| thesis/dissertation | |
| Expected completion date | Aug 2013 |
| Estimated size (number of pages) | 200 |
| Elsevier VAT number | GB 494 6272 12 |
| Permissions price | 0.00 USD |
| VAT/Local Sales Tax | 0.00 USD / 0.00 GBP |
| Total | 0.00 USD |



## Brain Research Manuscript:

Authors can use their articles for a wide range of scholarly, non-commercial purposes as outlined below. These rights apply for all Elsevier authors who publish their article as either a subscription article or an open access article.

We require that all Elsevier authors always include a full acknowledgement and, if appropriate, a link to the final published version hosted on Science Direct.

For open access articles these rights are separate from how readers can reuse your article as defined by the author's choice of Creative Commons user license options.

**Authors can use either their accepted author manuscript or final published article for:**

- Use at a conference, meeting or for teaching purposes
- Internal training by their company
- Sharing individual articles with colleagues for their research use* (also known as 'scholarly sharing')
- Use in a subsequent compilation of the author's works
- Inclusion in a thesis or dissertation
- Reuse of portions or extracts from the article in other works
- Preparation of derivative works (other than for commercial purposes)

*Please note this excludes any systematic or organized distribution of published articles.